UNIVERSITETET I AGDER

ENE500

Photovoltaic facade systems in Norway: An assessment of energy performance, building integration, and costs

Christian Hals Frivold

Supervisor:
Professor Anne Gerd Imenes

University of Agder, 2018
Faculty of Engineering and Science
Department of engineering

Individual declaration

The individual student or group of students is responsible for the use of legal tools, guidelines for using these and rules on source usage. The statement will make the students aware of their responsibilities and the consequences of cheating. Missing statement does not release students from their responsibility.

1.	I hereby declare that my thesis is my own work and that I/We have not used any other sources or have received any other help than mentioned in the thesis.	☑
2.	I further declare that this thesis: - not been used for another exam at another department/university/university college in Norway or abroad; - does not refer to the work of others without it being stated; - does not refer to own previous work without it being stated; - have all the references given in the literature list; - is not a copy, duplicate or copy of another's work or manuscript.	☑
3.	I am aware that violation of the above is regarded as cheating and may result in cancellation of exams and exclusion from universities and colleges in Norway, see Universitets- og høgskoleloven §§4-7 og 4-8 og Forskrift om eksamen §§ 31.	☑
4.	I am aware that all submitted theses may be checked for plagiarism.	☑
5.	I am aware that the University of Agder will deal with all cases where there is suspicion of cheating according to the university's guidelines for dealing with cases of cheating.	☑
6.	I have incorporated the rules and guidelines in the use of sources and references on the library's web pages.	☑

Publishing agreement

Authorization for electronic publishing of the thesis. Author(s) have copyrights of the thesis. This means, among other things, the exclusive right to make the work available to the general public (Åndsverkloven. §2). All theses that fulfill the criteria will be registered and published in Brage Aura and on UiA's web pages with author's approval. Theses that are not public or are confidential will not be published.	
I hereby give the University of Agder a free right to make the task available for electronic publishing:	Yes ☑
Is the thesis confidential? (confidential agreement must be completed)	No ☑
- If yes: Can the thesis be published when the confidentiality period is over?	
Is the task except for public disclosure? (contains confidential information. see Offl. §13/Fvl. §13)	No ☑

Abstract

In this master thesis, different PV facade systems located in Norway have been evaluated and analyzed. It will thus contribute to the ongoing development of a national database of BIPV. Also, technical and economic aspects of the PV systems are analyzed. Data series from the web-based monitoring systems have been evaluated, cross-sections of the PV facades are examined, and the economic costs associated with the PV systems have been evaluated.

The specific yield and cost of the analyzed cases have been compared with simulated data and traditionally clothed facades and with each other. The results showed that the facade PV systems can be compared to the roof installations with regard to specific yield and with traditional facade cladding on cost. From May 2017 to April 2018, the annual specific yield is in the range 500-770 kWh/kWp for the analyzed cases. The facades have a more even annual distribution contrary to the summer season, which has a typical peak for the roof installation. When comparing the specific yield for the PV systems on the facades with the roof PV systems, the facade systems produced 80-98 % of the roof systems.

As the development of installed PV systems are rapidly increasing, the importance of evaluating operative PV systems with regard to expected energy production and cost is necessary. The findings from this master thesis can be used as a guideline for expected specific yield and technical solutions on the PV facade systems in Norway.

Preface

Personally, I have a background from a bachelor degree in Mechatronics from the University of Agder. The renewable energy sources are the future, finding new solutions and develop the sources available is fundamental. The utilizing of the photon energy conversion from solar radiation is an essential part of the contribution. The limited information on facade mounted PV systems in Norway, together with the ongoing development of a Norwegian database gave motivation and drive to write this master thesis.

Acknowledgements

Firstly, I would like to sincerely thank Prof. Anne Gerd Imenes for all of her dedication and support during the master thesis. There has always been an open door and she has always given constructive feedback to the master thesis.

I would like to thank Vegar Myklebust at Kiwi Norge, who helped with the access to all of their PV systems, and providing further contact information on their PV suppliers.

Thanks to all of the contributors from the solar companies, providing insight and knowledge about their operating PV systems. FUSen with Trygve Mongstad, Geir Flikke, and Steinar Nilsen and for SoleL, Per Urdahl.

I would like to acknowledge all of the positive and welcoming contacts that have helped with providing information during the master thesis, Ole-Christian Østereng, Bodil Motzke, and Ine Maribu.

I sincerely appreciate the time and effort spent by Roger Nilsen on evaluating and giving remarks on my master thesis.

Finally, I would like to thank my girlfriend Maria Tønnessen, for her motivation and understanding during my work on the thesis.

University of Agder, Grimstad, June 1, 2018

Christian Hals Frivold

Christian Hals Frivold

Contents

Individual declaration **I**

Publishing Agreement **II**

Abstract **III**

Preface **IV**

Nomenclature **XI**

1 Introduction **1**

1.1 Background and motivation 1
1.2 Problem statement 2
1.3 Limitations 2
1.4 Thesis layout 3

2 Theoretical background **4**

2.1 Solar radiation 4
2.1.1 Direct and diffuse solar radiation 5
2.1.2 Solar geometry 5
2.2 The PV cell and its characteristics 5
2.2.1 PV cell material technologies 5
2.2.2 Maximizing the output power of the PV cell 6
2.2.3 Effect of temperature and irradiation changes 6
2.3 PV modules 7
2.3.1 The structure of a PV module 8
2.3.2 Standard test condition and efficiency of PV module 8
2.3.3 The temperature and irradiance matrix 8
2.3.4 The PV module efficiency of different cell technology 9
2.4 Degradation rates and failure of PV modules and systems 9
2.5 The grid connected PV system 9
2.6 Balance of system components 10
2.6.1 DC and mismatch losses 10
2.6.2 Inverter conversion efficiency 11
2.6.3 AC cabling and losses 11
2.7 The albedo effect 11
2.8 The air-gap 12
2.9 PV system performance parameters 12
2.9.1 Specific yield 13
2.9.2 Performance ratio 13
2.9.3 System efficiency 14
2.9.4 Uncertainties of measuring devices for solar radiation 14

3 State of the art in PV system performance **15**
3.1 Development of PV performance internationally 15
3.2 Development of PV performance in Nordic countries 16

4 Method **18**
4.1 Equations used to evaluate the PV systems 18
4.2 Data collection and quality 18

5 Cases and results **20**
5.1 Solsmaragden 20
5.1.1 System description 20
5.1.2 Building technical integration 22
5.1.3 Economy 24
5.1.4 Performance 25
5.1.5 Lessons learned 29
5.2 Brynseng school 30
5.2.1 System description 30
5.2.2 Building technical integration 31
5.2.3 Economy 34
5.2.4 Performance 35
5.2.5 Lessons learned 37
5.3 Bjørkelangen school 38
5.3.1 System description 38
5.3.2 Building technical integration 39
5.3.3 Economy 40
5.3.4 Performance 41
5.3.5 Lessons learned 41
5.4 Kiwi Dalgård 42
5.4.1 System description 42
5.4.2 Building technical integration 44
5.4.3 Economy 46
5.4.4 Performance 47
5.4.5 Lessons learned 48
5.5 Kiwi Fjeldset 49
5.5.1 System description 49
5.5.2 Building technical integration 50
5.5.3 Performance 51
5.6 ASKO washing hall 53
5.6.1 System description 53
5.6.2 Building technical integration 54
5.6.3 Economy 55
5.6.4 Performance 55
5.6.5 Lessons learned 57
5.7 Haldenterminalen 58

5.7.1 System description . . . 58
5.7.2 Building technical integration . . . 59
5.7.3 Economy . . . 59
5.7.4 Performance . . . 60
5.7.5 Lessons learned . . . 62

6 Comparison of analyzed cases and discussion **63**
6.1 Individual comparison between simulated and measured values . . . 63
6.1.1 Solsmaragden . . . 63
6.1.2 Brynseng school . . . 64
6.1.3 Bjørkelangen school . . . 68
6.1.4 Kiwi Dalgård . . . 69
6.1.5 Kiwi Fjeldset . . . 70
6.1.6 ASKO washing hall . . . 71
6.1.7 Haldenterminalen . . . 71
6.2 Comparison of the specific yield of the analyzed cases . . . 72
6.2.1 Cost comparison . . . 74
6.3 Lessons learned about the different fastening solutions . . . 76
6.4 Summarized discussion of compared cases . . . 77

7 Conclusion **78**
7.1 Recommendations for further work . . . 78

Appendix A Solsmaragden **85**

Appendix B Brynseng **92**

Appendix C Bjørkelangen **99**

Appendix D Kiwi Dalgård **103**

Appendix E Kiwi Fjeldset **106**

Appendix F ASKO washing hall **109**

Appendix G Haldenterminalen **112**

Appendix H Screen shot of web-based monitoring software **119**

List of Figures

1.1 The development of new installed PV systems in Norway from 2011-2017 1
2.1 The spectral distribution of the radiation from the sun 4
2.2 The illustration of a module with tilt angle θ_T, azimuth angle θ_a and incidence angle S_β 5
2.3 Graphically illustrated maximum power point 6
2.4 The effect of temperature and irradiation changes on a PV cell 7
2.5 Illustration of the PV system from the cell, module, string and array 7
2.6 Thickness comparison between the c-Si and CIGS modules 8
2.7 Illustration of how The grid-connected PV system works 10
2.8 The efficiency of a SMA inverter 11
2.9 The albedo effect 12
5.1 The BIPV and BAPV system of Solsmaragden 21
5.2 Structure of the green printed panel from ISSOL 22
5.3 Cross-section of the south facade on Solsmaragden 23
5.4 Pictures of the mounting of the PV modules on the facades at Solsmaragden 24
5.5 Specific yield comparison between the south facade and roof on Solsmaragden 26
5.6 Comparison of the monthly specific yield of the south facade (Inv 7 and Inv 8 combined), with the solar irradiance of 2017 27
5.7 Monthly development of PR for south facade 28
5.8 System efficiency of the south facade, on a monthly basis 28
5.9 System efficiency and solar irradiance on a clear sunny day in February 29
5.10 System efficiency and solar irradiance on a clear sunny day in July 29
5.11 Picture of the BIPV facade at Brynseng school 30
5.12 The section divisions and the building extension on the south facade of Brynseng . . . 32
5.13 Schematic illustration of the string design of Brynseng of each inverter 32
5.14 Illustration of module structure at Brynseng 33
5.15 Installation details, showing vertical battens and mounting hook 33
5.16 Cross-section of the Brynseng facade, including outer wall, brackets, and PV module . 34
5.17 BIPV cost distribution at Brynseng school 35
5.18 Comparison of different sections at Brynseng 36
5.19 The specific yield of each inverter at Brynseng, (May 2017-April 2018) 37
5.20 Picture of the south oriented BAPV at Bjørkelangen school 38
5.21 Vertical cross-section of the facade on Bjørkelangen 40
5.22 The specifc yield of the BIPV at Bjørkelangen school 41
5.23 Picture of the PV systems at Kiwi Dalgård 42
5.24 The main facade at Kiwi Dalgård with the different technologies 43
5.25 Structure of the modules used at Kiwi Dalgård 44
5.26 Cross-section of the south-west facade at Kiwi Dalgård 45
5.27 Illustration of the mounting details of the PV modules at Kiwi Dalgård 46
5.28 Gluing and installation of the PV modules at Kiwi Dalgård 46
5.29 Distribution of costs for the total PV system at Kiwi Dalgård 47
5.30 Specific yield of the mono-Si on the south oriented facade 48
5.31 Picture of the south oriented BAPV facade at Kiwi Fjeldset 49

5.32 PV module layers at the south facade on Kiwi Fjeldset 50
5.33 The framed PV module of Kiwi Fjeldset 51
5.34 Monthly development of specific yield of the south facade at Kiwi Fjeldset 52
5.35 Comparison between the facade and roof installation on Kiwi Fjeldset for 2017 52
5.36 The BAPV system on the facade of ASKO washing hall located in Vestby 53
5.37 Attachment details of the PV modules at ASKO washing Hall 55
5.38 The development on the specific yield of the south facade on ASKO washing hall . . . 56
5.39 Comparison between the PV system on the roof and facade on ASKO washing hall, 2017 56
5.40 The efficiency and temperature of the inverter on the south facade at ASKO washing hall 57
5.41 The BAPV system on the south facade of Haldenterminalen 58
5.42 Development on the inverter efficiency on the south facade 60
5.43 Monthly development of the south facade (BAPV) at Haldenterminal 61
5.44 Comparison between the PV system on the roof and facade 62
6.1 Monthly comparison between measured and simulated specific yield at Solsmaragden . 63
6.2 Monthly plotted measured irradiance on PV area and the simulated values from PVGIS on Solsmaragden 64
6.3 Monthly comparison between measured and simulated specific yield at Brynseng . . . 65
6.4 Individual inverter comparison between the measured specific yield and simulated data 66
6.5 The monthly simulated values from Matlab script and PVGIS 67
6.6 Monthly comparison between measured and simulated specific yield at the PV system of Bjørkelangen school 68
6.7 Monthly comparison between measured and simulated specific yield of the PV system at Kiwi Dalgård 69
6.8 Monthly comparison between measured and simulated specific yield of the PV system at Kiwi Fjeldset 70
6.9 Monthly comparison between measured and simulated specific yield of the PV system at ASKO washing hall 71
6.10 Monthly comparison between measured and simulated specific yield of the PV system at Haldenterminalen 72
6.11 Graphically monthly development from May 2017 to April 2018 of each case 74
6.12 Evaluation of different materials used on building facades 75
6.13 Typical cost distribution of the total PV system 76
A.1 The string design of inverter 7 and 8 on the south facade of Solsmarageden 86
B.1 Detailed mounting specifics on Brynseng 92
B.2 Different modules used at Brynseng 95
B.3 Electrical scheme of the strings at Brynseng 96
C.1 RedAir system 100
D.1 Illustration of the mounting details at Kiwi Dalgård 104
D.2 The standard sized PV module from Innos, the taylor made PV modules was not available to the author 105
G.1 IBC solar monitoring changing the values on energy generated per interval 112
H.1 Screen shot of the diagram creator of IBC Solar Pro 119
H.2 Example of front page on Sunny Portal and different analysis parameters 120

List of Tables

1 The coefficients of the albedo effect . . . 12
2 Some results from reviewed Nordic PV systems . . . 17
3 System description of the south oriented facade at Solsmaragden . . . 22
4 Measured data on Solsmaragden . . . 25
5 System description of the south facade oriented BIPV on Brynseng . . . 31
6 Measured data on Brynseng . . . 35
7 Description of BAPV system at Bjørkelangen . . . 39
8 Explanation of numbers in Figure 5.21 . . . 40
9 Measured data on Bjørkelangen . . . 41
10 Description of the operative crystalline facade at Kiwi Dalgård . . . 43
11 Measured data on Kiwi Dalgård . . . 47
12 Description of the south oriented BAPV system on Kiwi Fjeldset . . . 50
13 Measured data on Kiwi Fjeldset . . . 51
14 The characteristics of the BAPV on ASKO washing hall . . . 54
15 Measured data on ASKO washing hall . . . 55
16 System Description of Haldenterminal . . . 59
17 Measured data on Haldenterminalen . . . 60
18 Annual simulated values on the specific yield, irradiation, and PV system efficiency . . 73
19 Comparison on the specific yield of the different cases and air-gap . . . 73
A1 Efficiency and Performance Ratio on the south facade at Solsmaragden . . . 85
B1 Explanation of the mounting system at Brynseng . . . 92
B2 Detailed information on days of missing data on Brynseng . . . 93
B3 Calculation of cost with and without ENOVA support . . . 93
B4 The specific yield of each inverter at Brynseng . . . 93
B5 Specific yield of each inverter at Brynseng . . . 94
C1 Cost approximation of the BAPV on Bjørkelangen . . . 99
C2 Yield and specific yield of Bjørkelangen School . . . 99
D1 Yield and specific yield at Kiwi Dalgård main facade of Mono-Si . . . 103
E1 Yield and specific yield of BAPV at Kiwi Fjeldset . . . 106
E2 Days of missing data of BAPV on Kiwi Fjeldset . . . 106
F1 Energy production and specific yield of ASKO washing hall . . . 109
F2 South facade inverter efficiency at ASKO washing hall . . . 109
G1 Efficiency and mean temperature at Haldenterminalen . . . 113
G2 Yield and Specific yield of the south oriented BAPV on Haldenterminalen . . . 114

Nomenclature

Abbreviations

AM Air Mass

mono-Si mono-crystalline Silicon

NPV Net Present Value

NS Norwegian Standard

NTNU Norwegian University of Science and Technology

PVGIS Photovoltaic Geographical Information System

TMY Typical Meteorological Year

a-Si Amorphous Silicon

AC Alternating Current

BAPV Building Applied Photovoltaic

BIPV Building Integrated Photovoltaic

BIPVNO Building Integrated Photovoltaics for Norway

BOS Balance of system

c-Si Crystalline Silicon

CdTe Cadmium Telluride

CIGS Copper Indium Gallium Selenide

DC Direct Current

HIT Heterojunction with intrinsic thin-layer

IEA International Energy Agency

IEC International Electrotechnical Commission

m-Si Multi-crystalline Silicon

MPP Maximum Power Point

NOCT Nominal Operating Cell Temperature

NOK Norwegian krone

NREL National Renewable Energy Laboratory

nZEB Nearly Zero-Energy Beuilding

p-Si Polycrystalline Silicon

POA Plain of Array

PV Photovoltaic

PVPS Photovoltaic Power System Programme

RES Renewable Energy Sources

Si Silicon

STC Standard Test Conditions

UiA University of Agder

ZEB Zero-Energy Building

Symbols

η_{STC} Module efficiency at STC

η_{sys} System efficiency

η_{Inv} Inverter efficiency

$\mathrm{A_m}$ Module Area

$\mathrm{E_{A,D}}$ Measured Net AC energy production

H_2O Water vapour

$\mathrm{N_I}$ Days of missing irradiance data

$\mathrm{N_p}$ Days of missing production data

O_3 Ozone

$\mathrm{P_{sun}}$ Power from the electrical charge by the sun's radiation

ϕ_z	Solar zenith angle
θ_{a}	Azimuth angle
θ_{T}	Tilt angle
A	Area
CO_2	Carbon dioxide
G	Reference Irradiance
G_I	Reference Irradiance at STC
I	Cell current
I_{mp}	Maximum current point
I_{SC}	Short circuit current
P	Power
P_0	Nominal DC power
P_{AC}	Net Energy Output AC
P_{DC}	Array output DC power
P_{mpp}	Maximum power
P_{STC}	Power at STC
PR	Performance Ratio
S_β	The solar irradiance angle
T	Cell temperature
T_{STC}	STC temperature $25°C$
V	Cell potential
V_{mp}	Maximum voltage point
V_{OC}	Open cell voltage
W_{P}	Watt Peak
Y_A	Array Yield
Y_f	Final Yield
Y_r	Reference Yield
C	The economical cost
O	oxygen

1 Introduction

1.1 Background and motivation

In Norway, rivers and waterfalls running from high mountains and down to the fjords are making it possible to utilize the renewable energy of hydro power. According to the Norwegian electricity disclosure of 2016 [1], 98 % of the power production in Norway comes from renewable energy, mainly from the hydro power. The total renewable energy production was 146.3 TWh in 2016. This energy is not used explicitly by Norwegian consumers but sold to European countries through the renewable energy sources (RES) directive 2009/28/EC (guarantee of origin agreement) [2]. By buying these guarantees, the European nations can fulfill their quota on electricity from renewable energy production.

Norway is an elongated country which offers a wide diversity of climate throughout the year. Although solar irradiance is lower than in countries closer to the Equator, the cold seasons in Norway give favorable conditions for photovoltaic (PV) systems. This is because the PV systems effectiveness becomes higher as the module temperature drops, together with the high reflections due to snow on the ground.

According to the national survey report from Holm [3], in terms of installed PV capacity, the use of PV systems in Norway today are mainly from grid-connected, reaching an all-time high with 10.4 MW_p new installed building applied PV (BAPV) in 2016. Together with the off-grid PV of 1.05 MW_p installed, the total increase of PV capacity was 366 % from 2015 to 2016 [3].

According to a newly publicized report from Solenergiklyngen [4], there was an increase of 59 % of new installations of PV systems in 2017 compared with the previous year. The total installed PV capacity at the end of 2017 has almost reached 45 MW_p. The development of PV systems in the recent years is shown in Figure 1.1.

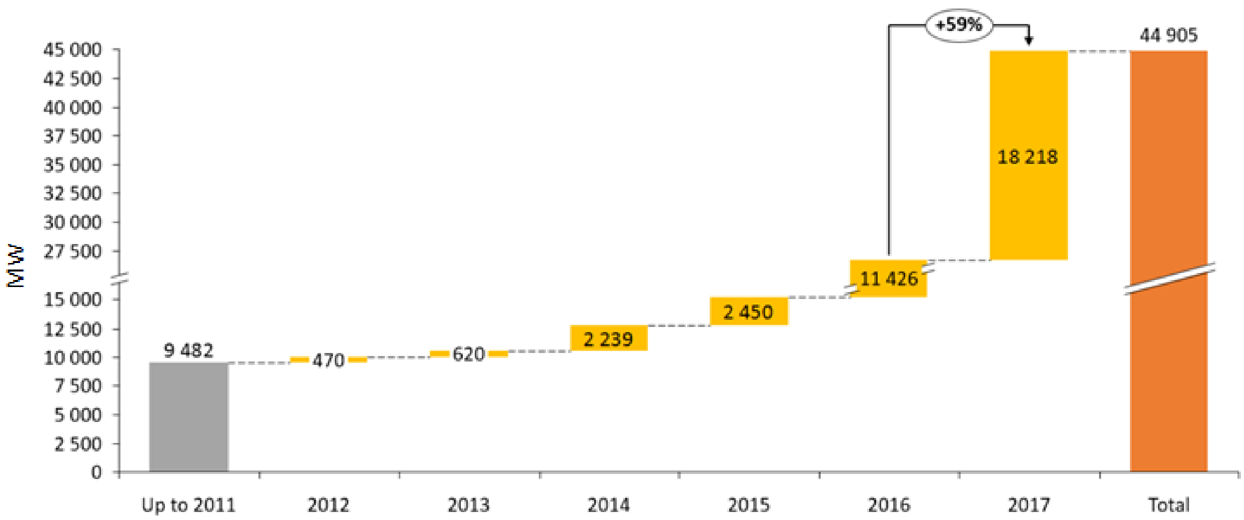

Figure 1.1: The development of new installed PV systems in Norway from 2011-2017, Figure 14 retrieved from [4]

As mentioned above, the majority of the installed PV systems in Norway are from BAPV systems. In the report from Holm [3], there are no registered installations on building integrated PV (BIPV) of 2016. The cost associated with having a BIPV is often the reason for the low interest. The additional costs of installing a facade of BIPV system contrary to glass facade is not that different, especially when the BIPV generates electrical energy. Because of limited information on BIPV, there seems to be misconceptions about the possibilities of its use.

1.2 Problem statement

In this master thesis, building integrated photovoltaic systems in different locations in Norway have been investigated and analyzed. This will give insight and contribute to knowledge about the BIPV performance in Norway, with particular emphases on facade systems. The systems will be examined by analyzing PV data, building integration, and total cost associated with the PV systems.

The main objective of this thesis is to implement a performance analysis of different BIPV facades, contributing to 1) BIPVNO project [5] and 2) the ongoing Task 15 from IEA-PVPS [6]. The master thesis provides data on the continuing development of a Norwegian database on BIPV. As the growth of new PV system installations is increasing rapidly [3], monitoring of BIPV performance and installations is crucial.

Another sub-objective is to evaluate the different solutions of technical building integration. This is achieved by examining the cross-sections of the building facade and how the configuration of the mounting details is solved. This will give insight into how the different PV systems utilize the air flow and the impact on the operating temperature of the PV modules.

The last sub-objective is to provide insight into costs associated with the PV system. The cost of the BIPV systems compared to standard facade cladding and distribution of cost directly connected to the BIPV system, such as planning, assembly, and modules prices.

Research questions

- Can PV systems become competitive to standard facade clothing?
- How does the performance of the individual PV systems compare to each other?
- What are the lessons learned so far, with regards to the operative PV systems?

1.3 Limitations

There are some important limitations to this master thesis as the access to available data on BIPV in Norway is limited. The data which has been available to analyze is for a limited time period, and the cost of BIPV is often embedded in the total building cost and sometimes not publicly accessible. The information on equipment used at the different sites is usually minimal. It is essential to be aware of these limitations because they may affect the quality of the data analyzed.

The performance analysis would have benefited from having on-site irradiance measurements, ambient temperature and direct current/alternating current output measurements in all locations available. This would have contributed to give a more accurately individual review and comparison of the analyzed cases. It is important to mention that there are uncertainties to the actual irradiance, seasonal variations, and the albedo effect (or reflection coefficient) on facades.

1.4 Thesis layout

- **Section - 1**
  The first section covers the introduction, with the problem statement, goals and limitations for the thesis.
- **Section - 2**
  Includes the theoretical information on PV system and factors affecting the PV system.
- **Section - 3**
  The section has a state of the art literature review of the development of historical and Nordic values of the performance ratio.
- **Section - 4**
  The method section gives the reader insight into how the data has been processed and collected. The method reflects on the workload and the technique for quantifying the results.
- **Section - 5**
  The cases analyzed, and results of the assessment are shown.
- **Section - 6**
  In this section there is an individual PV system comparison with simulated data and with each other, with subsequent discussion.
- **Section - 7**
  The conclusion brings back the research question and answers. The section includes recommendations on further work to the topic introduced in the thesis.

2 Theoretical background

The section contains the theoretical background on the solar radiation and the PV module characteristics.

2.1 Solar radiation

Section 2.1 to 2.1.1 contains information gathered from the book Applied Photovoltaics by Wenham et al. [7].

The solar radiation is created from the nuclear fusion processes at the sun. The energy from the extreme temperature at the core is absorbed by layers of hydrogen ions and re-radiated at sun's surface. The radiation at the surface is then emitted to the atmosphere. This gives rise to characteristic spectrum seen in Figure 2.1.

The path length radiation from the sun has to travel to get to the earth's surface is known as the air mass (AM), approximately calculated as:

$$AM = \frac{1}{cos\ \phi_z}, \tag{1}$$

where ϕ_z is the solar zenith angle, which is the angle between the sun and the point directly overhead.

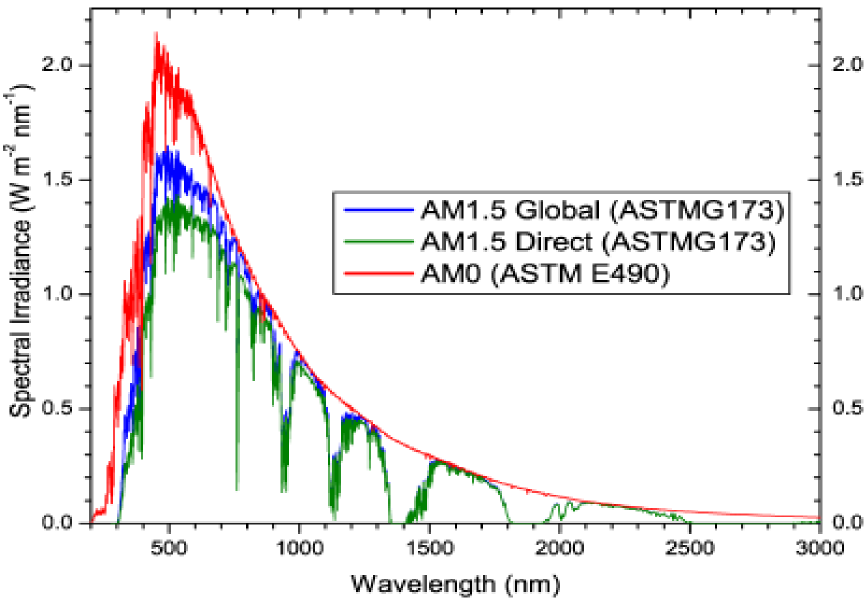

Figure 2.1: The spectral distribution of the radiation from the sun, figure retrieved from [8].

Figure 2.1 shows a typical energy distribution for air mass 1.5 spectrum, which is the one used with standard solar cell testing [7].

Before entering earth atmosphere, the spectral distribution of sunlight is defined as air mass zero (AM0). The power density at earth orbit is known as the solar constant, this value can vary slightly because of the earth's elliptic shape, but is commonly accepted to be $G_{sc} = 1366\ W/m^2$.

2.1.1 Direct and diffuse solar radiation

As the radiation from the sun travels through the atmosphere, it is scattered due to the Rayleigh scattering by molecules, dust particles and aerosols and absorption by atmospheric gases like CO_2, H_2O, O_3 and O. The scattering through the atmosphere reduces the radiation from the sunlight by roughly 30 % before it reaches the earth's surface. The sunlight reaching the earth's surface is divided into different components of radiation: the direct from the solar disk and the scattered sunlight from the sky, known as diffuse. The sum of direct and diffuse radiation is known as the global radiation.

2.1.2 Solar geometry

To understanding the radiation that enters earth's atmosphere, the position of the sun relative to the earth needs to be known. The most relevant angles for PV system characteristics are the tilt θ_{T} and azimuth angles θ_{a} of the PV modules, which are used to determine the solar irradiance angle S_β relative to the plane of array (POA) [9] [10]. In Figure 2.2 the angles used for positioning the sun is illustrated.

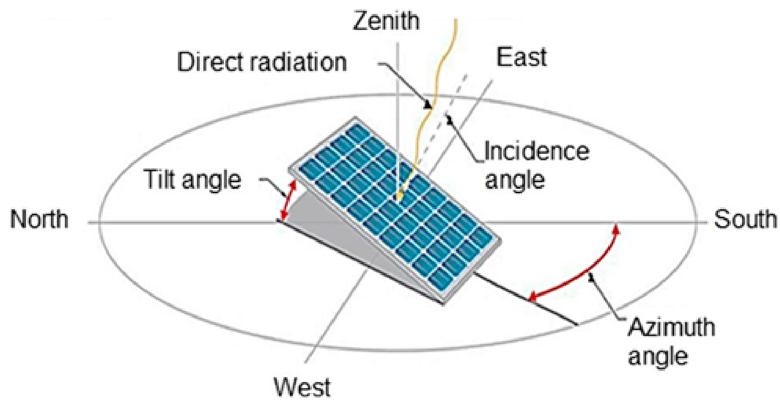

Figure 2.2: The illustration of a module with tilt angle θ_{T}, azimuth angle θ_{a} and incidence angle S_β, Figure 4 retrieved from [11]

2.2 The PV cell and its characteristics

This section will cover some typically used PV cell materials, how the output power is maximized, and different aspect of the changes in performance of a PV cell.

2.2.1 PV cell material technologies

This section is based on the 2017 annual trend report from IEA-PVPS [12]. The report divides solar cells into these categories: wafer-based crystalline either monocrystalline silicon (mono-Si) or polycrystalline silicon (poly-Si), compound semiconductor thin-film, and organic. The organic is still in the research and development phase. In countries with membership in IEA-PVPS, more than 94 % of the total production comes from crystalline silicon (c-Si), and 90 % of the worldwide production is from c-Si.

2.2.2 Maximizing the output power of the PV cell

When illuminated with sunlight, a single solar cell generates a voltage (V) and current (I) output. The desired voltage and current is obtained by connecting the cells in series and parallel, respectively.

The output of a solar cell is limited by the short circuit current (I_{sc}) and the open circuit voltage (V_{oc}) for a given irradiance, temperature and area. The maximum value of the product of I_{mp} and V_{mp} is known as the maximum power point (MPP). This could be graphically illustrated with the largest rectangle under the I-V curve, seen in Figure 2.3.

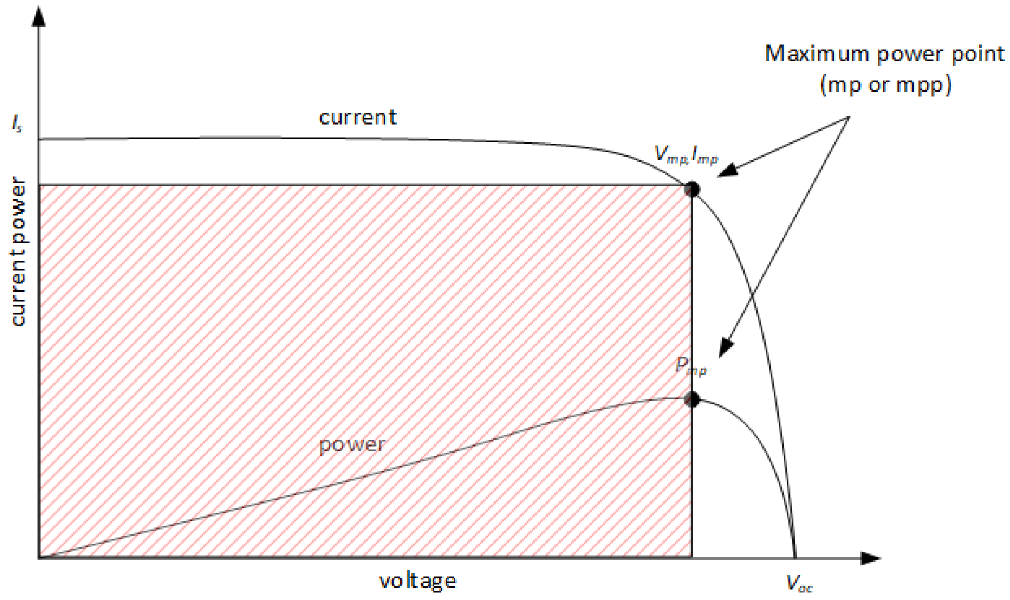

Figure 2.3: Graphically illustrated maximum power point, modification of Figure 3.5 in [7].

2.2.3 Effect of temperature and irradiation changes

The PV solar cell changes it performance with changes to the operating temperature, with the reference temperature as the standard test condition temperature 25°C ($\mathrm{T_{STC}}$), found in standard IEC 60904-3 [13]. The changes are affected by different variables, such as the ambient temperature, the encapsulation (making the PV cells into a module), and the intensity of the sunlight hitting the module [7].

Increasing the operating temperature above $\mathrm{T_{STC}}$ will reduce the performance of the PV cell, illustrated in Figure 2.4. On the other side, a lower operating temperature will increase the performance, with a typical temperature coefficient of a mono-Si cell of -0.40 %/K.

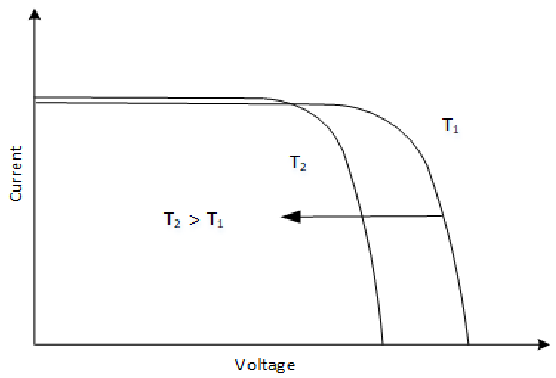

(a) The effect of increase in temperature

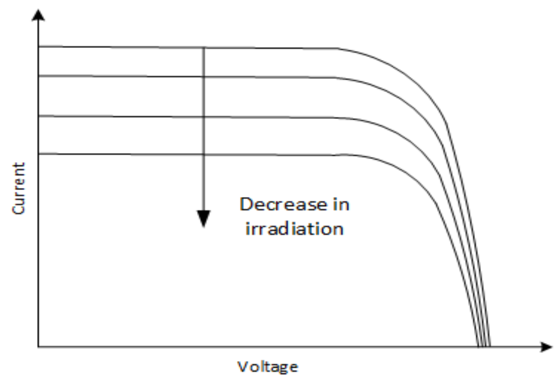

(b) The effect of decrease in irradiation

Figure 2.4: The effect of (a) temperature and (b) irradiation changes on a solar cell, modification of Figure 2 retrieved from [14]

In Figure 2.4 (a), an increase in the operating temperature from T1 to T2 shifts the I-V curve towards left. The effect is a minor increase in short-circuit current and a significant reduction in open circuit voltage.

In Figure 2.4 (b), it can be seen that if the operating temperature is held constant, a decrease in irradiation causes the IV-curve to step downwards as the short circuit current decreases with minor changes in the open circuit voltage [7] [14].

2.3 PV modules

The PV module is a construction of solar cells connected to a string, in series and parallel. Modules can then be connected in series to create a string. Connecting strings in parallel will result in an array [15]. Figure 2.5, illustrate the difference between cell, module, string, and array.

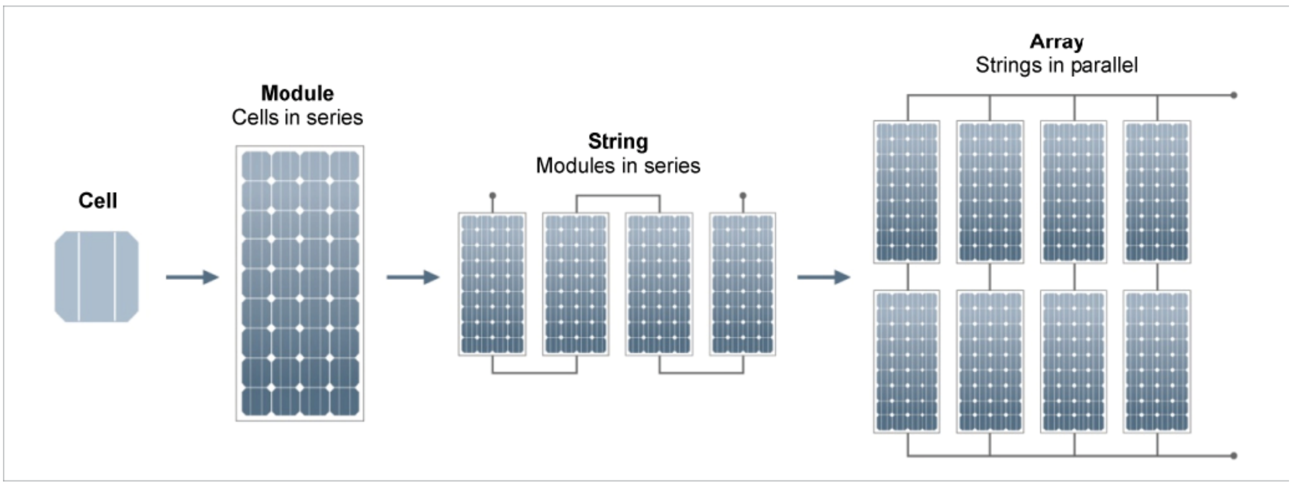

Figure 2.5: Illustration of cell, module, string and array. Retrieved from [15]

2.3.1 The structure of a PV module

The c-Si modules and thin-film modules are build up of different structures. The c-Si modules often have a transparent glass in front and on the back a glass or plastic material which encapsulates the wafer of c-Si in the middle. The thin-film differs from the c-Si modules as having the possibility of being flexible or fixed, as the modules are formed as a single substrate. The substrate is formed by encapsulating the PV cells, the front material is the same as the c-Si module [12]. In Figure 2.6, the different thickness layers of a c-Si module and thin-film copper indium gallium selenide (CIGS) module are illustrated.

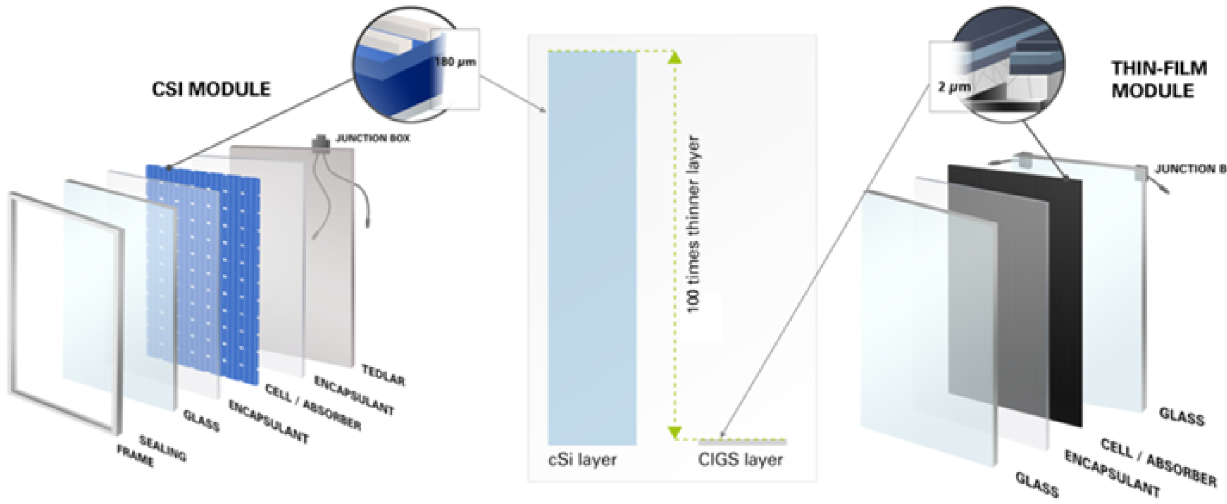

Figure 2.6: Thickness comparison between c-Si and CIGS modules, retrieved from [16]

2.3.2 Standard test condition and efficiency of PV module

The standard test condition (STC) is a test rating of the performance of PV modules [13]. The rating is performed in a laboratory where the cell temperature is 25°C, sunlight of 1000 W/m^2, and an air mass of AM1.5. Here, the maximum power of the PV modules is determined, known as the watt peak power of the module (P_{mpp}) [17].

The peak watt of the module under STC is then used to calculate the efficiency of the PV module [18]:

$$\eta_{\text{STC}} = \frac{P_{mpp}}{1000 \cdot A_m}, \tag{2}$$

where A is area of PV module, η_{STC} is the efficiency of the PV module, and P_{mp} is module peak power.

2.3.3 The temperature and irradiance matrix

The standard IEC 61853-1 [19] uses the outdoor sunlight to test the ratings of the PV module. The outdoor sunlight gives different temperatures and irradiance conditions, contrary to the STC. The rating method has a more similar exposure as the field operative PV modules [20]. As the test is of non-standard conditions, the uncertainty needs to be evaluated. According to the up to date publication (2018), the uncertainties are not yet known according to IEA-PVPS, Task 13 [21].

2.3.4 The PV module efficiency of different cell technology

The PV system is defined by the efficiency of the modules installed. The c-Si modules have an efficiency between 14 and 24.1 %. Depending on the cell technology used, thin-film modules can get an efficiency between 7 % for amorphous silicon (a-Si) and 18.1% for cadmium telluride (CdTe) [12].

2.4 Degradation rates and failure of PV modules and systems

The degradation rate is the reduction of the output power over time. Whereas there is no precise definition of failure, but typically referred to as degradation of 20 % of output power [22] [23].

According to Wenham et al. [7], the endurance of the encapsulation decides the operating life of a solar module. However, a range of degradation and failure modes have been observed [24].

National Renewable Energy Laboratory (NREL) [22] did a comprehensive literature review of degradation rates. The review included the summary from the last 40 years of literature. The report divides the gathered literature into pre and post year 2000.

For the mono-Si modules, the summarized post literature gives a degradation rate of 0.36 %/year for the module and 0.23 %/year for the system. The amount of literature is significantly lower for the thin-film technologies than the c-Si. Nevertheless, the post degradation rate is 0.96 %/year for the CIGS module and 0.02 %/year for the system.

For all literature summarized, independent of the technology used, is a degradation rate of 0.8 %/year for the module and a median of 0.5 %/year for the system.

2.5 The grid connected PV system

The PV system is either grid-connected or off-grid. In the grid-connected, the alternating current is distributed either to the electrical grid or directly to the end-user. The off-grid connected system, known as the stand-alone system, uses batteries to store the electrical energy. A third alternative is the hybrid system which combines the electrical grid connection with a battery bank used in the off-grid [7].

The PV conversion is the absorption of photon energy from the sunlight hitting the PV cell, generating an electric charge of electrons. The energy provided by the photons dislocates electrons from their electron shell, and the freed electrons generate an electrical charge [25].

Figure 2.7 illustrates a grid-connected photovoltaic system with the sun as the energy source. The PV array absorbs the radiation from the sun (P_{sun}), scattered throughout the atmosphere. The PV array consists of multiple solar modules, which utilize the photon energy conversion to generate an array output direct current (DC) power (P_{DC}). Cabling provides the passage to the inverter, which contains a direct to alternating current converter. The conversion gives an net energy output alternating current (AC) (P_{AC}), distributed to the connected end system type [26] [27].

There are system losses from the DC cabling, the conversion process, AC cabling and the distribution [28].

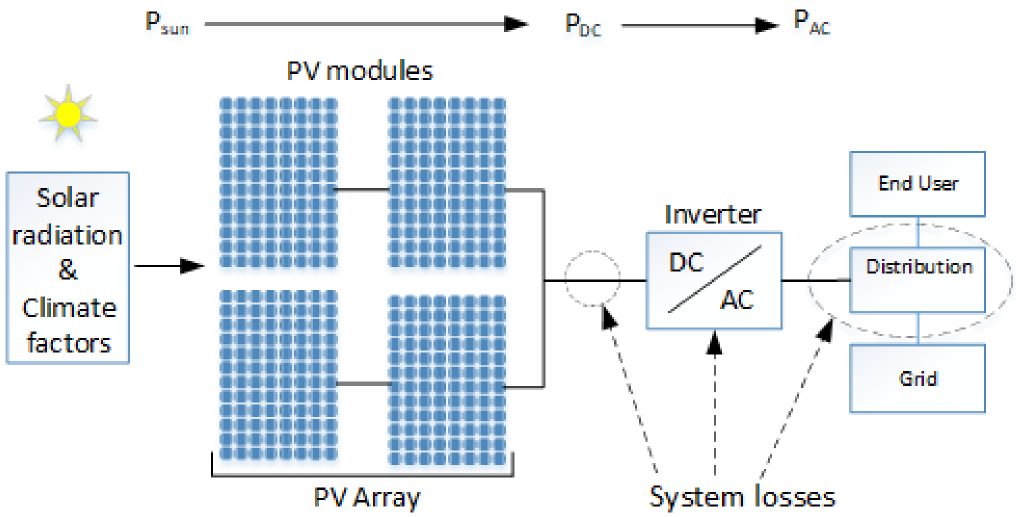

Figure 2.7: Illustration of how grid-connected PV system works, based on Figure 1 in [26]

2.6 Balance of system components

The balance of system (BOS) components includes inverters, batteries, wiring, transformers and other system components besides the PV module itself [7]. These components have losses and contributes to the overall efficiency of a PV system. The information in this section is retrieved from IEA-PVPS Task 13, Subtask 2 [28].

2.6.1 DC and mismatch losses

The operating voltage is controlled to maximize the PV system power output, usually by an inverter. The PV array and inverter is linked through DC cabling. The DC cabling has losses due to the resistance in the wiring. The losses depend on the cable length, cross-section, and temperature.

When the PV modules are in a serie-connected string, the current is determined by the module with the lowest current. As the modules need to operate at the same current, the module with the lowest current limits the remaining modules. This causes mismatch losses in the PV system, often caused by partial shading, module inconsistency, and uneven soiling.

2.6.2 Inverter conversion efficiency

The primary objective of the inverter is to convert the DC power to AC power, by using converters. The inverters have different efficiency ratings depending on the manufacturers, often in the region from 97 % to 98 %. The variation of a typical inverter efficiency as a function of output power and operating DC voltage is illustrated in Figure 2.8.

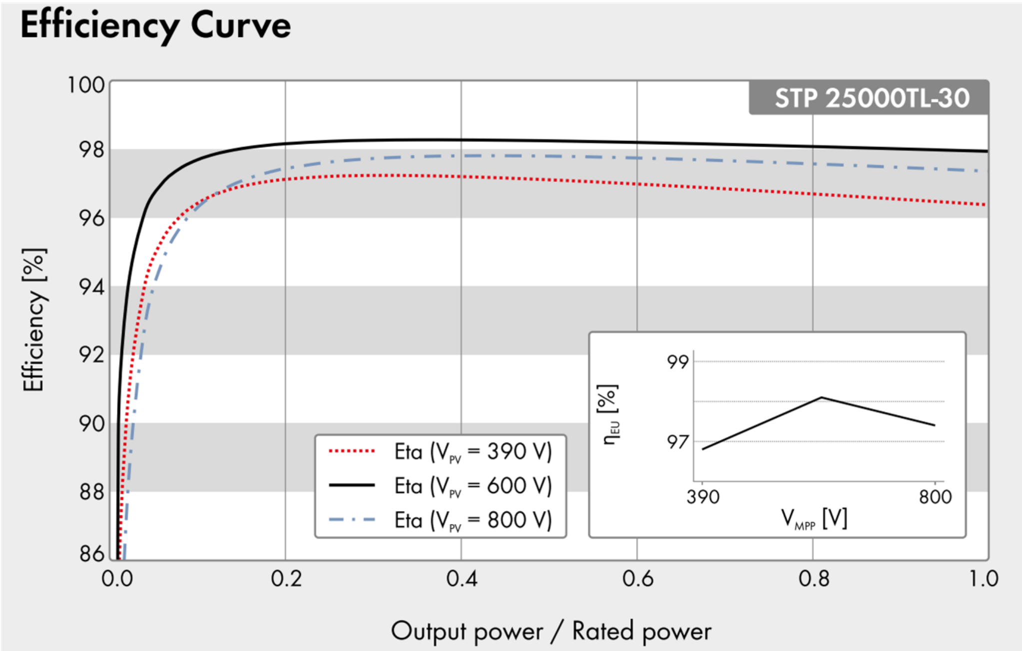

Figure 2.8: The efficiency of a SMA inverter STP 250000TL-30 [29]

2.6.3 AC cabling and losses

After the inverter has converted the DC power to AC, the power is delivered to a utility meter connected through AC cabling. In residential PV systems, losses with AC cabling are neglected due to the meter, and the inverters are directly adjacent to one another.

According to Reich et al. [30] common standard assumptions of fixed cabling losses are values of 1.5 % for DC-wiring and 1 % for AC cabling at maximum rated power.

2.7 The albedo effect

The radiation which is reflected by the sunlight hitting the surface is known as the reflection coefficient and often referred to as the albedo effect. The coefficient is between number 0 and 1, depending on the surface material. The albedo effect is an essential part of the evaluation of a PV system, especially for the facade systems. Some selected surface values of the albedo effect can be seen in Table 1, were high number gives higher diffuse radiation on the PV modules [31].

Table 1: The coefficient of the albedo effect, parts of Table 2.1 in reference [31]

Surface	**Albedo (%)**
Snow	
Fresh	80-90
Melting Snow	40-60
Sea ice and old snow	30-40
Dry land	
Concrete	17-27
Sand	30-35
Asphalt	5-17
Grass	18-25

2.8 The air-gap

The air-gap is the distance between the outer building construction barrier to the backside of the PV module. According to Kalogirou et al. [32] on air flow of BIPV panels, the most significant effects on the panel temperature is the wind velocity and the air-gap. In Figure 2.9 the effect of different air-gap distances on the panel temperature, with a wind velocity of 0.2 ms^{-1} are given [32].

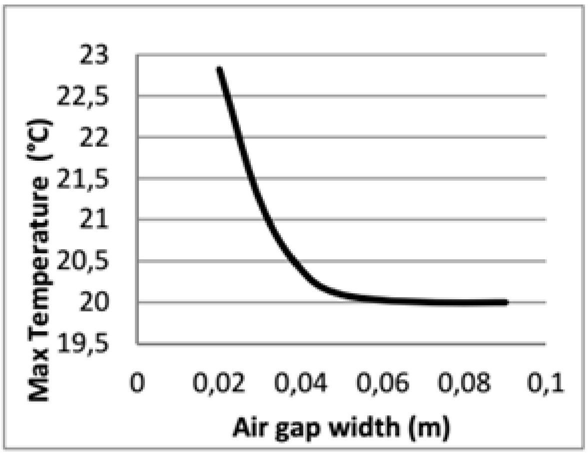

Figure 2.9: How the air-gap effects the module temperature, measured with a wind velocity of 0.2 ms^{-1}, Figure 7 retrieved from [32]

2.9 PV system performance parameters

For quantifying the performance of a PV system, some parameters have to be introduced. This section uses the standard definitions from IEC 61724 [33] on PV system performance. The equations below can either be used for evaluating the DC or AC output. The energy or power production can either be measured before the inverter (DC) or after (AC). The PV array area can also be seen as the active PV area.

2.9.1 Specific yield

The specific yield is quantified as the standard metric for analyzing a system and is often the first indication used for evaluating the system value [34]. The specific yield is the energy generated by the PV array divided by the installed rated output of the array P_0. The specific yield (Y_A) is the array energy output per kW of installed capacity:

$$Y_\mathrm{A} = \frac{E_\mathrm{A,d}}{P_0} \ [\mathrm{kWh/kW_p}], \tag{3}$$

where $E_\mathrm{A,d}$ is the measured AC energy production, and P_0 is the nominal DC power.

2.9.2 Performance ratio

The performance ratio (PR) is a parameter used to evaluate the inverter inefficiency and wiring, mismatch, and other losses when converting from DC to AC power. The effect of losses is also affected by PV module temperature, incomplete use of irradiance by reflection, soiling, or snow. System downtime and component failures also make an impact.

Before quantifying the PR, the final PV system yield Y_f needs to be evaluated. This is the portion of the total energy produced on the PV plant supplied by the specific yield of the PV array.

$$Y_\mathrm{f} = Y_\mathrm{A} \cdot \eta_\mathrm{LOAD}, \tag{4}$$

where η_LOAD refers to load percentage of the measured PV array to the total PV system and Y_A is the specific yield given in Eq.(3).

The reference Y_r yield is the total in-plane solar irradiation (G_I) divided by the module's reference in-plane irradiance ($G_\mathrm{I,ref}$). Therefore, the reference yield is the number of peak sun-hours. Reference yield is used when calculating PR.

$$Y_r = \frac{G_\mathrm{I}}{G_\mathrm{I,ref}} \tag{5}$$

The PR is the specific array yield divided by the reference yield, represented by Eq. (6):

$$PR = \frac{Y_\mathrm{f}}{Y_\mathrm{r}} = \frac{Production\ energy}{Expected\ energy} = \frac{Production\ energy}{\sum[I \cdot \frac{Peak\ Power}{1000}]} \tag{6}$$

Where Y_f is given in Eq. (4) and Y_r is given in Eq. (5)

2.9.3 System efficiency

The efficiency of the system is determined by dividing the energy output on the irradiation hitting the area of the PV array.

$$\eta_{\mathrm{AC}} = \frac{E_{\mathrm{A,d}}}{G_{\mathrm{I}} \cdot A_{\mathrm{m}}} \cdot \eta_{\mathrm{LOAD}}, \tag{7}$$

where A_{m} is the active PV module area.

2.9.4 Uncertainties of measuring devices for solar radiation

There are mainly used two measuring senors for detecting the solar radiation: the pyranometer and the reference cell.

The pyranometer has a black surface that is heated when sunlight hits it, and it responds to the temperature changes. The pyranometer sends out a voltage signal which is proportional to the irradiance measured. The pyranometer design is such that every angle of sunlight is permitted, the distribution is equally flat to all energy photons hitting the black surface. The output is held steady when there are changes in the ambient temperature and shifting sky conditions [35] [36]. The thermal response time is typically 5-18 seconds with rapidly changing irradiation.

According to a World Meteorological Organization report from 2008 [37], a good quality pyranometer has an achievable uncertainty on hourly exposure of 8 % and total daily of 5 %. For stations with special facilities and staff, a high-quality pyranometer could achieve an hourly uncertainty of 3 % and a total daily uncertainty of 2 %. The values are obtained with 95 % confidence level.

The PV reference cell values the irradiance by the number and spectral distributing of the photon current generated by the reference cell. The current is measured with a small resistor which measures the voltage across it [35]. The uncertainty in PV reference cell depends on the PV cell technology used.

Dunn et al. [38] published a paper on the comparison of pyranometers vs. PV reference cells. The uncertainty analysis was performed on a clear sky day with the two different devices beside each other. The daily result of the expanded uncertainty for the pyranometer was 5.29 % and 2.44 % for the reference cell. The expanded daily uncertainty corresponds to a confidence interval of 95 %.

Using the same approach and setup as Dunn et al. [38], researchers from NREL [36] did a daily comparison between the pyranometer and reference cell on the uncertainties on the broadband irradiance. The broadband irradiance is the total amount of solar radiation and includes photons from the spectrum which the PV cell cannot utilize. The result on a clear sky day with 1000 W/m^2 and 95 % confidence interval, was equal for both devices with an approximated value of 4.3 % [36].

3 State of the art in PV system performance

This section starts with a historical development of PV performance in Europe, with annual performance ratio and specific yield as methods for quantifying performance. Then the development of PV systems in Nordic countries with emphasis on Norwegian systems is evaluated. The focus of this section is to evaluate BIPV performance in Norway. The findings will be essential to get some statistical data on expected performance in this type of climate.

3.1 Development of PV performance internationally

As a part of the IEA Photovoltaic Power Systems Programme Task 2 [39], U. Jahn et al. [40] compared PV modules installed before and after 1995. Both monthly and annual data was analyzed from a total of 334 grid-connected PV systems in 10 European countries and Japan. The results showed an annual PR of 0.65 on systems installed before 1995 and an increase to 0.70 on those installed after 1995. According to the authors, this development is due to three possible reasons; more realistic ratings, more efficiency inverters, and higher system availability.

A later study by Reich et al. [30] in 2010 evaluated 94 PV systems located in Germany. They found that annual PR was between 0.70 and 0.90, with a median PR of 0.84. The results showed that 50 % of the modules had a PR larger than 0.83 and one-third of the systems had a PR larger than 0.85. This paper's object was to evaluate if it is realistic with a higher PR than 0.90. Even though none of the measured systems had a PR larger or equal to 0.90, the authors concluded that with improvement related to mechanical losses and the absence of shading, PR values of 0.90 are realistic.

In 2012, Leloux et al. [41] published a study on the performance of 1635 residential PV systems in France. The authors found that after a mean exposure time of 2 years, the mean PR value was 0.73 and the average annual specific yield was 1163 kWh/kW$_p$.

Leloux et al. [42] also studied operational data of 993 residential PV systems in Belgium. Though, through the year of 2009, only 158 PV system owners reported monthly production. This resulted in a net average annual specific yield of 902 kWh/kW$_p$. The authors also did a performance assessment of the 352 PV systems that provided more than 12 months of data between January 2009 and August 2010. The analysis resulted in a PR of 0.78 after an average exposure time of 2 years.

The estimations on in-plane irradiation are done with solar radiation models. This is reported to give some uncertainty in their findings, as ideally on in-plane irradiation data should be collected from installed pyranometer or reference cell.

In a report from IEA-PVPS Task 13 published in 2014, Nordmann et al. [43] analyzed 347 PV systems in the Netherlands by using web-scraping techniques. The web-scraping technique scans the net for requested data input, collects, and organizes it in databases.

The analysis showed an average PR of 0.78 ± 0.16 in 2012 and 0.78 ± 0.14 in 2013. In the same period, the average annual specific yield was 865 kWh/kWp in 2012, with an increase to 874 kWh/kWp in 2013. There were noticeable differences in the PR between summer and winter.

The winter season had an average PR value of 0.821 in contrasts to summer with 0.732. These seasonal variations are expected when not using temperature corrected PR.

3.2 Development of PV performance in Nordic countries

As a collaboration between Norway, Sweden, and Finland, Kleven et al. [44] studied the performance of three solar tracking PV systems, one in each country. The first system, a PV power plant of two dual tracking systems in Piteå, Sweden had a total system specific yield of 1288 kWh/kW_p in 2012, 1520 kWh/kW_p in 2013 and 1477 kWh/kW_p in 2014. In the analysis of yield, the values for kW_p installed are obtained from supplier testing the cells under (STC) before delivery.

The the second system, a solar tracking system, located at the University at Tromsø, had not sufficient data for performing a performance analysis. The system had 606 days of downtime between from 2010-2014.

In the third location in Tervola, Finland, there was an estimation of the annual specific yield of 1350 kWh/kW_p in 2013 based on measured values from February to November. The PV modules studied by Kleven et al. [44], are of different technologies and for research and development purposes.

Mutungi [45] analyzed two different PV systems in Finland as a part of a master thesis at the University of Jyväskylä. The poly-Si PV system had an average PR of 0.83 from 2010-2012. A heterojunction with intrinsic thin-layer (HIT) PV system at Saarijävi had a PR range 0.78-0.89 (2006-2012).

In 2015, Imenes et al. [46] published a paper on the performance of a PV system in Kristiansand. The PV system contains eight inverters connected to multi-crystalline silicon (m-Si) modules and one with micromorphous silicon thin-film. In 2013, the system had an annual specific yield of 925 kWh/kW_p and PR of 0.70. The following year, the system had an increase in both annual specific yield and PR to 951 kWh/kW_p and 0.79, respectively. The low PR in 2013 was reported to be due to start-up phase problems.

To assess the performance of BAPV and BIPV in Norway, Imenes [47] analyzed thirteen PV systems in 2016. The BAPV system located at Agder Energi had an average specific yield of 937 kWh/kW_p and PR of 0.74 over the time-period of four years. Another BAPV system at ASKO Vestby had a specific yield of 810 kWh/kW_p and PR of 0.86. The authors empathize that the results in this paper are preliminary, as larger time series are required for a more thorough analysis.

As part of a master thesis Camout [48] studied a PV plant of multi-crystalline cells located at Øker in Oslo and found an annual PR and specific yield, 0.81 and 691 kWh/kW_p, respectively (from 1 May 2016 to 30 April 2017). The PV plant is equipped with 25 string inverters. The string inverters are divided into sub-systems classified with installed PV power. For almost all of the 25 sub-systems, there is an average decrease of 7 % from PR to temperature corrected PR.

In Åsheim's master thesis [49] from Norwegian University of Science and Technology (NTNU), there was an analysis of a BIPV system of poly-Si, located at Evenstad, Norway. The results from the analysis showed an annual specific yield of 899 kWh/kW$_p$ in 2014, 887 kWh/kW$_p$ in 2015, and 880 kWh/kW$_p$ in 2016.

In Table 2, some of the results reviewed in this literature review section are listed.

Table 2: Some results from reviewed Nordic PV systems

Name/location	**Type**	PR	Annual Specific Yield [kWh/kWp]	Year measured	Reference
Saarjàrvi,Finland	BAPV (free-standing)	0.78-0.89	-	2006-2012	[45]
Jyváskylá,Finland	BAPV (free-standing)	0.81-0.85	-	2010-2012	[45]
Piteå, Sweden	dual tracking	-	1288-1520	2012-2014	[44]
Tervola, Finland	dual tracking	-	1350	2013	[44]
Kristiansand, Norway	BAPV	0.70-0.79	925-951	2013-2014	[46]
Øker, Oslo (Norway)	BAPV	0.81	-	2016-2017	[48]
Evenstad, Norway	BAPV	-	887-899	2014-2016	[49]

If comparing the systems mentioned in Table 2, there should have been more detailed data on PV technology, the angle of installation, and preferably variations in annual irradiation. The purpose of the Table 2 to give a general overview of research results within Nordic PV systems.

4 Method

This section presents the method used in evaluating the different cases, including how the collection of data is performed and the evaluation of efficiency and costs.

4.1 Equations used to evaluate the PV systems

For performance assessment of the PV system case study in this master thesis, several metrics are used to analyze it. Those are specific yield (Eq. 3), PR (Eq. 6), inverter efficiency (Eq. 8), and the PV system efficiency (Eq. 7). Further used equations are listed below. All of the listed parameters are essential for quality analysis.

The inverter efficiency η_{inv} is calculated by the dividing the net AC output power (P_{AC}) by the DC output power (P_{DC}).

$$\eta_{inv} = \frac{P_{\mathrm{AC}}}{P_{\mathrm{DC}}} \tag{8}$$

For evaluating the cost per area of PV modules installed, the total cost of the PV system is divided by the total area covered by PV modules.

$$\text{Cost per area of module} = \frac{Total\ \mathrm{C}}{Total\ A_{\mathrm{m}}}\ [\mathrm{NOK/m^2}] \tag{9}$$

Where C is the total cost of the PV system, and A_{m} is the area covered by PV modules. This equation is relevant for the building sector, as they often use cost per square meter as the reference.

The cost of a PV system is also evaluated as the cost per installed PV capacity ($\mathrm{W_p}$), which is mainly used as a reference in the PV community. The equation is shown below.

$$\text{Cost per installed watt peak} = \frac{\text{Cost per area of module}}{W_{\mathrm{p}}} \cdot \text{Total } A_{\mathrm{m}}\ [\mathrm{NOK/W_p}] \tag{10}$$

4.2 Data collection and quality

The first part of the case analysis was to evaluate the PV system performance and system value. In assessing the performance and system values, data on energy production, irradiation, and DC/AC power was downloaded from the different online monitoring software systems. The data was gathered and sectioned by the numbered inverter with the installed capacity.

Data has been collected from two different PV system monitoring programs depending on the case, which is Sunny Portal [50] and IBC SolPortal Pro [51].

Sunny Portal is a web based PV monitoring system, where data produced by the PV plant is monitored. The system has a user-friendly design and offers multiple sections of information and visualizations of the PV system. The professional packaged, provides 15-minutes data resolution, live data, and graphs. The system can be connected to different sensors such as irradiation, battery status and so on. Screen shot of the Sunny Portal main web page can be found in Appendix H.2 .

The PV monitoring program from IBC, SolPortal Pro has multiple features and provides live data monitoring of yield, AC/DC, voltage, and module temperature in addition to visualizations. Especially the feature where different tables of chosen parameters can manually be generated is useful. The tables can be downloaded to CSV files. The program provides resolution of 5-minutes data. Screen shot of the SolPortal Pro main web page can be found in Appendix H.1.

The data retrieved from the different web monitoring software systems has been based on individual inverters on hourly data series. The data series have been on energy production and mean power production. Where irradiance data is available, the data has been used to evaluate the monthly values and performance ratio. The monthly values were plotted in graphs, showing the development of combined inverters and individual inverter. In the cases with both facade and roof installation, a monthly comparison was plotted. Months without full data series were marked in the figures in the different sections.

Where there are PV modules both on the facade and roof, the quality of the data retrieved can be verified better than when PV modules are only on the facade. Missing data series and the available time period of data collection and evaluation have made some constraints on the results in this master thesis. Since there are few installed BIPV systems in Norway, reference on expected yield and performance is limited.

Information retrieved on building technical details and different technological configurations on the various PV systems has been done with e-mail communication and telephone interviews. The technical solution on especially the mounting details is often sensitive and confidential. Nevertheless, Solidworks and Microsoft Visio have been used to draw parts of the structural details on the mounting of the modules and the build-up of glass-glass modules, where used. Through personal communication with building professionals, the drawings presented in this master thesis have been approved.

In the cost analysis sections of this master thesis, the economy is evaluated by calculating the cost per area of PV modules (Eq. 9) and the cost per installed watt peak (Eq. 10). The individual values from the different cases were used to compare the costs. Also, through personal communication and online searches, the economic cost was collected. Absolute numbers were not granted, nevertheless the total cost, and in some case the distribution of cost, was provided.

As only one of the PV facade systems had an irradiance sensor installed, simulations on the expected monthly specific yield were done in PVGIS [52]. PVGIS is a web-based simulation program, where the particular location, capacity installed, azimuth angle, and tilt angle of the PV system is entered as input. The program then simulates irradiance and energy production on a monthly basis. These values were used to compare the system values for the individual cases.

5 Cases and results

This section contains the detailed description and analysis of the chosen case studies consisting of buildings with grid-connected vertical south oriented BIPV and BAPV systems.

The information and pictures used in Sections 5.1-5.7 are retrieved from interviews performed by Teknova [53] [54] [55], as part of the research project "Building integrated photovoltaics for Norway" (Norwegian Research Council project number 244031). In addition interviews with Kiwi Dalgård and Kiwi Fieldset was performed by the author [56]. Further used references are cited in the specific section.

5.1 Solsmaragden

Union Eiendomsutvikling is the owner of Solsmaragden, an office building located in Drammen on the south side of Drammenselven. The company wants to present itself as an innovating company with focus on the environment image to attract tenantries. The building has met the requirements of the passive house standard NS 3701 [57]. PV panels are mounded on the roof and facade. The BIPV system was developed with the intention to make the building aesthetic an the focus was not the economic gain from the PV production. As can be seen by the adding of an extra layer of green printed glass, which reduces the energy production. The Belgium supplier ISSOL did the system design of the facades, the company FUSen was adviser and inspector, the project designers were Asplan Viak, and the installer was a local entrepreneur.

5.1.1 System description

The PV system was commissioned in January 2016 with a total area of 1534 m^2, installed PV power of 181.97 kW_p and 13 operating SMA [29] inverters. Figure 5.1 illustrates the PV facades and roof layout with two different system types, BIPV (5.1a) and BAPV (5.1b).

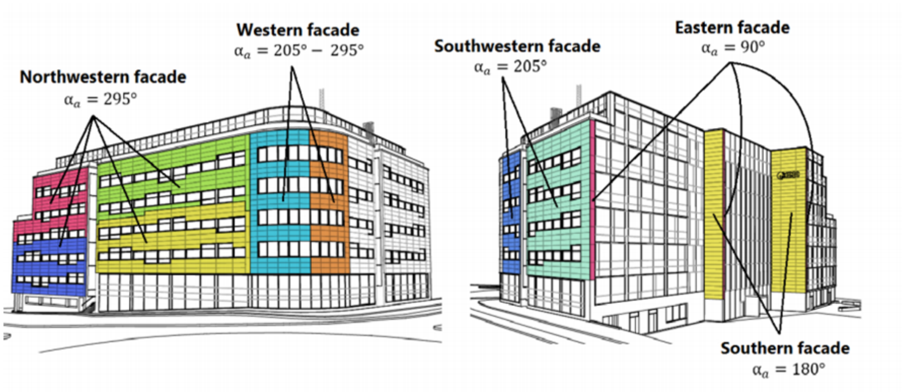

(a)

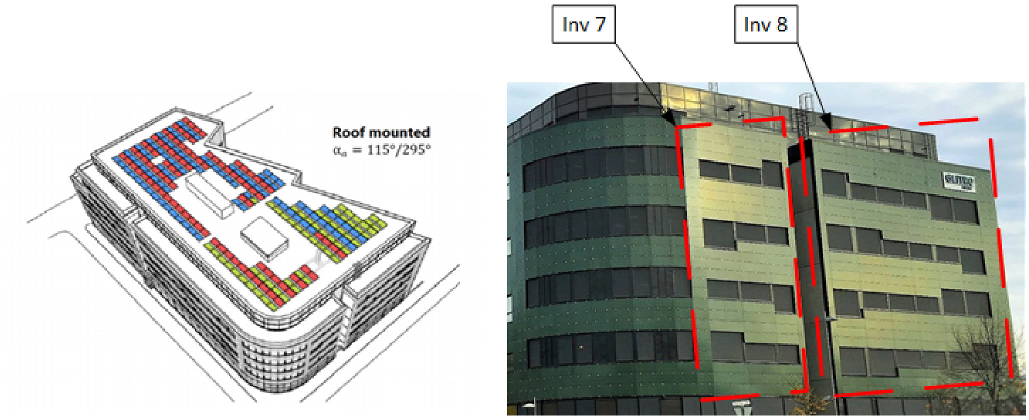

(b)

Figure 5.1: (a) The different BIPV facades of Solsmaragden (b) The flat roof of east/west BAPV installation and the south oriented facade with inverter seven and eight retrieved from Haumann [58] and with original sketches from Christine Wangsnes, Union Eiendom [59]

On the flat roof, a traditional east/west BAPV system is mounted, with a tilt angle of 10°and standard mono-Si modules. The BAPV has an installed capacity of 67.8 kW$_p$ over an module area of 388 m^2. On the facades, there are BIPV with standard mono-Si solar cells with green printed glass, with a total module area of 1146 m^2 and installed capacity of 114.2 kW$_p$. There are PV modules on the south, east, and the west facade. Detailed information on the south oriented facade is listed in Table 3. In addition, there are a few on the north facade but they are not connected (only visual). On the right-hand side of Figure 5.1b the two inverters on the south oriented facade are illustrated with red rectangles. The string design can be seen in Appendix A.1.

Table 3: System description of the south oriented facade at Solsmaragden

System description of the BIPV system on the Solsmaragden south facade	
Installed capacity	27.09 kW_p
Area:	267.5 m^2
Tilt angle	90°
Orientation	205°
Inverter properties	
Inverter type	Sunny Tripower 6000TL and Sunny Tripower 15000TL
Number of inverters	2
European efficiency	97.4 % and 97.8 %
Topology	Transformerless
Nominal AC output power	6000 W/15000 W
DC/AC ratio	1.27/1.30
Module characteristics	
Module type	Cenit 220 Model-70/90/130/150-6112
Number of modules	62/138
Module design	Green printed, glass-glass
Cell technology	mono-Si
Module power	From 70 W_p to 150 W_p
Weight module	From 18 to 30 kg unframed
Module size	From 1670x590x8 mm^3 to 2490x590x8 mm^3
Module efficiency	From 7.89 % to 10.80 %
NOCT	N/A
Temperature coefficient of P_{mpp}	-0.391%/°K

5.1.2 Building technical integration

The technical solutions used on the facade, is taylor-made to this specific building. The idea of the design was to create an outstanding environmentally friendly architecture. In Figure 5.2, the custom-made green printed glass-glass module used on the BIPV is shown. According to ISSOL [60], the green printed glass gives 83 % yield compared to non-printed glass.

Figure 5.2: Structure of the green printed panel from ISSOL

In Figure 5.3, an illustration of the cross-section at Solsmaragden is shown. The air-gap between the wind barrier and the green printed module is 60 mm. The cladding is ventilated, with the outside air as the source. The specially made modules caused a need for extra reinforcement to the outer wall because of the added weight. The modules also resulted in a more complex string design than ordinarily PV systems.

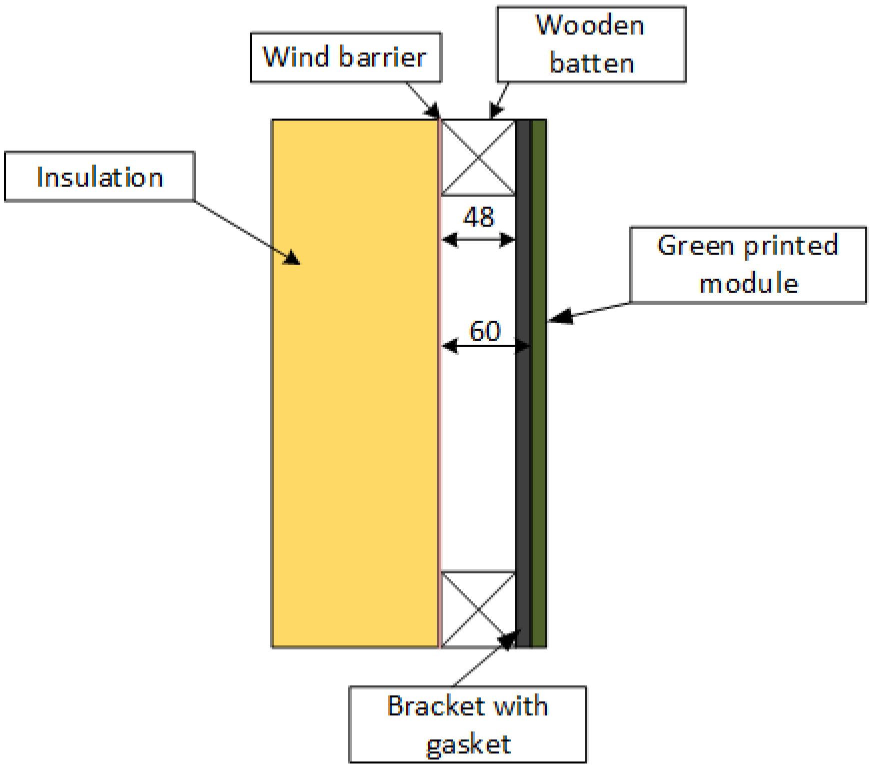

Figure 5.3: Cross-section of the south facade on Solsmaragden, drawn by the author, approved by Gregertsen at Union Eiendomsutvikling [61]

The PV modules are screwed on the battens of the outer wall, using standard glass clamps. The fastening solution with glass clamps on Solsmaragden is shown on the left-hand side of Figure 5.4b and a standard glass clamp on the right-hand side. Behind the PV modules, there is a moisture resistant undercoat.

(a)

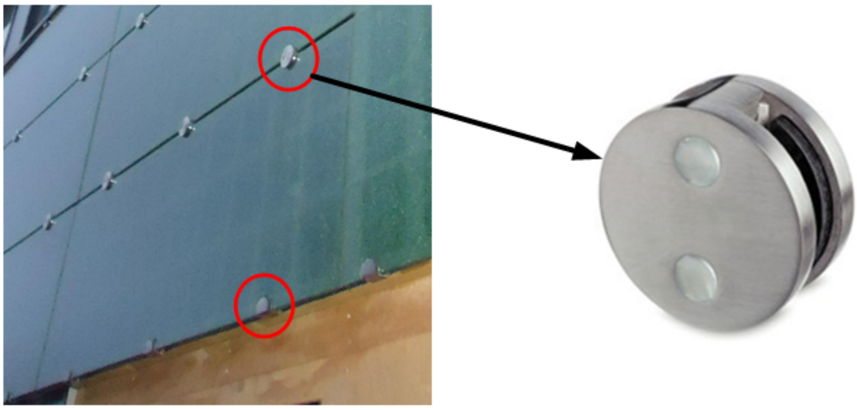

(b)

Figure 5.4: (a) Ongoing installation on the facades at Solsmaragden (b) Picture of the glass clamps used to fasten the PV modules to the batten and a picture of a typical glass clamp, retrieved from [62]

5.1.3 Economy

The total added cost for the BIPV system was 3.4 million NOK. The calculation is done with BIPV as a facade material, with the subtraction of cost associated with traditional facade materials. The total added cost of the BIPV equals 1.4 % of the total cost associated with the building. There is no information available on the budgetary allocation of cost on the BIPV.

The solution with facades covered with colored solar panels released economical support from ENOVA of 1.5 million NOK, as a part of their program "New technology for future buildings" equivalent to 44 % of the total added cost of the BIPV. Including the support from ENOVA the total added cost for the BIPV is reduced to 1.9 million NOK. ENOVA is owned by the Norwegian Ministry of Climate and Environment, with the ambition to reduce the greenhouse gas emissions, strengthen the supply support of energy and contribute to the development of new energy and climate technology [63].

The added cost per installed capacity for the BIPV facade excluding the support from ENOVA is calculated to be 29.8 kr/W_p, by using Eq. 10. The added cost per module area was 2967 NOK/W_p.

More details on the calculations can be found in Appendix B3.

5.1.4 Performance

Table 4: Measured data on Solsmaragden

Solsmaragden	Description	Data resolution	Time period
Weather data	Irradiance, pyranometer on the south facade	Hourly	Oct 2016 →
Production data	AC power	15-min	Jan 2016 →

This section covers the south facade of the building. The original analysis made by the system installer of the anticipated outcome of the PV energy production was 55.5 MWh for the total BIPV system and 50.5 MWh energy production on the BAPV system [53]. The supplier (ISSOL) performed the simulation on the BIPV, and the roof is estimated using IBC's solar calculator, according to the master thesis of T.Haumann [58].

The south facade had in 2016 an annual production of 16.44 MWh resulting in a specific yield of 607 kWh/kW$_p$. In 2017 the energy production was 15.48 MWh, which gives a specific yield of 560 kWh/kW$_p$.

There are days of missing production data (N_p) for both years, with N_p=34 days in 2016 (22 days in January, 12 days in April) and N_p=16 days in 2017 (15 days in January, 1 day in February). In Figure 5.6 the distribution of the data available are plotted on monthly basis.

From Figure 5.5, which compares the monthly development of specific yield of the roof installation. It can be seen that the distribution from February to October is more even for the facade. The annual specific yield of the BAPV system on the roof was 730 kWh/kW$_p$ in 2016 and 710 kWh/kW$_p$ in 2017. Comparing the specific yield of the south facade and the BAPV on the roof gives a yield of 83 % in 2016 and 80 % in 2017 for the south facade, with the annual specific yield of the BAPV system as the reference.

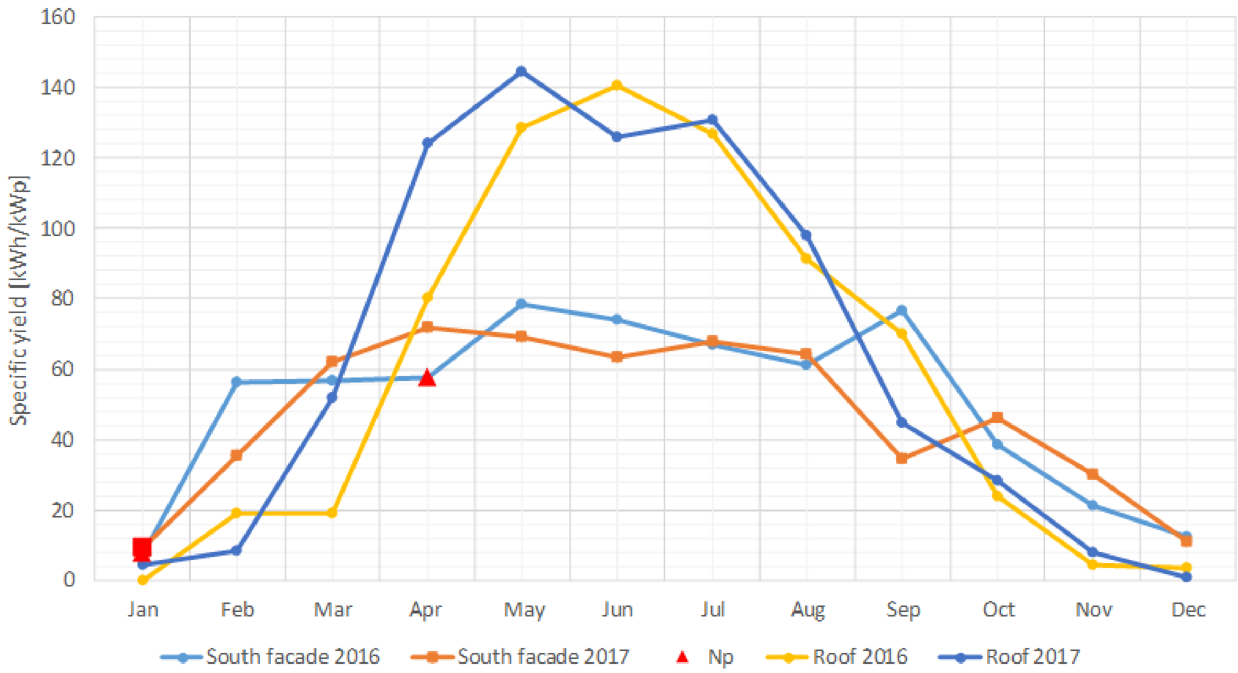

Figure 5.5: Specific yield comparison between the south facade and roof on Solsmaragden

The first data of irradiance was logged in October 2016, which means there is only one complete year of irradiance data available for analysis. In Figure 5.6, the specific yield of the south facade combined with the irradiance measured is plotted. In 2017, there are 27 missing days of data on irradiance N_I=27 (15 days in January, 12 days in February).

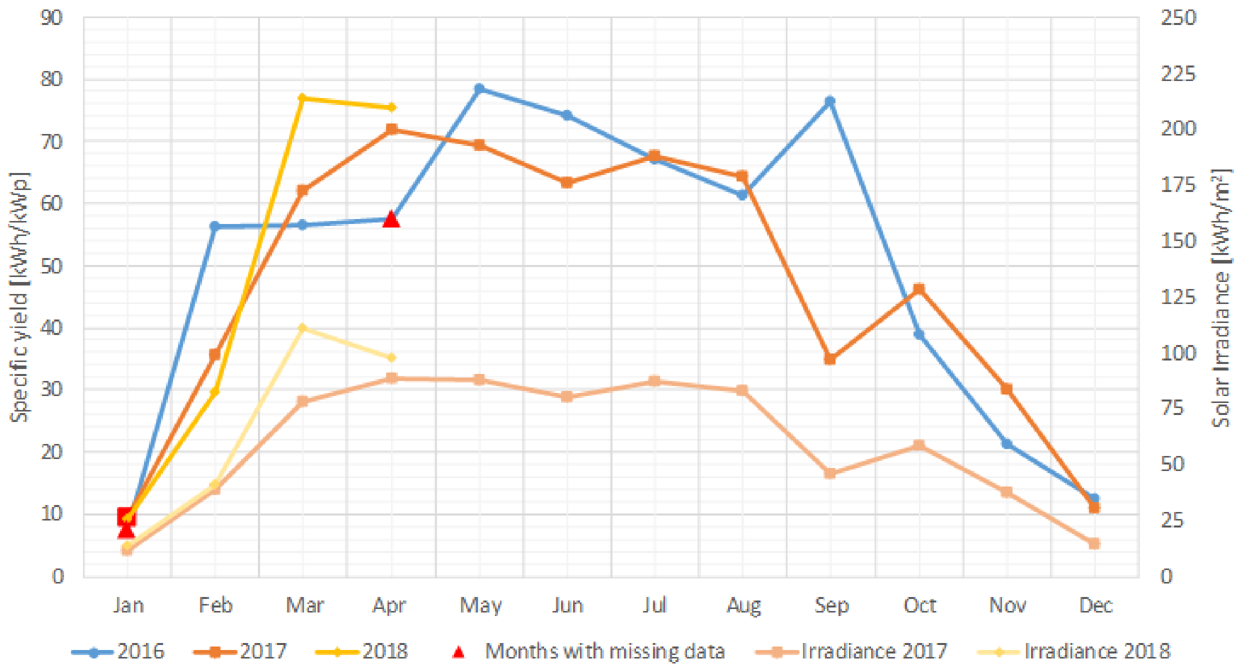

Figure 5.6: Comparison of the monthly specific yield of the south facade (Inv 7 and Inv 8 combined), with the solar irradiance of 2017

In Figure 5.7, the development of the PR value throughout the year of 2017 is shown. The red triangles indicate months with days of missing data. When calculating the PR, days, where there are missing N_p or N_I, are not implemented in the evaluation. PR decreases from the highest value in April of 0.81 to the lowest of 0.76 in September. The yearly PR for the south facade was 0.79 in 2017. Since almost half of the irradiance data for two first months of 2017 is missing, analyzing the PR from March 2017 to February 2018 may give a more significantly view of annual performance.

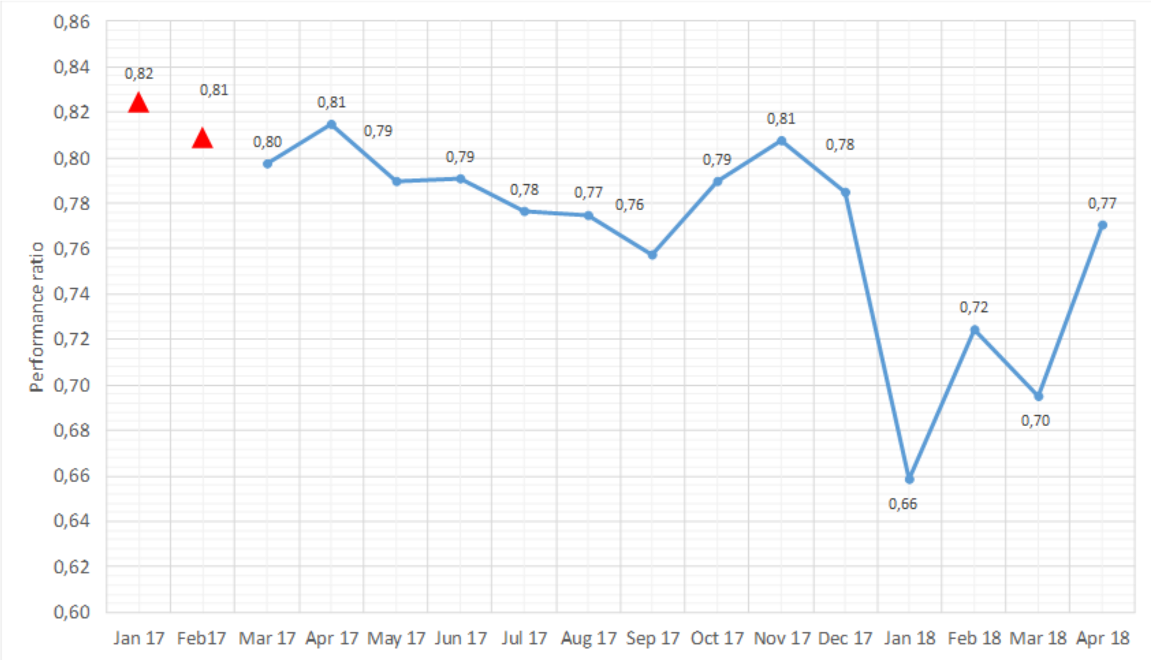

Figure 5.7: Monthly development of PR for south facade

The PV system efficiency is calculated by using Eq. 7. The monthly development of the PV system efficiency is plotted in Figure 5.8. The annual PV system efficiency is evaluated from March 2017 to April 2018, as there are numerous days of missing data in the two first months of 2017. The PV system efficiency (η_{sys}) was 7.80 % in the specified time period.

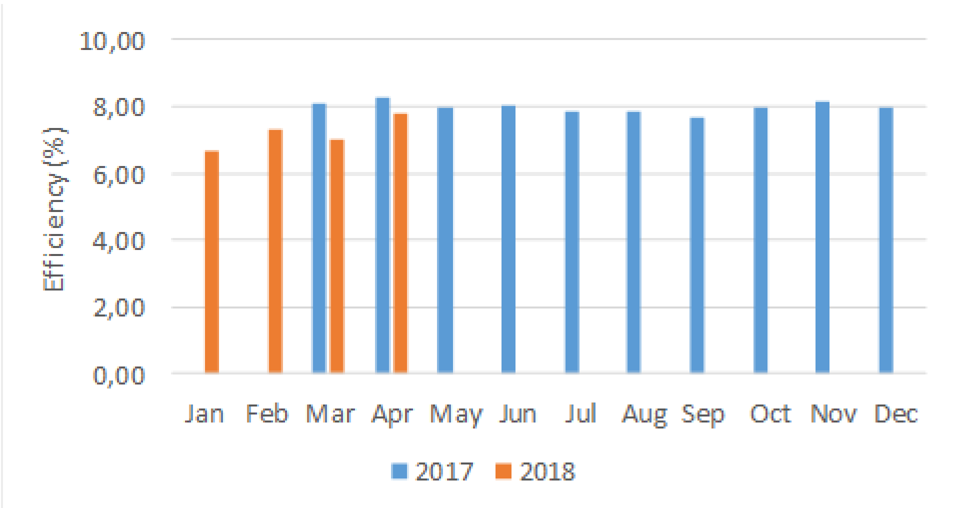

Figure 5.8: System efficiency of the south facade, on a monthly basis

Figure 5.9 and Figure 5.10 show data from a clear sunny day in February and July, respectively. The two days have been plotted to see the variation of PV system efficiency in typical winter and summer days. It is evident that the clear day in February, has a higher maximum hourly PV system efficiency than for the more evenly distributed efficiency in July.

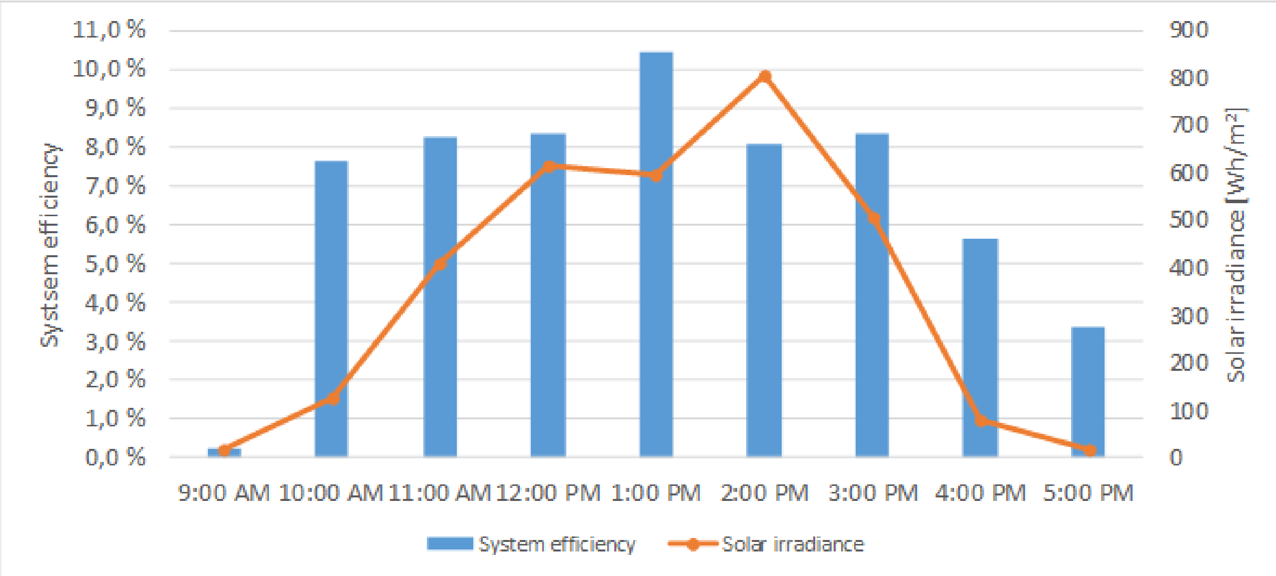

Figure 5.9: System efficiency and solar irradiance on a clear sunny day in February

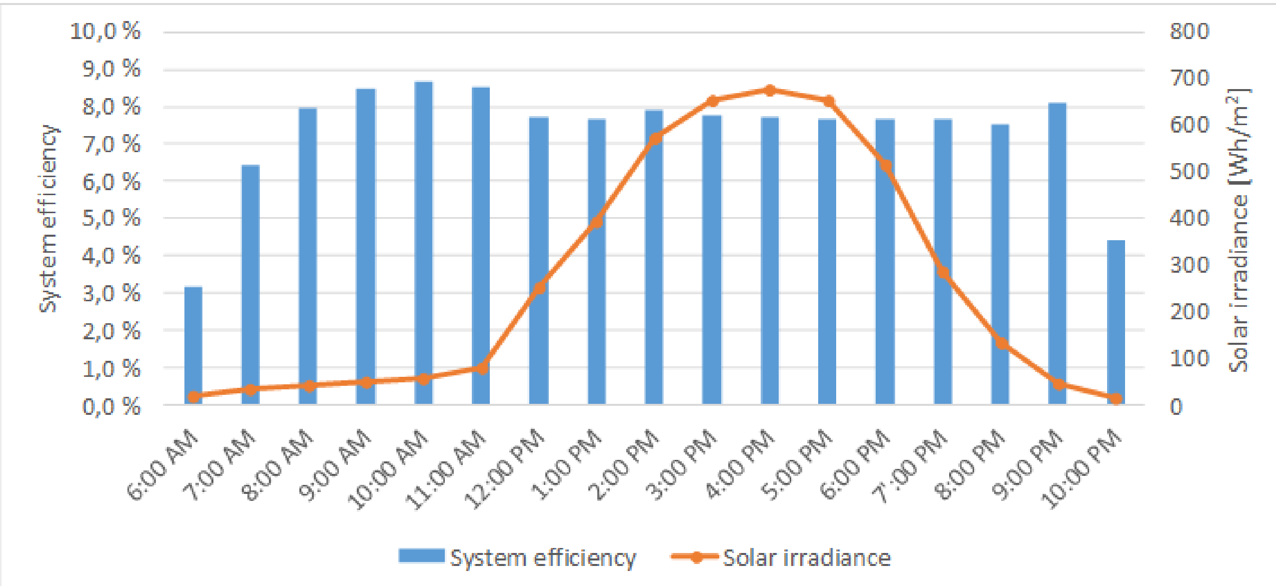

Figure 5.10: System efficiency and solar irradiance on a clear sunny day in July

5.1.5 Lessons learned

FUSen and the owner of the Solsmaragden reported that the BIPV facade was costly, especially with the custom-made green printed glass-glass modules. The reason was that there were not many suppliers available and the use of colored PV technology was in the initial phase of development. FUSen together with the Belgium supplier ISSOL developed a suitable fastening and installation solution for this specific project. The initially proposed fastening solution was costly and proved not to be suited for Norwegian building methods. Despite high costs, the Solsmaragden owner stated that they would do it again even without support from ENOVA.

5.2 Brynseng school

Brynseng is a new public primary school for children from the age of 6 to 12 with a multipurpose hall, owned by the Undervisningsbygg Oslo KF. The PV system was part of a project to test the nearly-zero energy building (nZEB) concept. Implementing the BIPV facades was an idea set forth by the Environmental Counsellor at Undervisningsbygg at a later stage in the project. The roof was then not available for PV module installation.

The architect wanted a uniform black surface, as can be seen on the picture of the building in Figure 5.11. The BIPV facade design and projecting were a cooperation between the module supplier ISSOL, the facade installer Staticus, and the main contractor NCC.

Figure 5.11: Picture of the BIPV facade at Brynseng school, retrieved from [64]

5.2.1 System description

The BIPV system was commissioned in April 2017 with a total module area of 1045 m^2, installed PV power of 165.6 kW_p, and 8 operating string inverters from SMA [29]. The modules are supplied from the Belgium company ISSOL, with taylor-made modules of the model CENIT 220. More system details are given in Table 5.

Table 5: System description of the south facade oriented BIPV on Brynseng

System description of the BIPV facade at Brynseng school	
Installed capacity	165.585 kW_p
Area	1046.5 m^2
Tilt angle	90°
Orientation	185°
Inverter properties	
Inverter type	Sunny Tripower 15000TL-10/12000TL-10/25000TL-10
Number of inverters	4/1/3
European efficiency	98 % / 97.9 % / 98.1 %
Topology	Transformerless
Nominal AC output power	15000 W/12000 W/25000 W
DC/AC ratio	From 1.06 to 1.28
Module characteristics	
Module type:	CENIT 220, details listed in Appendix B.2
Number of modules	656
Module design	ISSOL black glass-glass, unframed
Cell type	mono-Si
Module power	From 35 W_p to 448 W_p
Weight module	N/A
Module size	From 400x664 mm^2 to 2760x1080 mm^2, details listed in Appendix B.2
Module efficiency (%)	Typically around 16 % (average for all)
NOCT	N/A
Temperature coefficient of P_{mpp}	N/A

Table 5 lists the characteristics on the BIPV on Brynseng. Detailed information on the different modules performance and size is given in Appendix 5.14. There are some conflicting opinions if there are 28 or 26 sizes used in the project, this master thesis uses 28 sizes with a total installed capacity of 165.585 kW_p. This is verified by examination of the electrical string design plotted for each of the 656 modules (given in Appendix B, by examine Appendix B.3 and Appendix B.2) .

5.2.2 Building technical integration

Because the concept of a BIPV was introduced late in the pre-project, some of the ideal adjustments were not possible to implement in the architecture. The facade with BIPV is divided into three sections, the right, central and left side, as shown in Figure 5.12. The central section has a building extension in the upper part and is broader than the other sections. The section causes partial shadow during the day on the PV modules. The PV modules had no negative impact on the building structure, but additional work was required. The inverters on the different sections are illustrated in the string design in Figure 5.13.

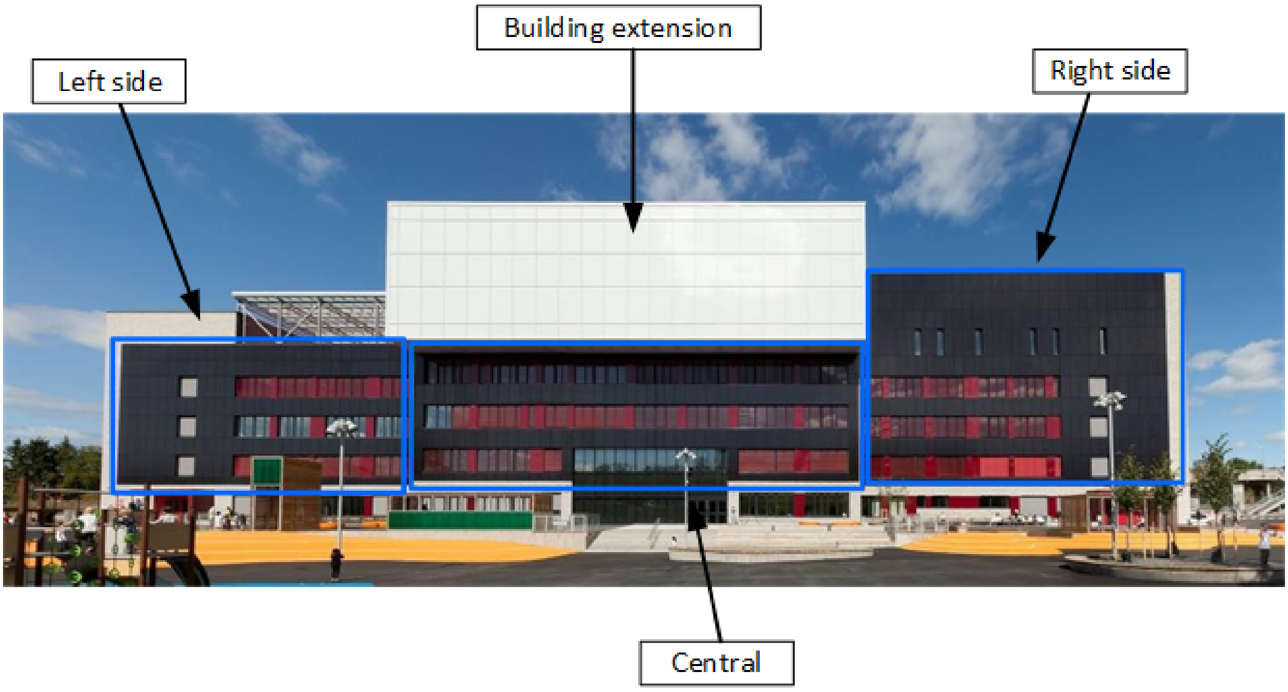

Figure 5.12: The section divisions and the building extension on the south facade of Brynseng illustrated with blue rectangles

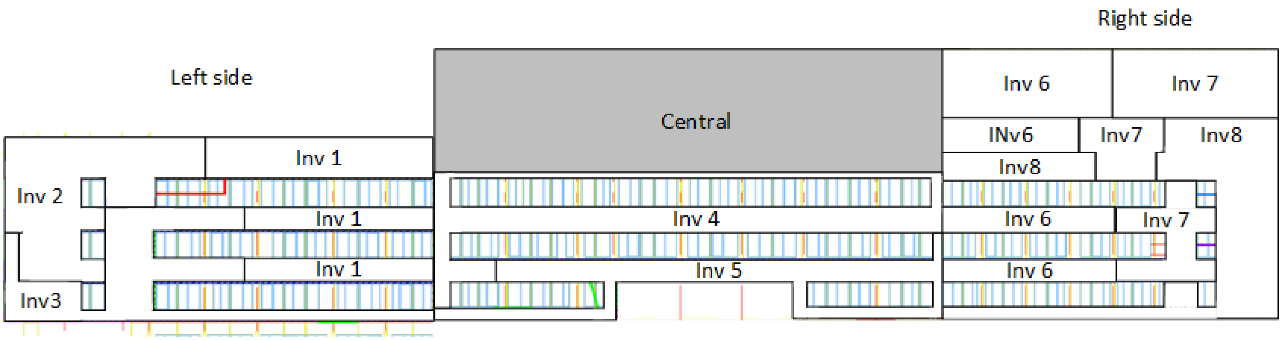

Figure 5.13: Schematic illustration of the string design of Brynseng of each inverter, more information is given in Appendix B.3

The PV module structure shown in Figure 5.14 is a simplification of the layers, as the encapsulation which is on both sides of the mono-Si is not shown. The outer layer of safety-glass prevents pieces of any broken glass from falling and allows the sunlight to pass through.

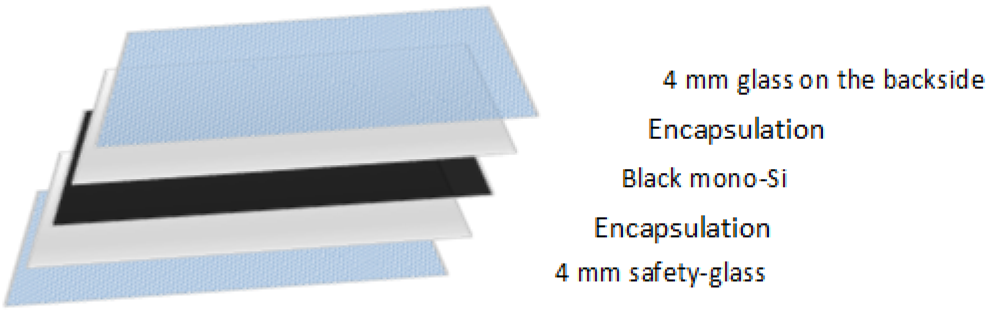

Figure 5.14: Illustration of module structure at Brynseng

The vertical battens and mounting hooks are illustrated in Figure 5.15. The insulation handling the moisture intrusion is shown on the left-hand side. This insulation is located behind the modules. All cabling is UV resistant and can handle Norwegian winter temperatures.

Figure 5.15: Installation details, showing vertical battens and mounting hook

In Figure 5.16, the cross-section of Brynseng facade is shown. The air-gap between the insulation and the PV modules is 239.5 mm. The outdoor air is free to flow behind the modules, reducing the temperature. The detailed information on the fastening developed by Staticus is given in Appendix B.1.

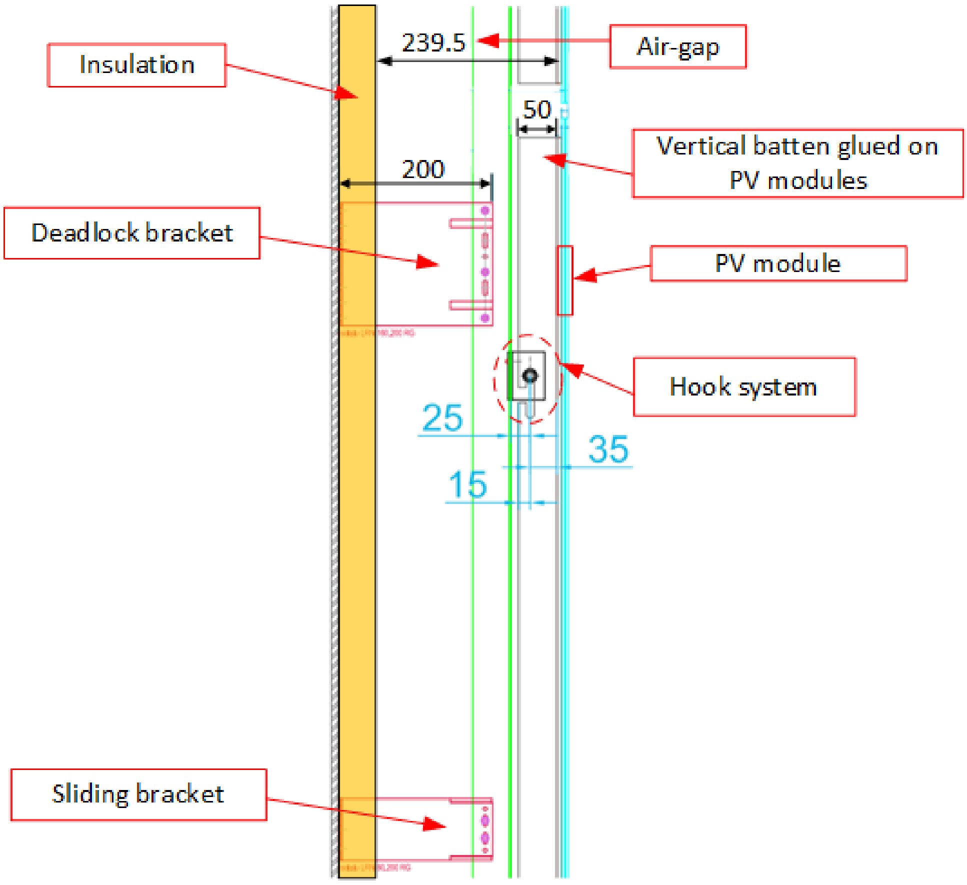

Figure 5.16: Cross-section of the Brynseng facade, including outer wall, brackets, and PV module, measurements in mm. Explanations from the author, original picture retrieved from [54]

5.2.3 Economy

The Brynseng project applied for funding from the "Energy efficient buildings" program from ENOVA and was given a total of 4.5 million NOK, being a pilot project for nZEB. This do not only include founding to the PV but also the additional equipment such as building envelope, heat pump, etc.

In the budget, the BIPV was a labeled as an investment and initially compared with the cost of an expensive brick facade option. The conclusion was that the extra cost was acceptable, because of the desire to get an nZEB status. Some economic calculations on the income of the PV system where done, but the income from el. production was found to be minimal. Therefore, the income was not the driver for getting the BIPV system.

The total cost of the BIPV facades was 7.7 million NOK or 7360 NOK per area of PV module (NOK/A_m). Compared with the price of standard facades tiles of 3000 NOK/m^2 the added cost of getting BIPV facade equals 4360 NOK/m^2. By using Eq. 10, the added cost is 27.5 NOK/W_p, detailed calculation is given in below.

$$\text{cost pr W}_\text{p} = \frac{4360 \text{ NOK/m}^2 \cdot 1046m^2}{165.6 \ \cdot 10^3 \text{ W}_\text{p}} = 27.5 \text{ NOK/W}_\text{p}$$

In Figure 5.17, the distribution of cost for the BIPV system is shown. The main cost is the installation including materials and work, with 40 % of the total cost. Undervisningsbygg used 350 000 NOK on solar cell advisory services which are not included in the total cost for the BIPV system. The project group had to spend extra on finding out the unclear legal framework regarding safety and building codes (technical, electrical, project design, what laws and regulations to follow). More clear guidelines regarding the Norwegian rules and regulations will contribute to lowering the total cost.

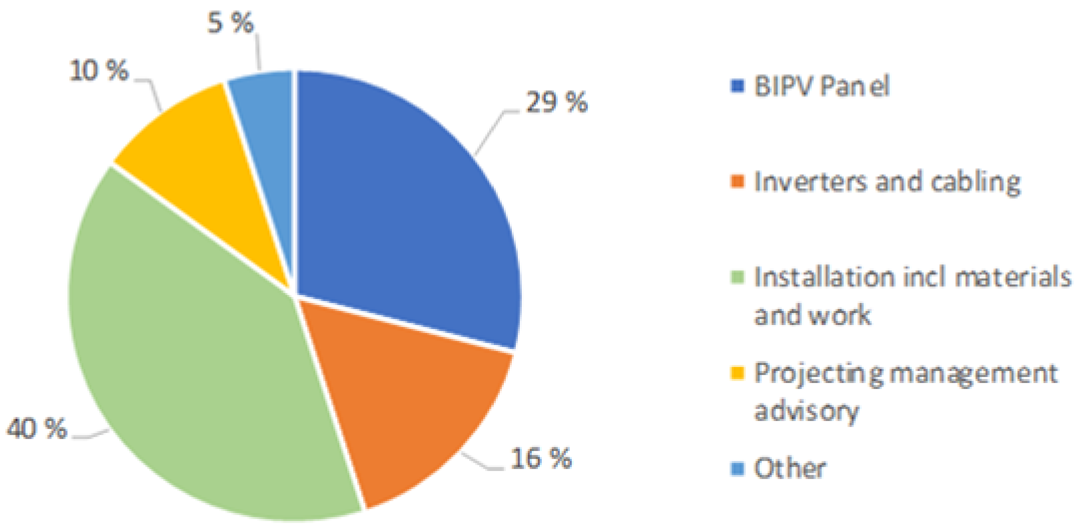

Figure 5.17: BIPV cost distribution at Brynseng school

Disregarding the financial support, the net present value (NPV) is negative, meaning that the project will not be paid back during the lifetime of 20-25 years. Including the financial support from ENOVA than the NVP becomes positive and the project is paid back during the lifetime. Undervisningsbygg has estimated one inverter shift and 0.5 % of the investment for operation and maintenance.

5.2.4 Performance

Table 6: Measured data on Brynseng

Brynseng	Description	Data resolution	Time period
Weather data	N/A		
Production data	AC power	15-min	May 2017 →

There has been a thorough initial estimation of yield based on simulation during the design phase. In a report from ISSOL [65], the annual specific yield for the total BIPV system is estimated to be 635 kWh/kW$_p$. The report from ISSOL uses a total installed PV system capacity of 166.4 kW$_p$.

In Figure 5.18, the plot of the monthly development of the specific yield of the three sections of the BIPV facade at Brynseng is shown. Details are shown in Appendix B. The red triangles indicate days of missing data N_p (April and June), more details are found in Appendix B. From May 2017 to April 2018 (1 year) the energy production was 91.2 MWh, and the specific yield was 551 kWh/kW$_p$. Taking into account the N_p missing days, the production was close to the anticipated value retrieved from the simulated analysis. The values for the central part are lower than the two others from June to August, with N_p indicating missing days in June.

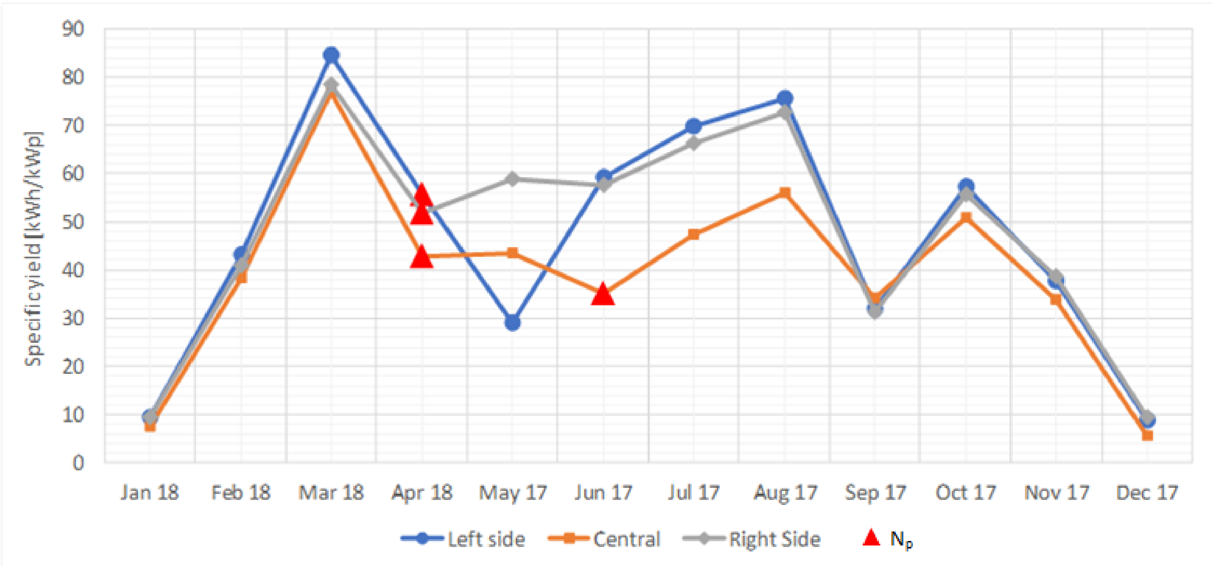

Figure 5.18: Comparison of different sections at Brynseng

The annual specific yield of each inverter is plotted in Figure 5.19. Appendix B gives more detailed information on yield and specific yield. The plot in Figure 5.19 indicates that inverter 4 is underperforming relative to the other ones. As seen in Figure 5.13, the modules connected to inverter 4 is just beneath the building extension.

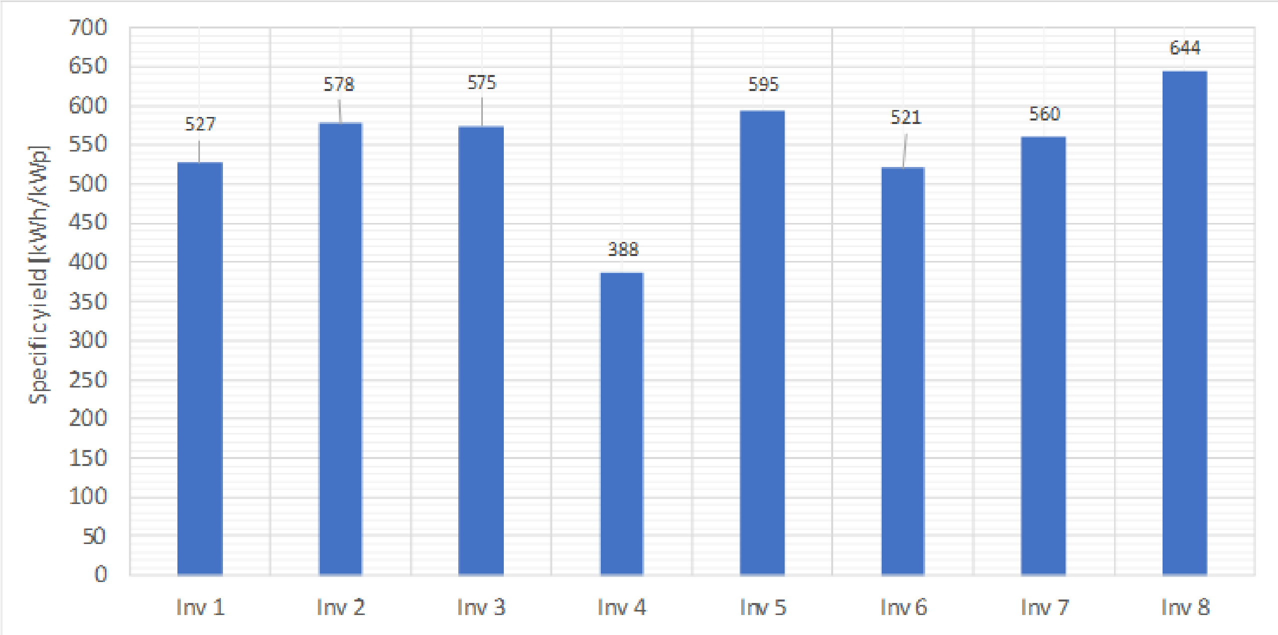

Figure 5.19: The specific yield of each inverter at Brynseng, (May 2017-April 2018)

5.2.5 Lessons learned

The Brynseng school BIPV project became more costly than anticipated because of the added time of projecting and design and unclear regulation framework for the fire safety and electrical requirements. It was not a sufficient amount of knowledge on the topic available, there were only a few reference projects up and running at the time.

Knowledge gained during this first pilot project will be valuable for new projects. This knowledge will be expected to reduce the cost in future BIPV projects. This project would not have been possible without the financial support from ENOVA. New projects have to be feasible on their own and be independent of financial support.

5.3 Bjørkelangen school

Bjørkelangen school is located in a small town in Aurskog-Høland municipality. The school is for children from the age 6 to 16 and was first used in February 2018. The south oriented facade of the building has a visually integrated PV system installed, as can be seen in Figure 5.20. One of the criteria from the municipality was that it should be "eye-catching" for people passing by, whereas the aesthetics were the driver for the BAPV system. The total entrepreneur of the building was HENT and Sørum Elektriske was the subcontractor for the electrical work. Solel was responsible for the PV system as a subcontractor of Sørum Elektriske.

Figure 5.20: Picture of the south oriented BAPV at Bjørkelangen school

5.3.1 System description

The BAPV system was commissioned in December 2017 with a total module area of 208 m^2, installed PV power of 35.2 kW_p and two operating string inverters from SMA [29]. The standard PV modules are delivered from the supplier Elite and are of black mono-Si. More system details are given in Table 7.

Table 7: Description of BAPV system at Bjørkelangen

System description of the BAPV system at Bjørkelangen	
Installed capacity	35.2 kW_p
Area:	208.2 m^2
Tilt angle	90°
Orientation	203°
Inverter properties	
Inverter type	Sunny Tripower 15000TL-30
Number of inverters	2
European efficiency	98 %
Topology	Transformerless
Nominal AC output power	15000 W
DC/AC ratio	N/A
Module characteristics	
Module type	EliTe Black (ET-M660275BB)
Number of modules	128
Cell type	mono-Si
Module design	Standard black, with frame
Module power	275 W_p
Weight module	18.5 kg
Module size	1640x992x35 mm^3
Module efficiency	16.90 %
NOCT	45 ± 2 °C
Temperature coefficient of P_{mpp}	-0.43%/°K

5.3.2 Building technical integration

The Bjørkelangen school building is of massive wood with ore pine as the outer panel. Solel was introduced early in the design phase and started to install the modules simultaneous as the construction of the outer wall. The technical integration that Solel uses is from Rockwool and is called RedAir [66]. The system contains insulation plates which have the benefit of not requiring a wind barrier and the wooden batten is treated against fire, fungal and rot, more details are found in Appendix C.1.

Figure 5.21 illustrates the vertical cross-section from the facade with the BAPV system. The PV module (1) is fastened to the vertical rails (2) with clamps. The rails are screwed onto the horizontal wooden batten (3). Behind the horizontal wooden batten there is a black cloth (4), which are screwed to the vertical wooden batten (5). The vertical wooden batten is fastened to the insulation (6) by using a fastening system from Rockwool. The air-gap behind the PV modules is 51 mm. The details on the fastening solution between the PV modules and the vertical rails are a business secret and not allowed to be reproduced.

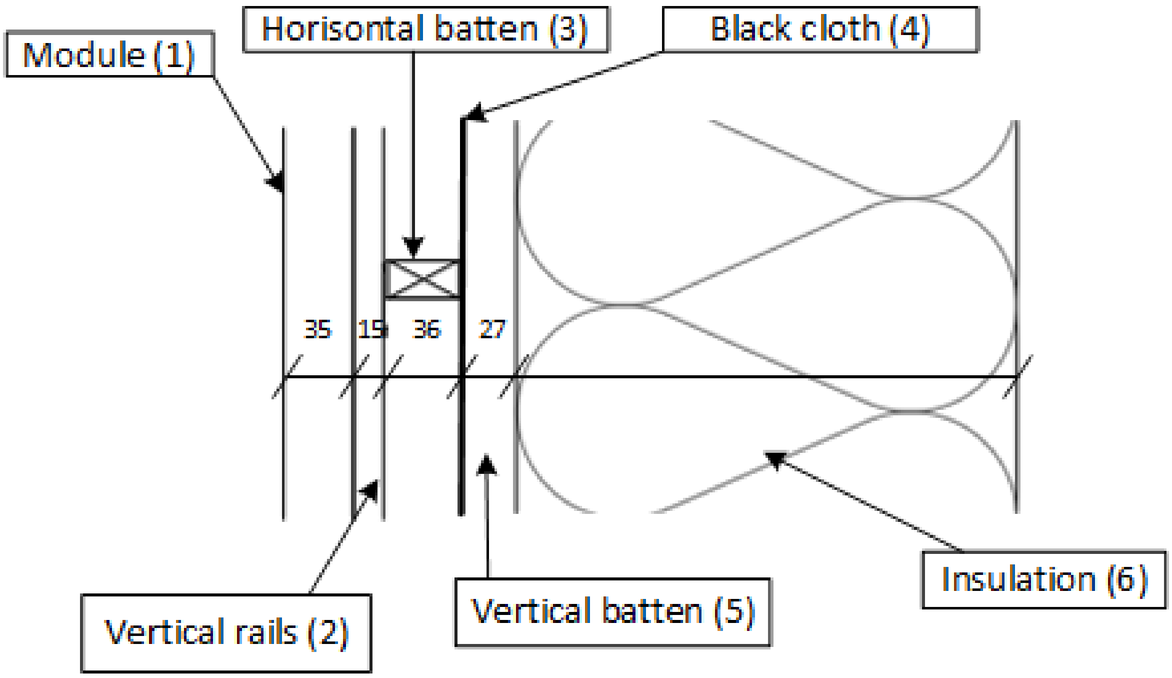

Figure 5.21: Vertical cross-section of the facade on Bjørkelangen, numbers refer to Table 8

Table 8: Explanation of numbers in Figure 5.21

Number	Technical description
(1)	Solar module
(2)	Vertical rails of Al with profile from the REDAir system
(3)	Horizontal wooden batten
(4)	Isola Tyvek Cloth (black)
(5)	Vertical REDAir FLEX LVL (See Appendix C.1)
(6)	Insulation (REDAir Flex plates) (See Appendix C.1)

5.3.3 Economy

The cost directly associated with the BIPV facades has not been possible to obtain, mainly because it is embedded in the total cost of the building of 300 million NOK.

From direct communication with the system supplier [67], the general cost of their solutions, without the cost associated with projecting and other indirect costs, were given as 2065 NOK/m^2 for a PV system in the region of 20-75 kWp. Based on this information, an assumption on the cost associated with this project is calculated to 2200 NOK/m^2, calculation details are given in Appendix C1.

The cost of 2200 NOK/m^2 is estimated and may differ from the actual cost. By using the assumption, the calculated cost per installed W_p, using (Eq. 10) gives:

$$\text{Cost per installed } W_\text{p} = 2200\ \frac{NOK}{m^2} \cdot \frac{208.2\ m^2}{35.2 \cdot 10^3\ W_\text{p}} \approx 13.0\ \text{NOK/W}_\text{p}$$

5.3.4 Performance

Table 9: Measured data on Bjørkelangen

Bjørkelangen	Description	Data resolution	Time period
Weather data	N/A		
Production data	AC power	15-min	Dec 2017 →

The system supplier did not perform a simulation on the expected energy production in the design phase. The PV system was commissioned in December 2017, therefore it is only five months of data available. Consequently, the system performance analysis presented here will be preliminary.

In Figure 5.22, the monthly development of the specific yield from December 2017 to April 2018 is shown. The detailed results on energy production and specific yield are give in Appendix C2. There was N_p=1 day of missing data in December 2017.

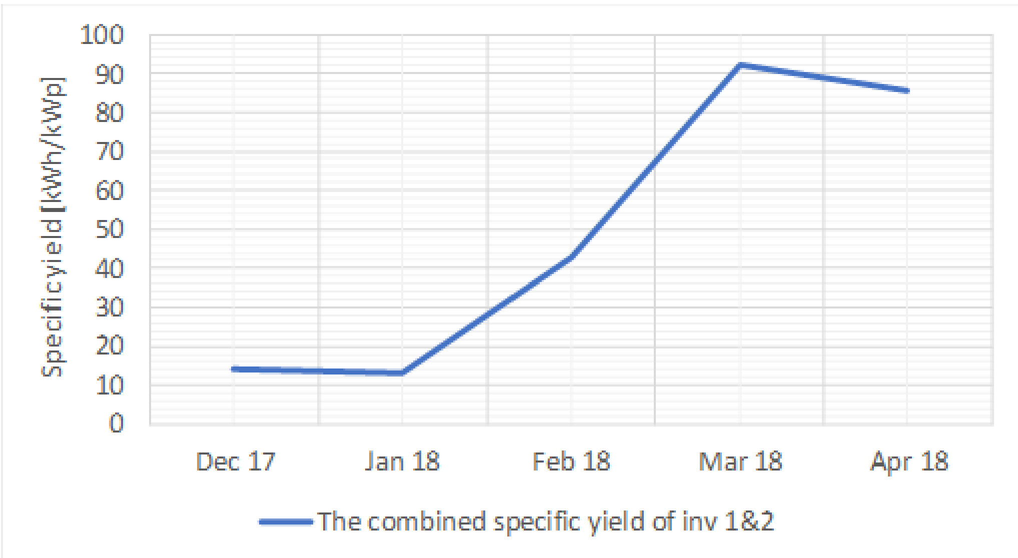

Figure 5.22: The specifc yield of the BIPV at Bjørkelangen school

5.3.5 Lessons learned

Solel reports that there were no problems in the installation phase and the system is producing well [68]. The municipality has only positive feedback on the BIPV system installed on the facade [69]. (Early access to the wall and no complex architectural features, is important for low costs)

5.4 Kiwi Dalgård

Kiwi Dalgård is a grocery store located in Trondheim. Kiwi is owned by Norgesgruppen, a multi-corporate business in Norway with around 1850 grocery stores around the country [70]. Norgesgruppen wanted to test new PV technology by using crystalline and thin-film technology on the facade and roof. FUSen was responsible for the solar modules on the building and participated in the planning and installation as well [71]. The building meets the requirements for passive house standard NS 3701 [72].

Figure 5.23 shows two of the three BIPV facades and the roof configuration with east/west modules. The PV system is connected to battery packs, making it possible to use the energy stored when the production is low.

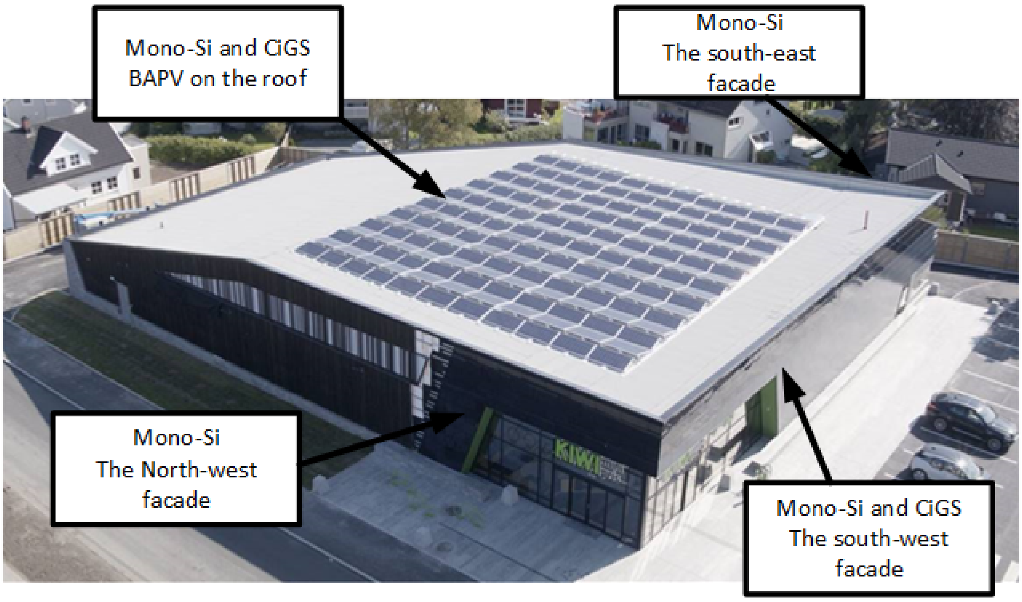

Figure 5.23: Picture of the PV system at Kiwi Dalgård, retrieved from [73]

5.4.1 System description

The building uses two types of PV technologies, thin film (CIGS) and mono-Si. Both technologies are installed on the southwest facade and the roof, as specified in Figure 5.23. The south-west facade has both technologies, with the mono-Si situated in the area above the area with the CIGS, indicated with the red and yellow frame, in Figure 5.24.

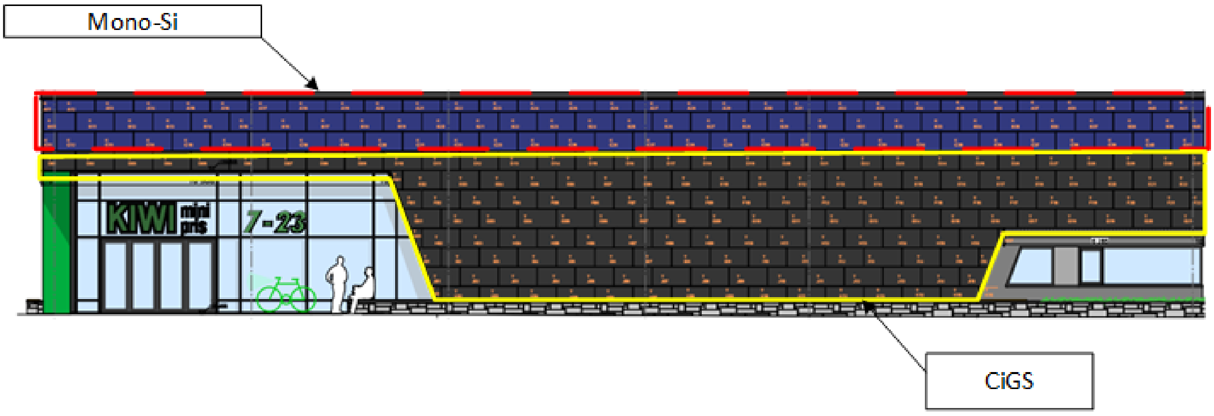

Figure 5.24: The main facade at Kiwi Dalgård with the different technologies, retrieved from [74]

Only one of the facades is currently operative, the mono-Si on the southwest facade. The BIPV system with mono-Si was commissioned in August 2017 with a module area of 58 m^2, installed PV power of 8.02 kW_p with one string inverter from SMA [29]. The mono-Si modules are supplied from Innos and are taylor-made to the Kiwi Dalgård project. More system details are given in Table 10.

Table 10: Description of the operative crystalline facade at Kiwi Dalgård

System description of the mono-Si facade at Kiwi Dalgård	
Installed capacity	8.018 kW_p
Area	58 m^2
Tilt angle	90°
Orientation	240°
Inverter properties	
Inverter type	Sunny Tripower 7000TL-20
Number of inverters	1
European efficiency	97.5 %
Topology	Transformerless
Nominal AC output power	7000 W
Module characteristics	
Module type	Innos Black Facade
Number of modules	93
Cell type	mono-Si
Module power	N/A
Module design	Glass-glass with laminated colored foil
Weight module	N/A
Module size	N/A
Module efficiency	N/A
NOCT	N/A
Temperature coefficient of P_{mpp}	-0.40 %/°K

Each module is customized to fit the building design. Therefore, information on module weight, size, and efficiency has not been possible to retrieve. The thin-film CIGS modules were delivered by a

German company Manz [75], but no data sheet has been made available.

5.4.2 Building technical integration

The frameless mono-Si module at Kiwi Dalgård is build up of laminated colored glass-glass layers and mono-Si with encapsulation on both sides. The module design of the mono-Si, is illustrated in Figure 5.25, based on retrieved information from the standard sized PV module. Datasheet is given in Appendix D.2.

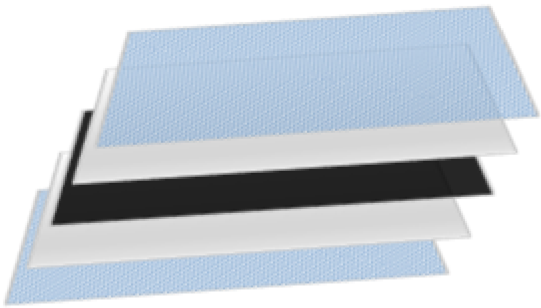

Figure 5.25: Structure of the modules used at Kiwi Dalgård, retrieved from [74]

In Figure 5.26, the cross-section of the southwest facade at Kiwi Dalgård is shown, the thickness of the CIGS modules is greater than the mono-Si thickness. Therefore, the cross-section shows PV modules of 12 mm, which is representative for the thin film CIGS modules and not the thinner mono-Si.

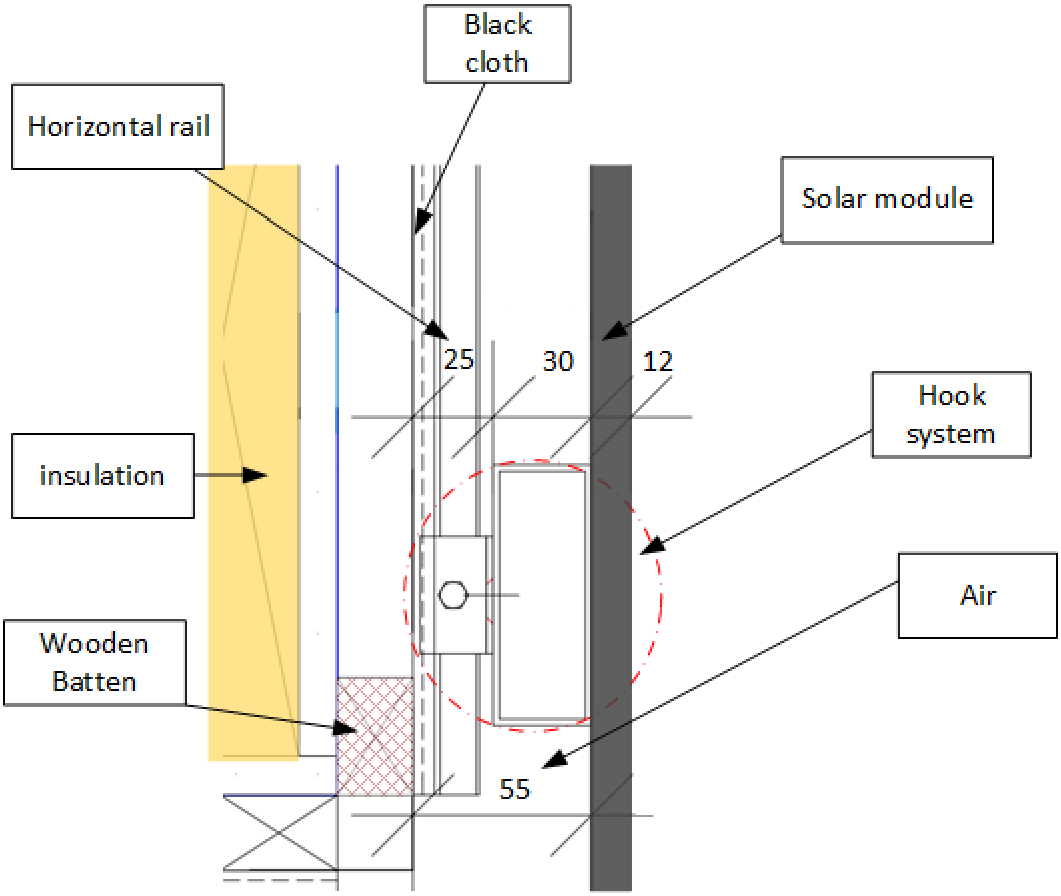

Figure 5.26: Cross-section at the south-west facade at Kiwi Dalgård, with explanations, original picture retrieved from [74]

The air gap is 55 mm allowing the air to flow freely in and out behind the panels. The red circle indicates the mounting details reviewed in the section below. The modules are mounted without any reinforcements on the structure of the building. The modules are taylor-made to this specific Kiwi Dalgård project, as the modules are cut to fit the design.

The mounting details on the BIPV system have not been made available. Nevertheless, by studying received pictures from Fikke [74], an approximate replication of the mounting details have been performed in SolidWorks. The specific parts and the hooking mechanism are shown in Figure 5.27.

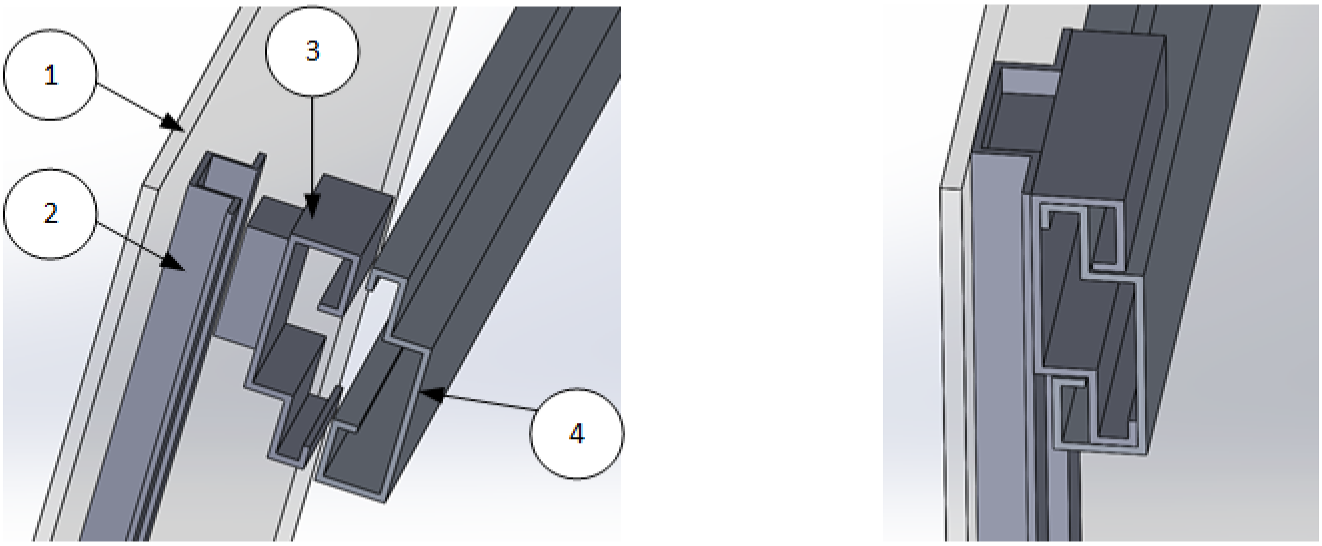

Figure 5.27: Illustration of the mounting details of the PV modules at Kiwi Dalgård

The first part (1) is the solar module, glued on the vertical rail (2), and the vertical rail is screwed on the bracket (3). Then the configuration is hooked on the horizontal rail (4), which itself is screwed on the outer structure of the building.

In Figure 5.28, pictures from the installation of the PV modules in progress are shown from the gluing of the PV modules to the installation on the outer wall of the building. The process of gluing the vertical rails onto the modules demands accurate and precise work [74].

Figure 5.28: Gluing and installation of the PV modules at Kiwi Dalgård, retrieved from [74]

5.4.3 Economy

The project recived funding of 3 million NOK by ENOVA [76]. The grant was given for the technical integration with CIGS and mono-Si on roof and facade. Together with a new the PV system, the project also included new technical solution for the refrigerating plant and common usage of the thermal solution on nearby households. Information was found from a interview with Ine Maribu [77].

The cost of the total PV system was 6.8 million NOK, with the distribution of cost shown in Figure 5.29. The main cost is from the PV modules, which have a combined share of 36 % of the total cost. The cost of the installation and projecting is not divided between the roof and facade, therefore further cost analyze is not satisfactory. Nevertheless, this project is a very costly due to the taylor made modules of both mono-Si and CIGS.

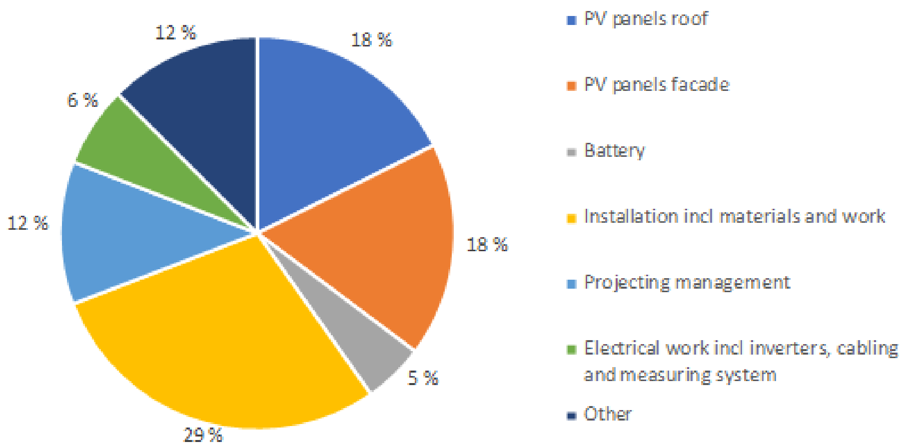

Figure 5.29: Distribution of costs for the total PV system at Kiwi Dalgård, information provided by Ine Maribu [78]

5.4.4 Performance

Table 11: Measured data on Kiwi Dalgård

Kiwi Dalgård	Description	Data resolution	Time period
Weather data	N/A		
Production data	AC power	15-min	August 2017 →

There has not been any simulation studies on the expected energy production of the Kiwi Dalgård BIPV system [74]. Figure 5.30 shows the development of specific yield of the operative inverter on the main facade. The PV modules on the facade started producing energy on 31 August 2017, giving data from a limited time period to analyze.

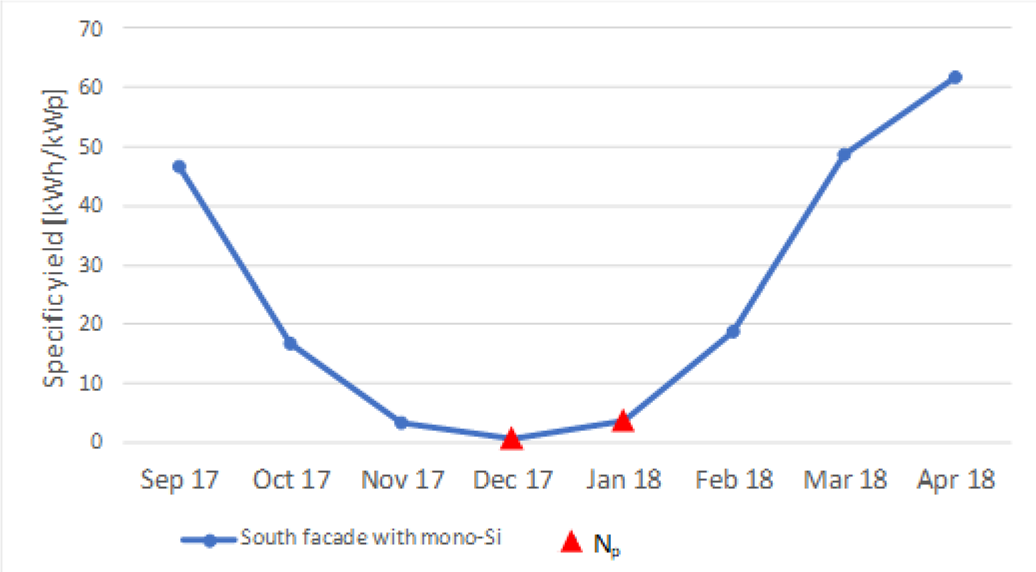

Figure 5.30: Specific yield of the mono-Si on the south oriented facade

There are two days of data missing in the operative period (N_p=1, a day in 2017, N_p=1, a day in 2018), indicated with the red triangles. More data is needed to make an adequate performance assessment of the system.

5.4.5 Lessons learned

FUSen reports that they would have liked to be involved in the design process at an earlier stage, mainly to plan the internal configurations such as the cabling and the technical room. This would have ensured a faster process, with reduced planning cost. As this is the first project with this fastening solution and mono-Si and CIGS modules together, they were all in all satisfied with the result. The fastening solution has been used in recent projects where FUSen has been involved. One note from the project leader was that the time and effort used for gluing the rails to the modules could have been done faster, nevertheless the technique of gluing improved as time and knowledge was obtained [74].

5.5 Kiwi Fjeldset

Kiwi Fjeldset is a grocery store located in Elverum. Kiwi is owned by Norgesgruppen. Kiwi Fjeldset has a BAPV system on the roof and facade delivered by FUSen [79]. The system was up and running 16 February, 2016. Figure 5.31 shows the main entrance of the grocery store and the nine modules making up the BAPV system on the facade. The building also has a protruding structure that can be seen in Figure 5.31, causing shadow during some time of the day.

Figure 5.31: Picture of the south oriented BAPV facade at Kiwi Fjeldset, retrieved from [80]

5.5.1 System description

The PV system contains a traditional east/west configuration on the roof with a total of 352 modules from IBC with an installed capacity of 91.52 kW_p and nine modules at the south facade with an installed capacity of 2.4 kW_p. The BAPV system on the south facade was commissioned in February 2016, with an total module area of 14.5 m^2, and one operating string inverter from SMA [29]. More system details for the south facade are given in Table 12.

Table 12: Description of the south oriented BAPV system on Kiwi Fjeldset

System description of BAPV system on Kiwi Fjeldset south facade	
Installed capacity	2.43 kWp
Area	14.5 m^2
Tilt angle	90°
Orientation	200°
Inverter properties	
Inverter type	Sunny Boy 2.5 1VL-40
Number of inverters	1
European efficiency	96.7 %
Topology	Transformerless
Nominal AC output power	2500 W
Module characteristics	
Module type	ISSOL 220/Model 270
Number of modules	9
Module design	glass-glass, framed
Cell type	mono-Si
Module power	270 W_p
Weight module	37.36 kg
Module size	1.637x984x50 mm^3
Module efficiency	16.8 %
NOCT	N/A
Temperature coefficient of P_{mpp}	-0.391 %/°K

5.5.2 Building technical integration

The module is build up of different layers with glass on both sides of the mono-Si with encapsulation, the safety glass enables safe passage around the building. Illustration of the structure is given in Figure 5.32. The modules are attached to a frame, as shown in Figure 5.33.

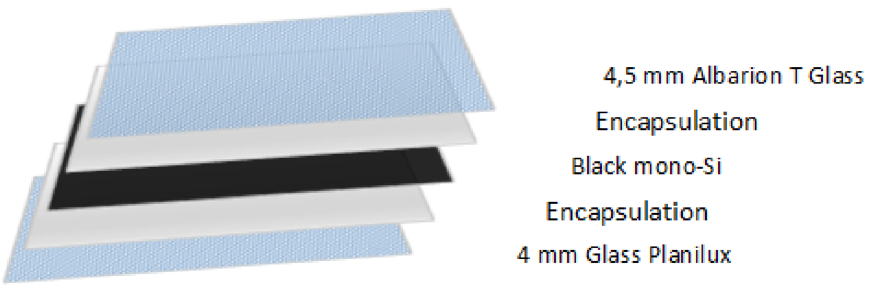

Figure 5.32: PV module layers at the south facade on Kiwi Fjeldset

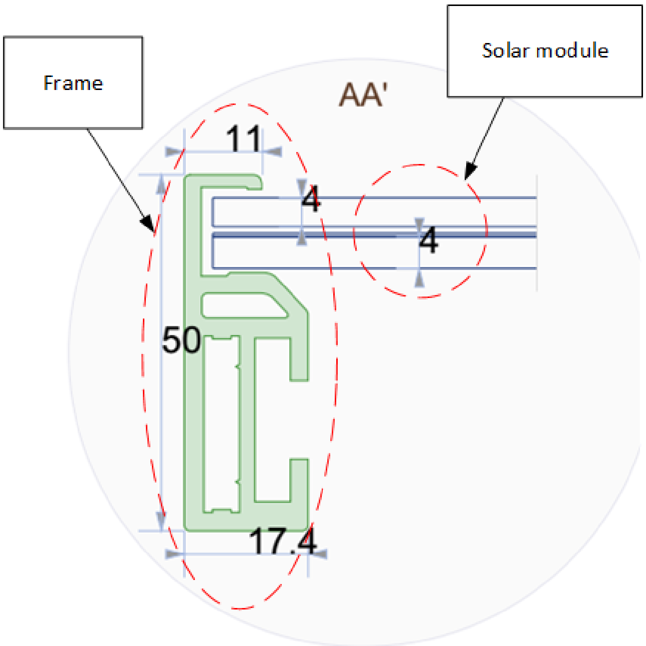

Figure 5.33: The framed PV module of Kiwi Fjeldset, retrieved from Appendix E

5.5.3 Performance

Table 13: Measured data on Kiwi Fjeldset

Kiwi Fjeldset	Description	Data resolution	Time period
Weather data	N/A		
Production data	AC power	15-min	February 2016 →

There have been no specific simulations on the expected yield and performance of the south oriented BAPV facade. The estimation of the total energy production of the roof and facade installation is 70 MWh per year [79].

Kiwi Fjeldset has nearly one year of full data series available (N_p of missing data in is given Table E2) for the facade, with energy production of 1208.82 kWh and a specific yield of 497.5 kWh/kW$_\mathrm{p}$ in 2017. The monthly development of the specific yield is shown in Figure 5.34 where the red triangles indicate days of missing data (given in Appendix E2). The development of specific yield in 2017 is evenly distributed from March to September. The specific yield has been compared to the roof installation, the result is shown in Figure 5.35. In Figure 5.35, typical peak during summer months is shown. When comparing the annual specific yield for the PV system on the facades with the roof PV system, the facade systems produced 77 % of the roof system.

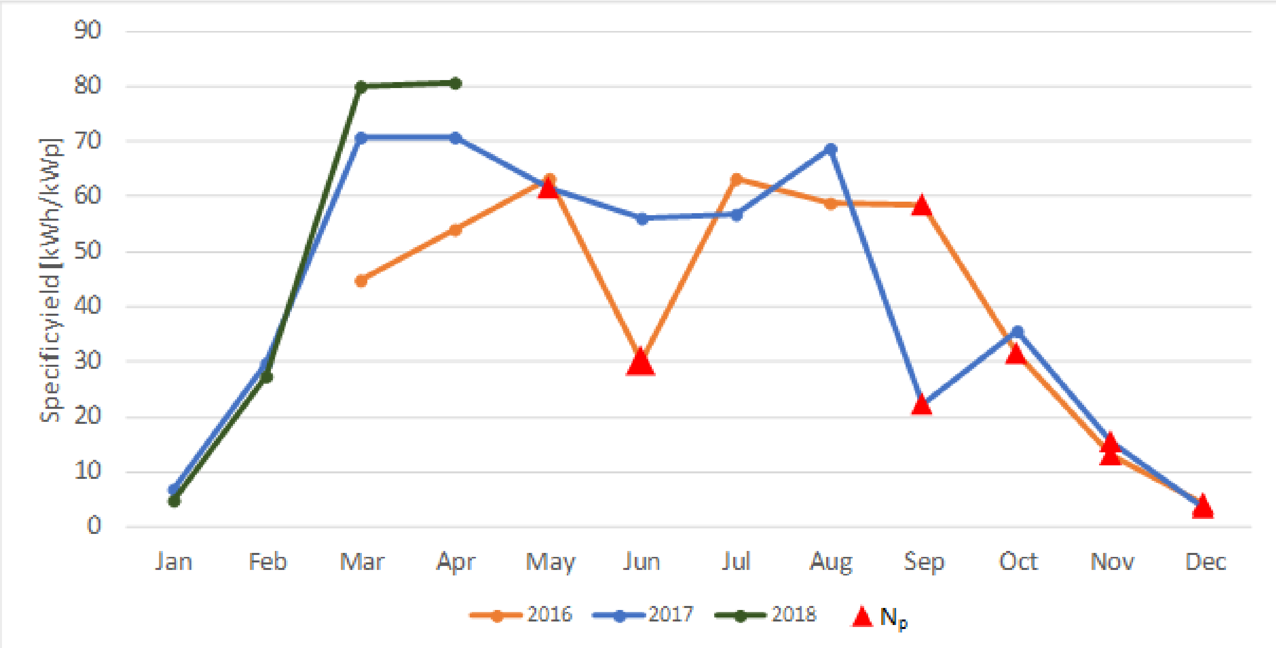

Figure 5.34: Monthly development of specific yield of the south facade at Kiwi Fjeldset

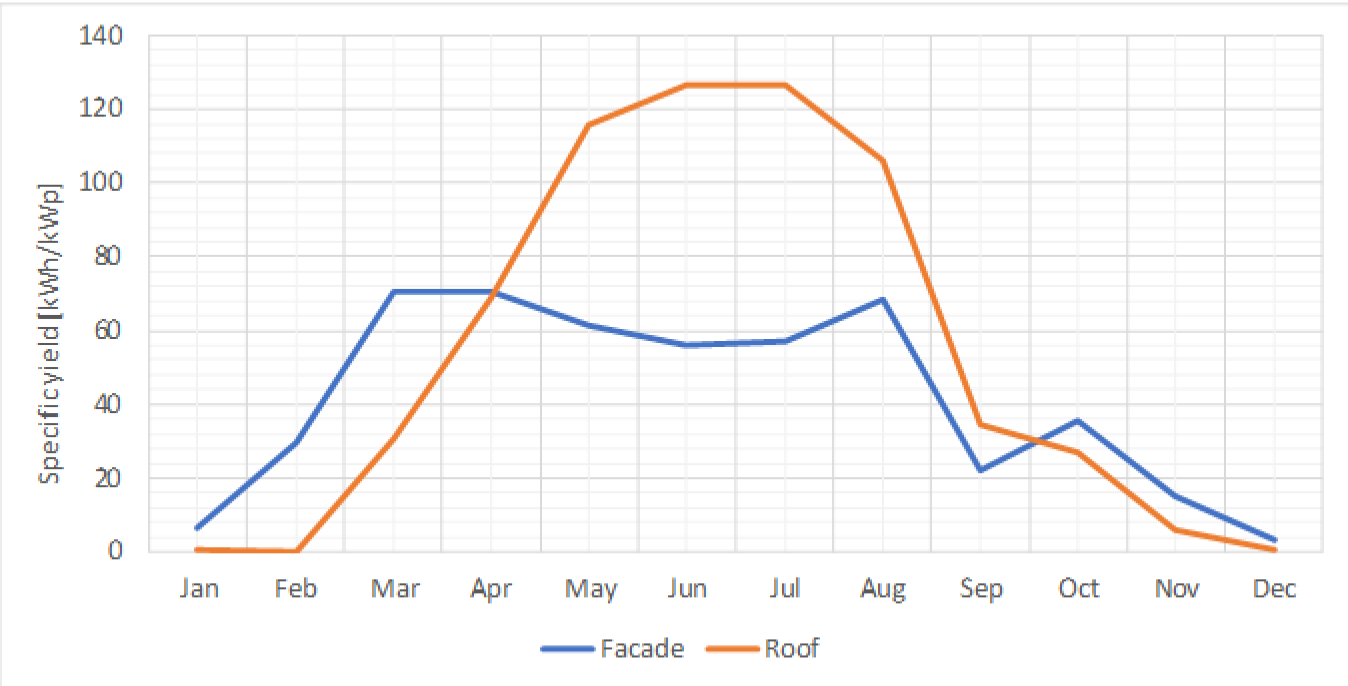

Figure 5.35: Comparison between the facade and roof installation on Kiwi Fjeldset for 2017

5.6 ASKO washing hall

ASKO washing hall is located in Vesby, east in Norway. The washing hall has PV modules on the roof and facade. This is part of an extensive solar cell investment project organised by Norgesgruppen.

The facade modules are visually integrated and are in reality a BAPV system with modules from LG. The recommendation of using BAPV facade combined with roof mounted PV modules came from FUSen, who designed and installed the system. The combined system gives a good energy production profile all year long.

As can be seen in Figure 5.36, no buildings or other objects are giving shadow on the modules. However, this may change as the washing hall us situated in an industrial park.

Figure 5.36: The BAPV system on the facade of ASKO washing hall located in Vestby

5.6.1 System description

The PV system consists of a roof and facade system, with 240 modules from IBC on the roof with a capacity of 62.4 kW_p and 107 modules with a capacity of 32.1 kW_p on the facade. The BAPV on the facade was commissioned in March 2017, more details are given in Table 14.

Table 14: The characteristics of the BAPV on ASKO washing hall

System description of the BAPV on ASKO washing hall	
Installed capacity	32.1 kW_p
Area	175.48 m^2
Tilt angle	90°
Orientation	180°
Inverter properties	
Inverter type	Sungrow SG 30kTL
Number of inverters	1
European efficiency	98.0 %
Topology	Transformerless
Nominal AC output power	30 000 W
DC/AC ratio	1.07
Module characteristics	
Module type	LG Electronics LG300N1K-G4
Number of modules	107
Module design	standard with backsheet
Cell type	mono-Si
Module power	300 W_p
Weight module	17.0± 0.5 kg
Module size	1640 x 1000x 40 mm^3
Module efficiency	18.3 %
NOCT	46 ± 3°C
Temperature coefficient of P_{mpp}	-0.38 %/°K

5.6.2 Building technical integration

The technical integration is different from the facade systems previously mentioned but similar to another system used on Haldenterminalen, see Section 5.7.2. The building wall is of insulated panels with polyurethane from Kingspan [81] and the specific panels used in this building is the KS 1200 NL (Appendix G Datasheet). The panels have an outer layer of steel, which the attachment used on the PV modules are directly screwed on. The attachment system is from K2 systems and the specific system used is the Speed Rail System [82], illustrated in Figure 5.37. The screw used is a unique screw of A2 stainless steel for usage on steel plates. The wiring is of standard copper solar cable (DC), with 4 mm^2 cross-section. The inverters are attached up under the ceiling inside the building.

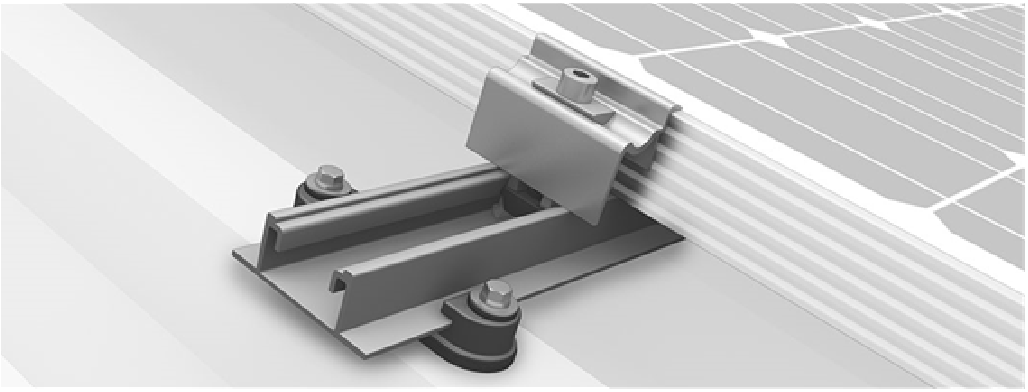

Figure 5.37: Attachment details of the PV modules at ASKO Washing Hall, retrieved from [82]

5.6.3 Economy

The system supplier/owner was not able to provide information on the economical aspects of the ASKO washing hall BAPV system.

5.6.4 Performance

Table 15: Measured data on ASKO washing hall

ASKO washing hall	Description	Data resolution	Time period
Weather data	N/A		
Production data	DC and AC power	15-min	March 2017 →

There are some uncertainties in the values logged in the IBC solar software. When generating hourly energy production data on the individual inverter, the values do not correspond to the data on hourly mean AC power. Hourly energy production is produced in kWh, without any values smaller than 1 kWh. This is showed in Appendix H.2, for Haldenterminal where there is actually a change during the month of July, with improved resolution.

The data available gives one year of data to analyze. For the period from April 2017 to March 2018, the energy production is 26.2 MWh on the south facade. The specific yield in the same period is 721.1 kWh/kW$_p$. The monthly development can be seen in Figure 5.38.

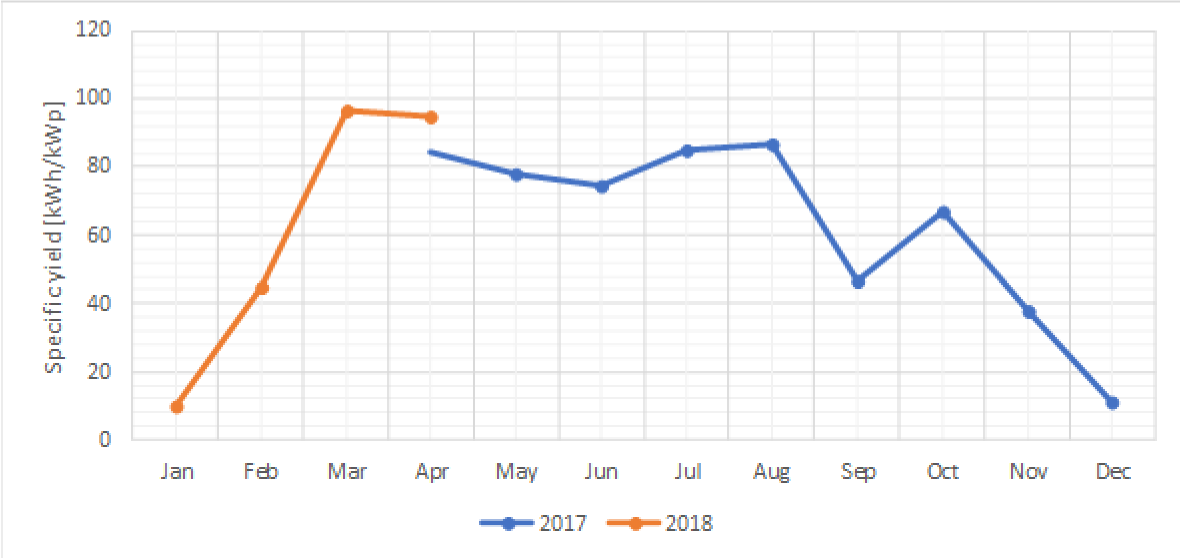

Figure 5.38: The development on the specific yield of the south facade on ASKO washing hall

The detailed monthly values are listed in Appendix F1. In Figure 5.38, the specific yield is evenly distributed from April 2017 to August 2017. There are only four full months with data in 2018, but the trend of an even distribution is apparent from March. This is contrary to the roof which has a peak in the summer months, which can be seen in Figure 5.39.

For the roof, the first full month of data was in March 2017, and for the facade, in April 2017. The comparison between the roof and facade on the specific yield is given in Figure 5.39. From April 2017 to March 2018 the facade produced similar energy per installed capacity as the roof, where the specific yield of the facade was 98 % of the roof installation.

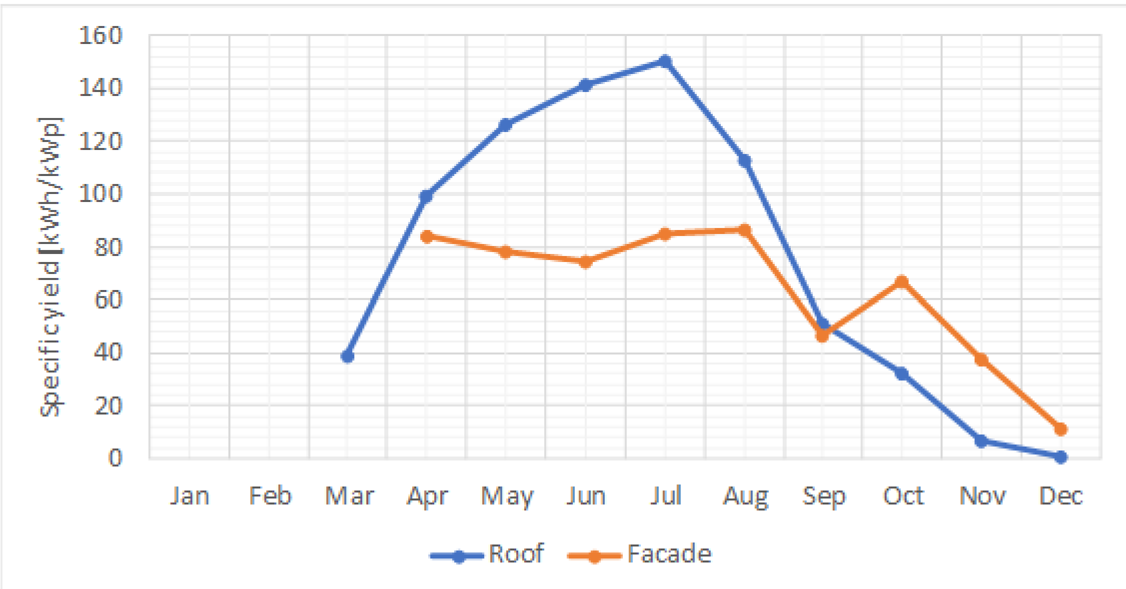

Figure 5.39: Comparison between the PV system on the roof and facade on ASKO washing hall, 2017

The IBC solar monitoring program as described in Section 4.2, enables monitoring the DC and AC output power of the inverter. This gives the possibility to find the efficiency of the inverter (η_{inv}). In the first full year of data, from April 2017 to March 2018, the mean efficiency of the inverter on the facade is $\eta_{\text{inv}} = 97.94\%$. The monthly development of the efficiency and temperature can be seen in Figure 5.40. There is minimal variation in the efficiency and temperature during the first operative year.

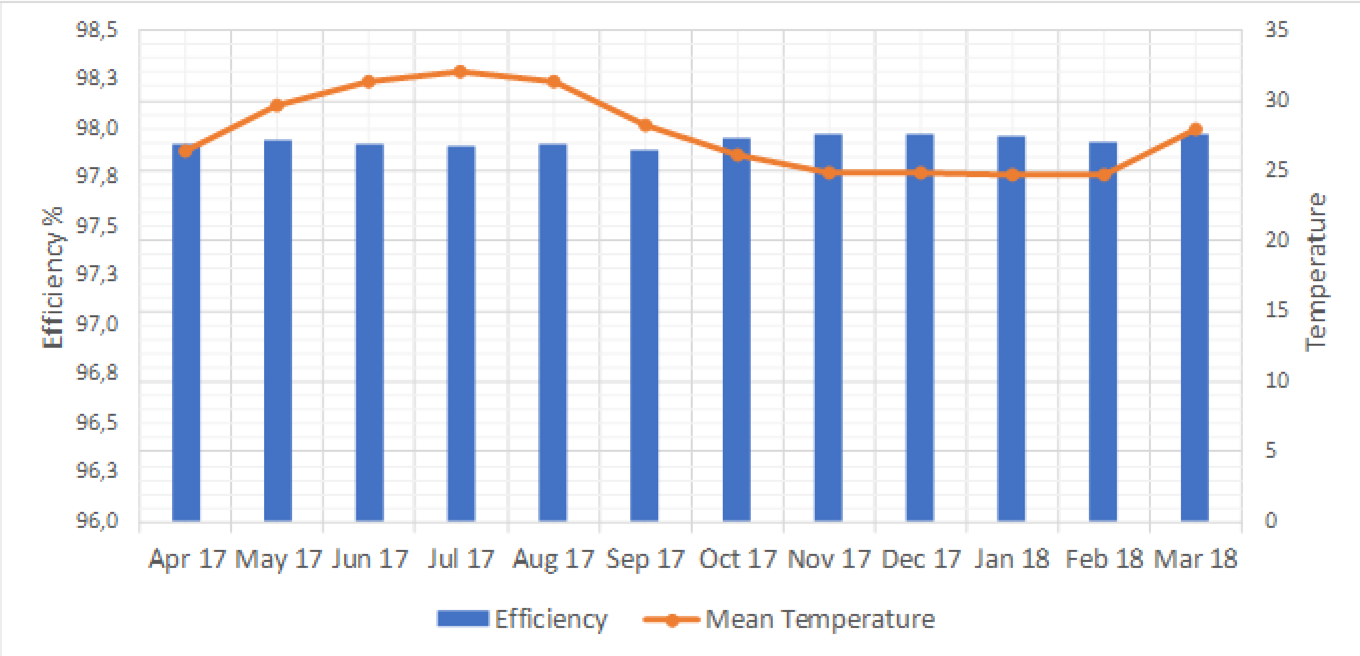

Figure 5.40: The efficiency and temperature of the inverter on the south facade at ASKO washing hall

5.6.5 Lessons learned

The owner of the ASKO washing hall and FUSen were overall satisfied with the result. Visually the panels had an excellent aesthetic look. FUSen emphasized the importance of choosing panels that are aesthetically pleasing and suppliers with good color control on their modules. According to FUSen, some panel producers struggle with the colour homogeneity.

5.7 Haldenterminalen

Haldenterminalen is located in Halden in the east of Norway. The building is owned by Ringstad Gruppen AS and is a building for rental. The PV system is installed as part of the extension of the existing building, with FUSen as system supplier and PV system installer. The PV system is of the type BAPV and is shown in Figure 5.41.

Figure 5.41: The BAPV system on the south facade of Haldenterminalen

5.7.1 System description

The facade PV system was commissioned in August 2015 and consists of standard sized modules from IBC, with 20.02 kW_p installed power. The PV module area of the facade is 126.04 m^2, with one operating inverter from Sungrow [29]. More system details are given in Table 16. There is a light pole on the car parking close to the Haldenterminalen causing some shadow on the modules during the day.

Table 16: System Description of Haldenterminal

System description of the Haldenterminal PV system	
Installed capacity	20.2 kW_p
Area	126.04 m^2
Tilt angle	90°
Orientation	195°
Inverter properties	
Inverter type	Sungrow SG 20KTL
Number of inverters	1
European efficiency	97.30 %
Topology	Transformerless
Nominal AC output power	20000 W
DC/AC ratio	1.00
Module characteristics	
Module type	IBC MonoSol 260 CS Black
Number of modules	77
Cell type	mono-Si
Module design	standard with backsheet
Module power	260 W_p
Weight module	19.5 kg
Module size	1.650x992x45 mm^3
Module efficiency	15.9 %
NOCT	46°C
Temperature coefficient of P_{mpp}	-0.493 %/°K

5.7.2 Building technical integration

FUSen used the same technique as for ASKO washing hall, described in Section 5.6.2 for the attachment of the PV modules on the building structure. The attachment used on the PV modules are directly screwed on to the outer steel layer of the building panels. The specific system used is the Speed Rail System [82].

5.7.3 Economy

The system supplier or owner was not able to provide information on the economic aspects of the Haldenterminalen BAPV system.

5.7.4 Performance

Table 17: Measured data on Haldenterminalen

Haldenterminalen	Description	Data resolution	Time period
Weather data	N/A		
Production data	DC and AC power	15-min	August 2015 →

The energy production data series has the same problems as mentioned in Section 5.6.4, in that the monitoring software changes the decimal values from what seems to be rounded numbers (1 kWh) to numbers with decimals at the end of July 2017 (see Appendix G.1). Data series were the energy production is below 1 kWh, the software set the value to 0.

Based on available DC and AC inverter power data, the monthly average inverter efficiency on the south facade BAPV system varies from the lowest 94.33 % in December 2017 to thee highest value in April 2018 of 97.78 % , more details found in Appendix G. In Figure 5.42, the development from January 2016 to April 2018 on the inverter efficiency is shown. Some of the low efficiency on December 2016 can be explained by the fact that there were five days where the monitoring software did not log any energy production, which could have been caused by the data logging resolution. The annual average inverter efficiency is 96.6 % for 2016 and 96.7 % for 2017.

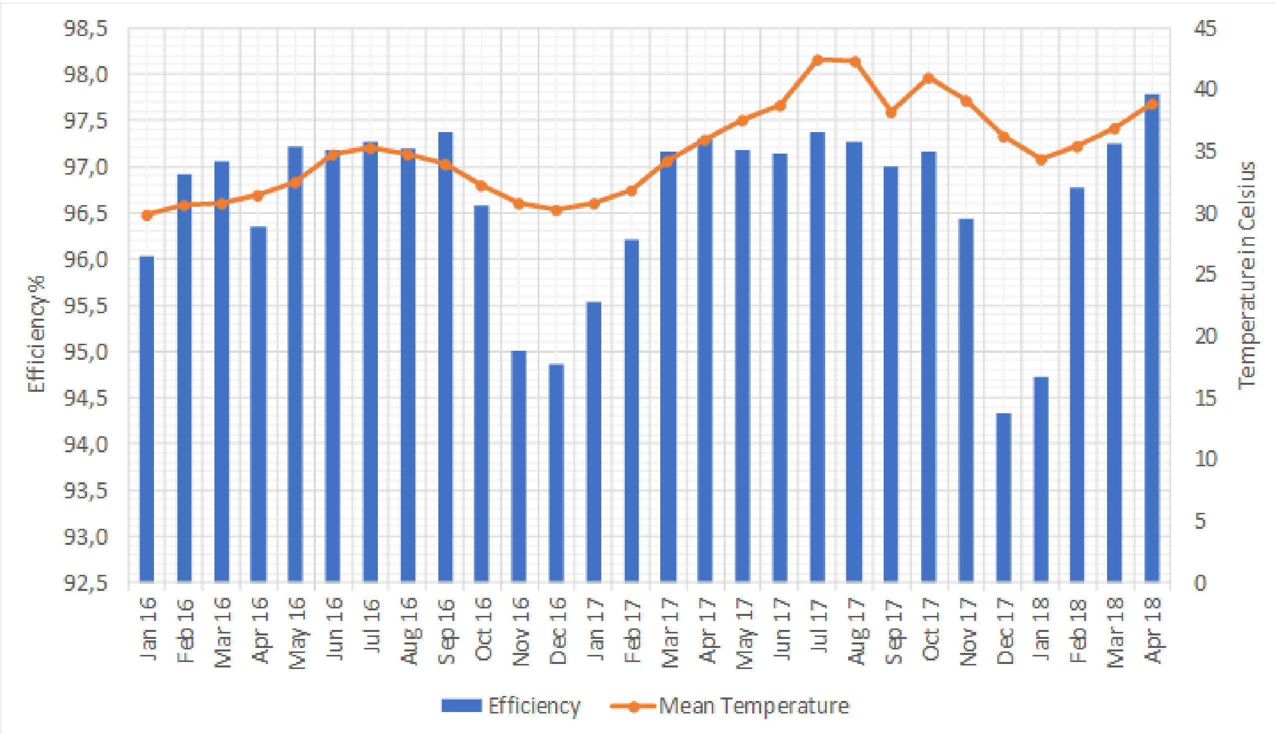

Figure 5.42: Development on the inverter efficiency on the south facade

There are two full years of data available for the energy production on Haldenterminalen. The energy production was 15.7 MWh in 2016 and 15.4 MWh in 2017. Except from some hours missing on a couple of days, the data set is complete. The specific yield in the respective years is 781 kWh/kW$_p$ in 2016 and 770 kWh/kW$_p$ in 2017.

The development of the monthly specific yield for the south facade can be seen in Figure 5.43. The absolute values for the monthly specific yield are given in Appendix G.

In Figure 5.44, the specific yield of both the south facade and the roof installation is given on a monthly basis for 2016 and 2017. The roof has the typical distribution as seen for previous cases, and the facade is evenly distributed from March to September. The facade has almost produced as much energy per installed capacity as the roof the full two first year of available data. Compared with the roof installation, the specific yield of the facade was 94 % in 2016 and 92 % in 2017.

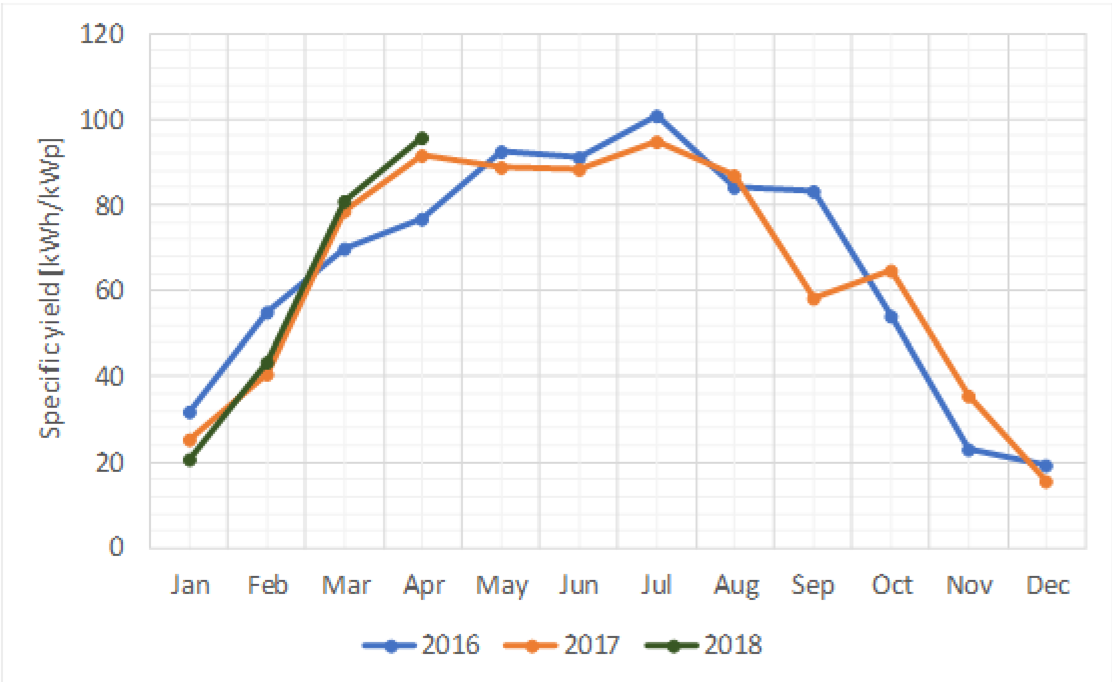

Figure 5.43: Monthly development of the south facade (BAPV) at Haldenterminal

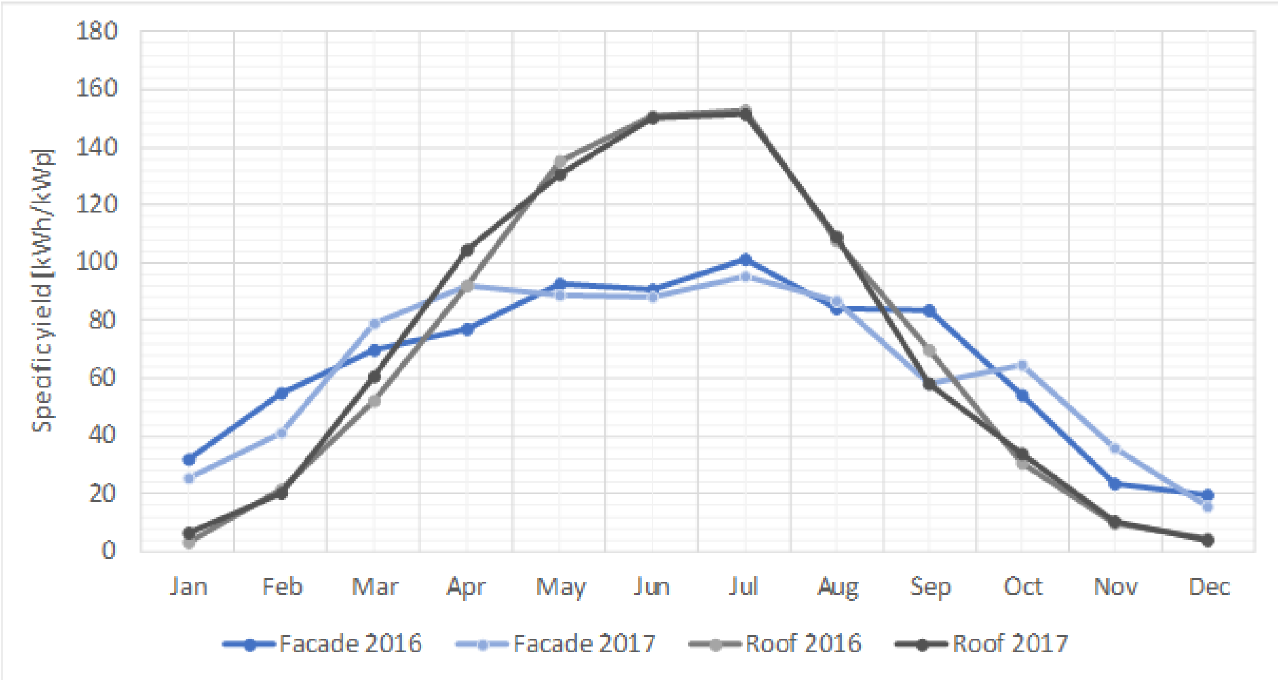

Figure 5.44: Comparison between the PV system on the roof and facade

5.7.5 Lessons learned

According to the system supplier and installer FUSen, there has only been positive feedback from the building owner. In the winter, when the roof was covered with snow, the vertical PV modules on the facade were producing well.

6 Comparison of analyzed cases and discussion

6.1 Individual comparison between simulated and measured values

In this section, the individual cases are compared with the simulated values from PVGIS [52] on the specific yield, and discussion around what can be the reason for variations from the simulated data. The simulated data values are from a typical meteorological year (TMY), not specified to a given time period.

6.1.1 Solsmaragden

Figure 6.1, shows the plotted measured values on site and the simulated values on a monthly basis of the specific yield for one year, with the measured values from May 2017 to April 2018. The tendency is that the measured specific yield is below the simulated data through the year.

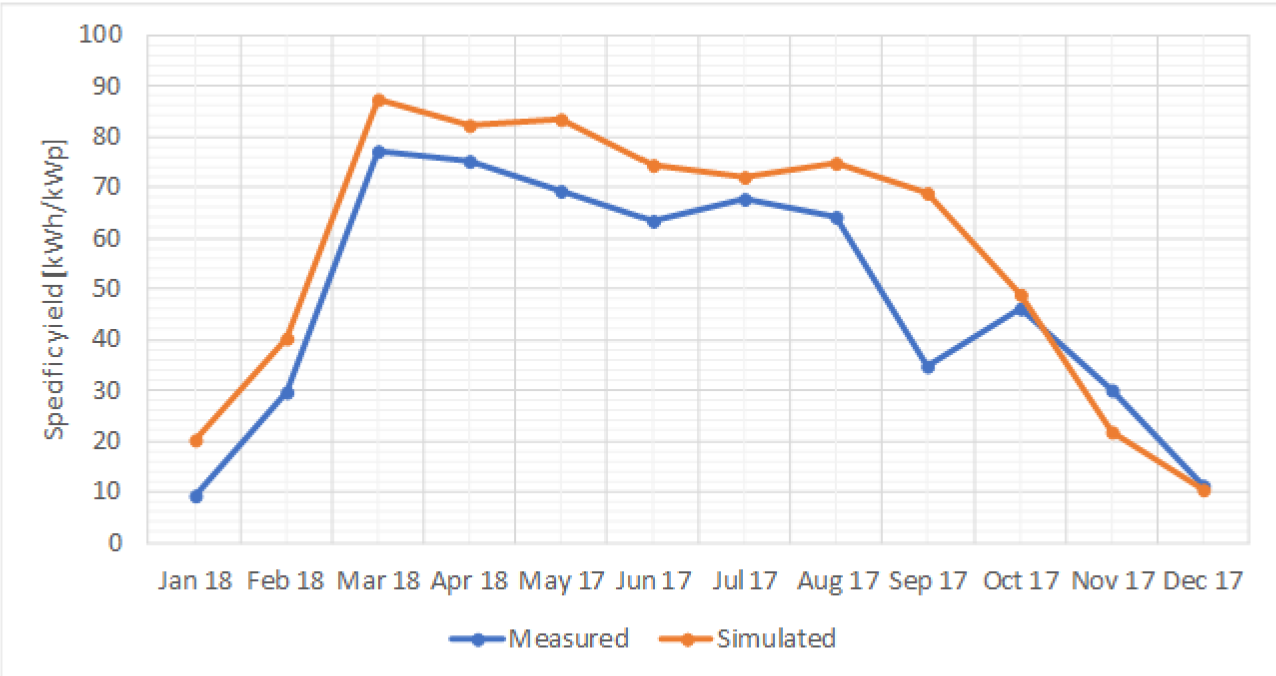

Figure 6.1: Monthly comparison between measured and simulated specific yield at Solsmaragden

Solsmaragden is the only site evaluated with irradiance data available on the south facade. The performance ratio was 0.79 in 2017, which can be seen as a reasonably good PR value, referring to review of literature given in Table 2. The on-site measurements of irradiance on Solsmaragden are compared with the simulated data in Figure 6.2. In September 2017, there is an abnormal low irradiance compared with the simulated data. This observation can explain the drop seen in Figure 6.1.

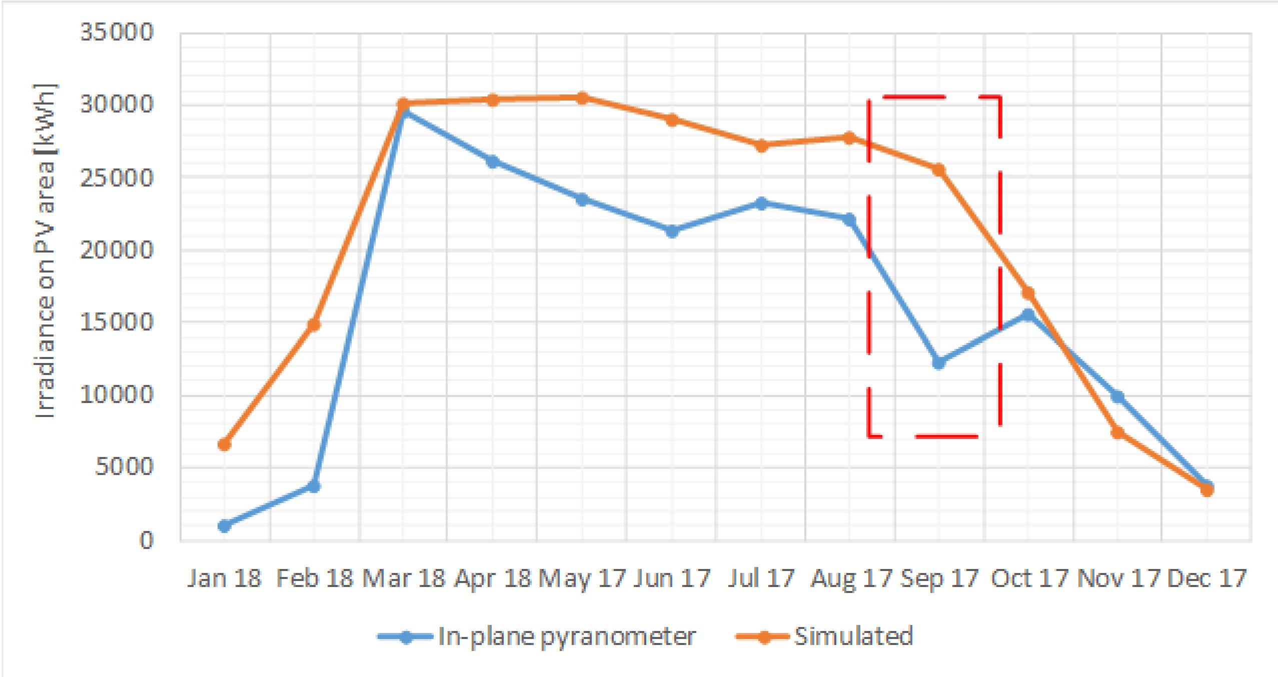

Figure 6.2: Monthly plotted measured irradiance on PV area and the simulated values from PVGIS on Solsmaragden

6.1.2 Brynseng school

In Figure 6.3, the monthly comparison between the simulated and measured data on specific yield is plotted. By examine the plotted graph, it can be seen a variation between the measured and simulated data. As there were missing days of production in both April and June, the contrast is not that significant as the graph illustrates in Figure 6.3. The drop in specific yield in September could be due to the low irradiance, seen in Figure 6.2 as Brynseng is located not that far away from Solsmaragden.

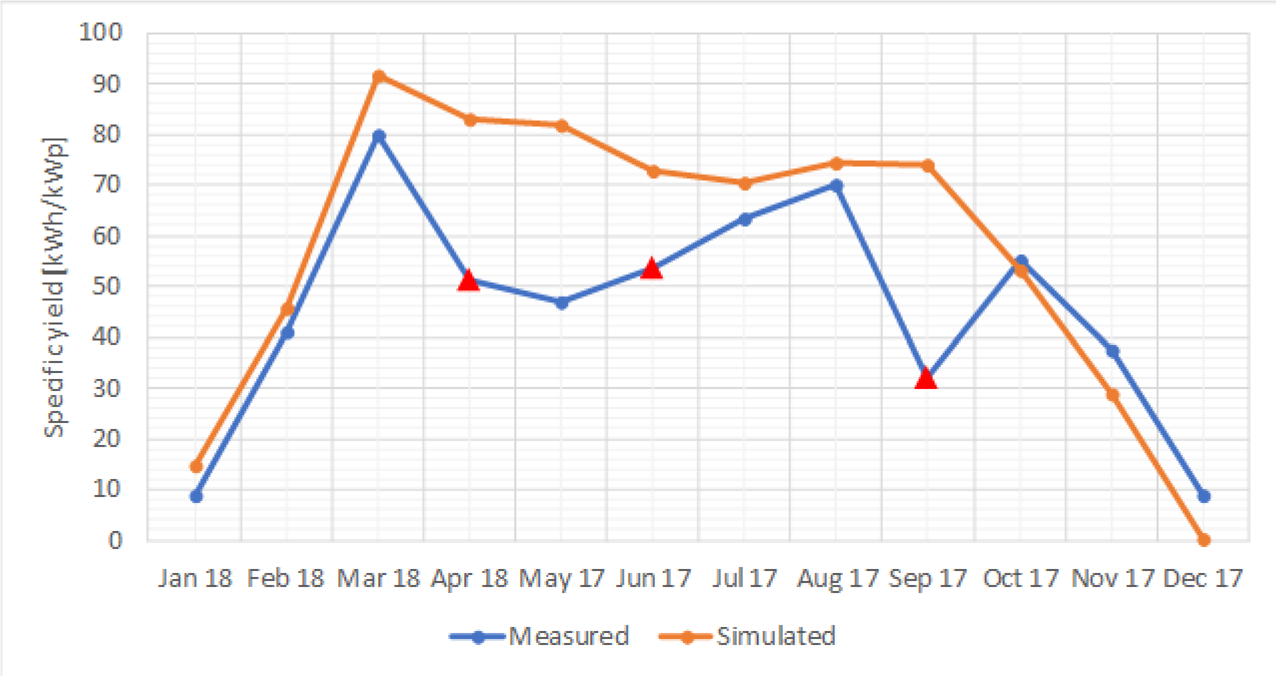

Figure 6.3: Monthly comparison between measured and simulated specific yield at Brynseng

In the simulated data values from ISSOL [65], each string inverter is evaluated on the specific yield. The simulated results from the ISSOL report and the measured values from Figure 5.19, are compared in Figure 6.4. The red dotted rectangles illustrate inverters which deviate from the simulated values from ISSOL.

By examining the graphical plot in Figure 6.4, it seems that the PV supplier has overestimated the specific yield of inverter 2, 3, 5 and 7. If the deviation is from low irradiance, it would have been evident on all of the string inverters, which seem to be close to the simulated values.

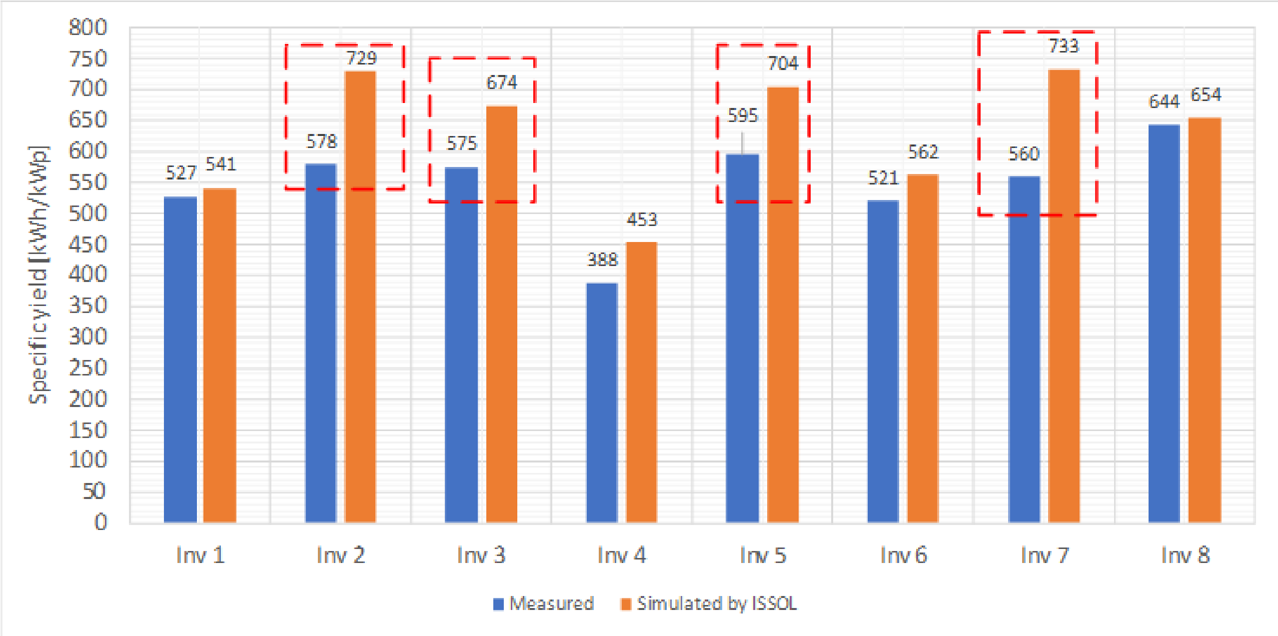

Figure 6.4: Individual inverter comparison between the measured specific yield and simulated data from ISSOL, on Brynseng

As a part of her research, Prof. Anne Gerd Imenes has developed a Matlab script by using equations from [83] on how to transpose the global horizontal irradiance to the plane of array. The global horizontal irradiance data has been retrieved by the author from access to the meteorological web page of eKlima [84] and was implemented in the Matlab code by Prof. Anne Gerd Imenes. In Figure 6.5, the compared values on monthly irradiance (May 2017-March 2018) from the simulations in Matlab and simulated values from PVGIS are shown.

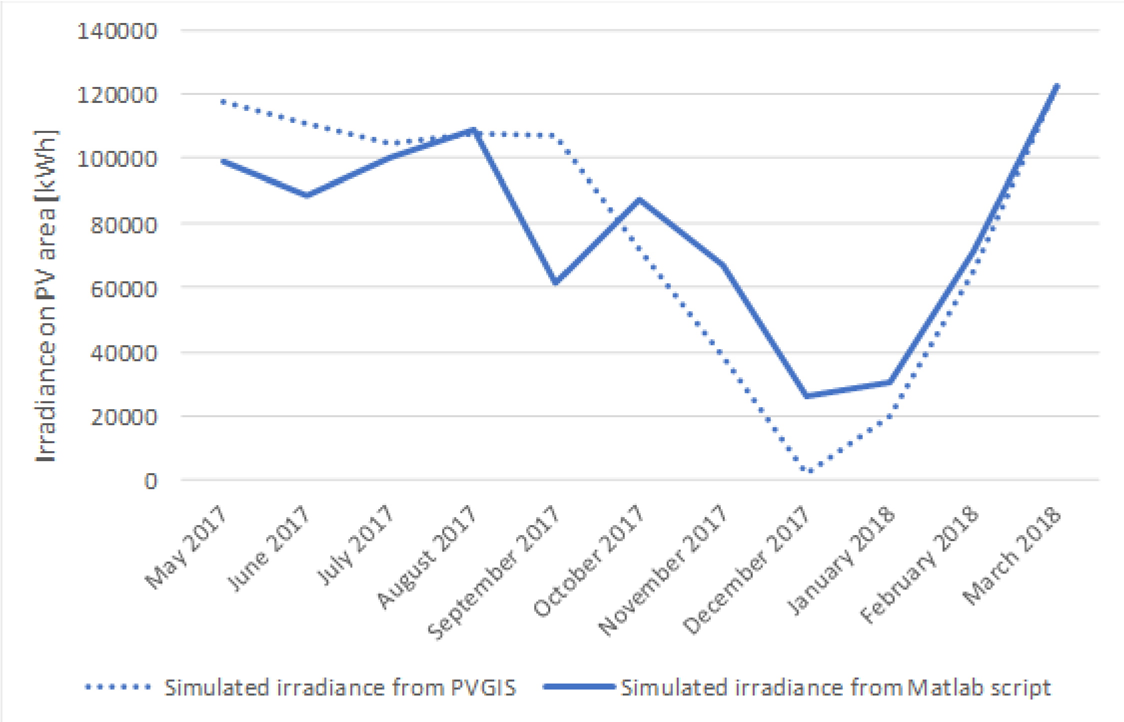

Figure 6.5: The monthly simulated values from Matlab script and PVGIS

By using the simulated irradiance values from the Matlab script in Eq.6 the PR was calculated to 0.58 (data from May 2017 to March 2018) for the total BIPV system on Brynseng.

6.1.3 Bjørkelangen school

Figure 6.6 shows the plotted monthly measured specific yield on site and the simulated values from PVGIS. The PV system was commissioned in December 2017 and this gives few available months of data to compare. Nevertheless, it seems by the plotted graph that the measured values are as expected by the simulation. As this is just a preliminary analysis, it seems that the system values so far are operating in the region of what can be expected.

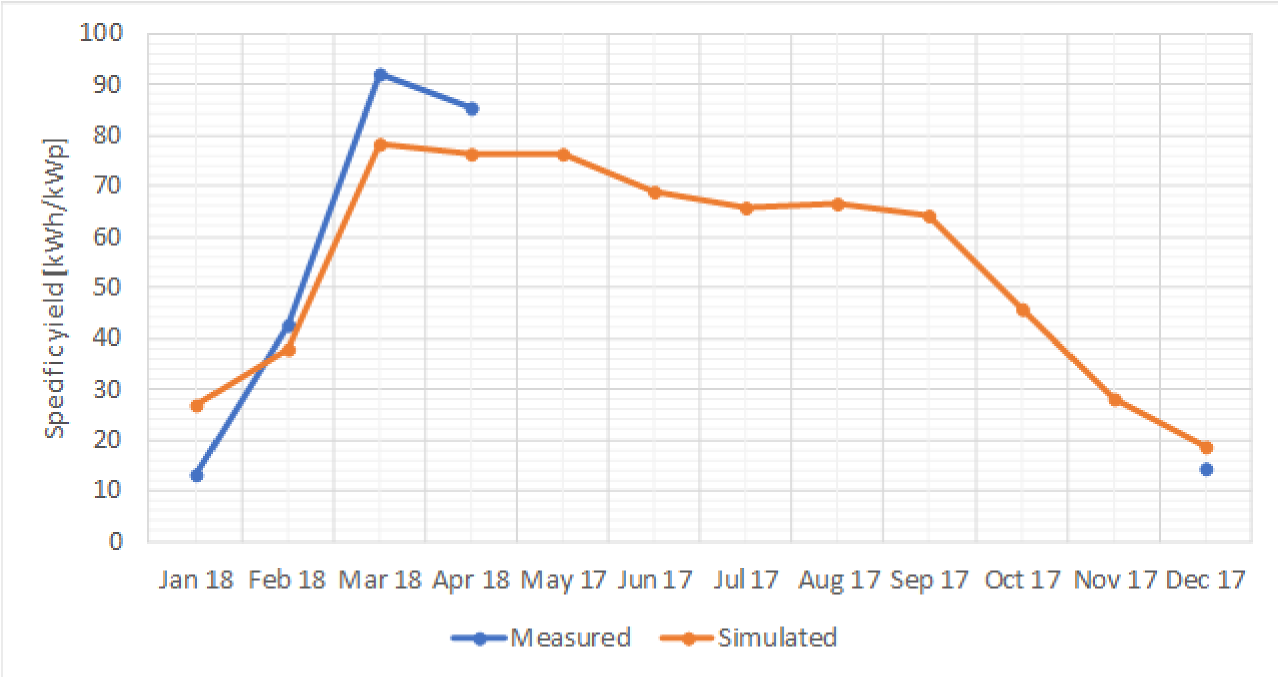

Figure 6.6: Monthly comparison between measured and simulated specific yield at the PV system of Bjørkelangen school

6.1.4 Kiwi Dalgård

There are few months of available measured data from Kiwi Dalgård, as the PV system was commissioned in September 2017. Nevertheless, by examining the comparison between simulated specific yield from PVGIS to the measured in Figure 6.7, the BIPV system is performing as to be expected from simulations.

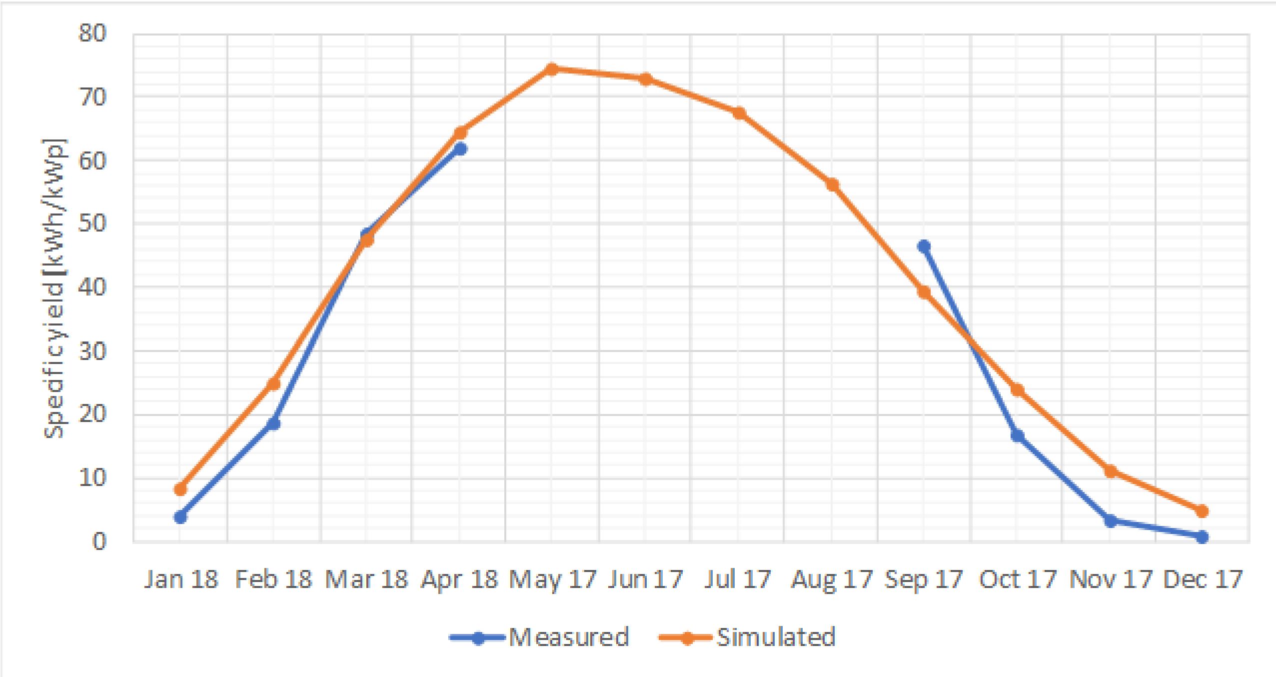

Figure 6.7: Monthly comparison between measured and simulated specific yield of the PV system at Kiwi Dalgård

When the CIGS modules and the two missing facades with mono-Si modules will become operative, the total production generated by the PV system will give more available data to give a more complete analysis.

6.1.5 Kiwi Fjeldset

The small BAPV system on Kiwi Fjeldset has a more even distribution of the monthly specific yield, contrary to the simulated data from PVGIS as shown in Figure 6.8. As the location of the PV system is in a different latitude than the other five cases presented in this master thesis, referring to the abnormal irradiance in September (seen in Figure 6.2 for Solsmaragden), is not adequate. Although, it seems to be representative of this location as well. Nevertheless, the PV system values are operating as expected, when using the simulated data from PVGIS as the reference values.

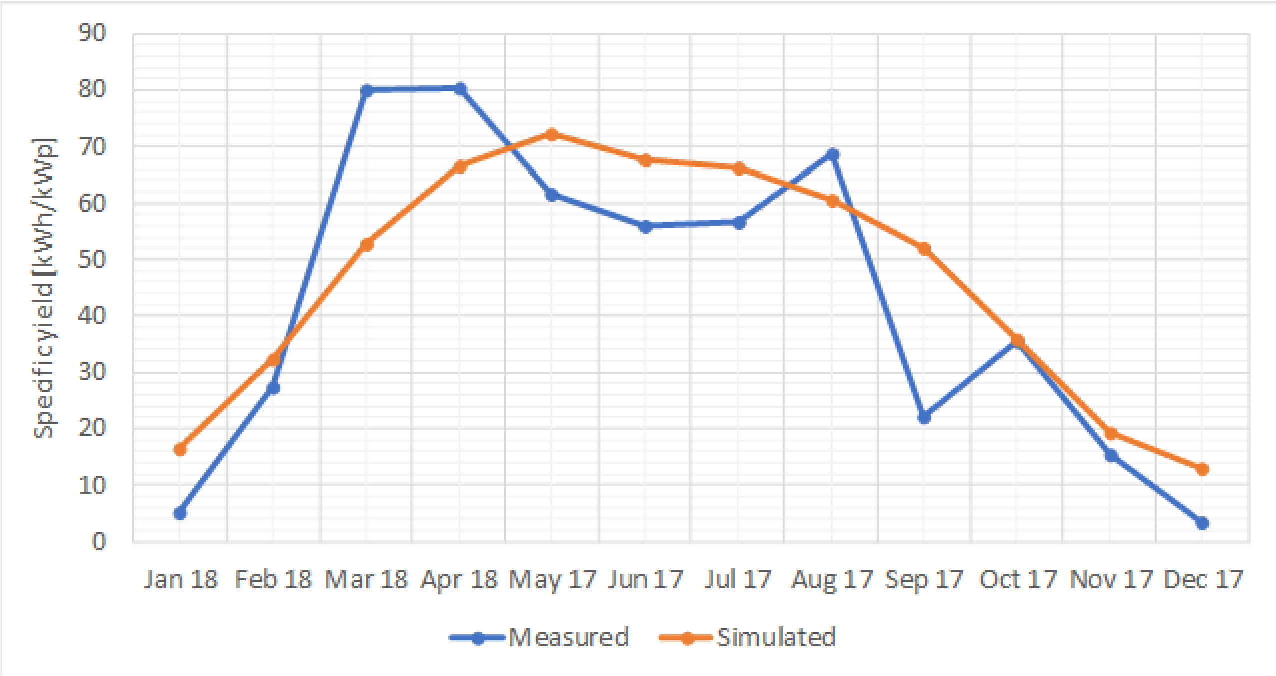

Figure 6.8: Monthly comparison between measured and simulated specific yield of the PV system at Kiwi Fjeldset

6.1.6 ASKO washing hall

As presented in Section 5.6.4, the BAPV system on ASKO washing hall is performing according to what to expect, compared with the Nordic systems in Table 2. in Figure 6.9 the simulated values obtained from PVGIS are compared with the on-site measured energy production data. The measured values correspond well to the simulated, except the drop seen in September 2017. The only reasonable explanation is referring to the low irradiance seen in Figure 6.2. ASKO washing hall is located in the nearby latitude as Solsmaragden.

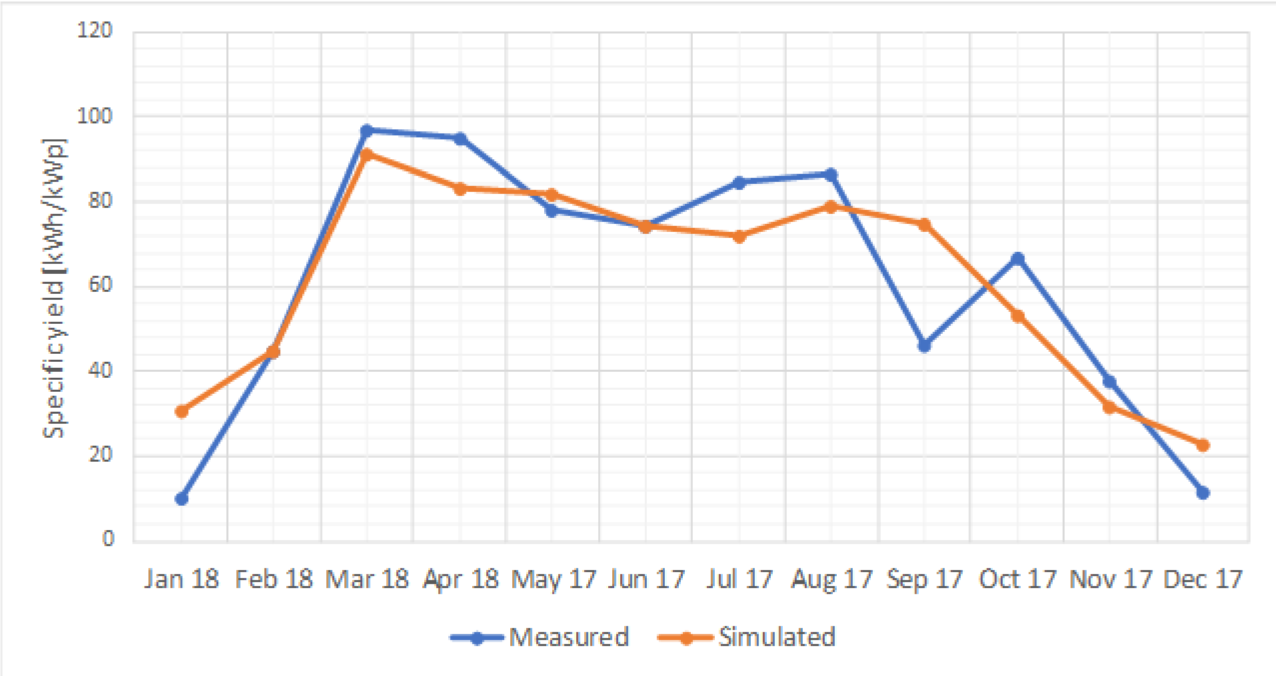

Figure 6.9: Monthly comparison between measured and simulated specific yield of the PV system at ASKO washing hall

6.1.7 Haldenterminalen

Haldenterminalen has the PV system with the longest operating time, with almost three years of available data. In Figure 6.10, the measured specific yield is plotted with the simulated data from PVGIS. It can be seen that the measured values are higher than simulated from March 2017 to August 2018. Through the years of data series, the PV system has performed well and continues to do it.

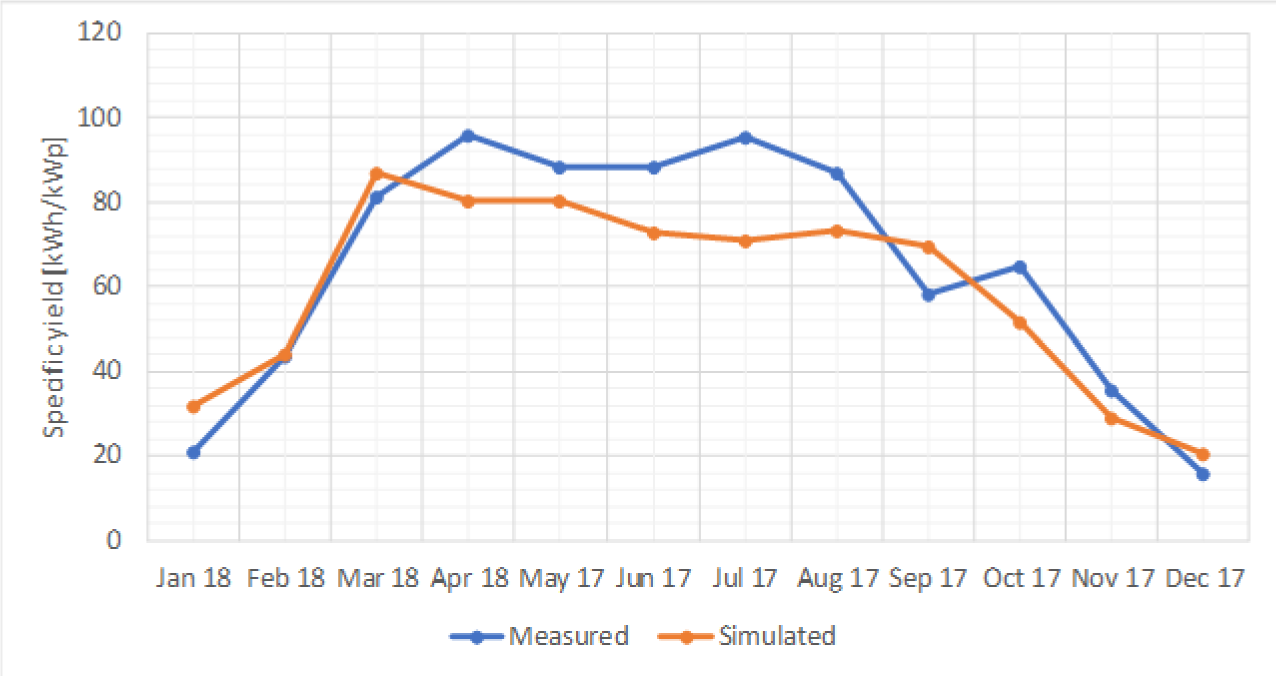

Figure 6.10: Monthly comparison between measured and simulated specific yield of the PV system at Haldenterminalen

6.2 Comparison of the specific yield of the analyzed cases

For evaluating the performance values correctly and comparing the different cases, some comparative conditions are necessary. The irradiance is the first parameter that needs to be known for comparing the different PV systems, as the irradiance varies from location to location and is usually not recorded.

Hence, using the web software provided by PVGIS [52], indicative data on the PV yield and the irradiance at a given side can be obtained. The data is used to evaluate the average irradiance expected on the different locations, and should not be misconceived with actual data on irradiance which occurs on the site.

Some other considerations are the angle of installation, orientation, type of system and technology. The angle of installation is 90° in all of the evaluated cases, but the orientation varies. The orientation is comparable for all the cases besides Kiwi Dalgård which is almost west-oriented. There are three cases with BIPV and four of BAPV systems, but all of them are of mono-Si modules.

Table 18 indicates the expected energy production, specific yield, irradiance, and PV system efficiency. The PV systems are sorted by location, from south to north.

Table 18: Annual simulated values on the specific yield and irradiation using the simulation tool provided by PVGIS [52]

Specific yield, irradiance, and PV system efficiency according to PVGIS simulations							
PV system and location	Halden terminalen (59°7'30"N)	ASKO Washinghall (59°35'18"N)	Solsmaragden (59°35'18"N)	Bjørkelangen (59°52'29"N)	Brynseng (59°54'31"N)	Kiwi Fjeldset (60°52'27"N)	Kiwi Dalgård (63°23'51"N)
Energy production [kWh]	14206	23755	18536	22987	114401	1349	3976
Specific yield [kWh/kWp]	710	740	684	653	690	555	496
Irradiance on PV area [kWh]	122062	176519	250599	184848	986222	10963	40581
PV system efficiency[%]	11.6	13.5	7.4	12.4	11.6	12.3	9.8

Table 19 gives the measured specific yield at the sites on a monthly basis. It can be seen that the annual measured specific yield varies from the simulated in Table 18. Any conclusions from the simulated data on how the PV systems are performing have to be taken carefully. Nevertheless, some irregularities are seen for Solsmaragden and Brynseng, with a measured specific yield 100 kWh/kW_p lower than simulated. Bjørkelangen and Kiwi Dalgaard have too few data available to give some good comparison, though the preliminary energy production at Bjørkelangen seems good. Contrary to the BIPV systems at Solsmaragden and Brynseng. Haldenterminalen and ASKO washing hall have an energy production close to the simulated and for Haldenterminalen even a little better. The PV systems where the air-gap was available are all within the limit that is recommended, according to Section 2.9.

Table 19: Comparison on the specific yield of the different cases and air-gap analyzed in presented section 5

PV system	Halden terminalen	Asko washing hall	Solsmaragden	Bjørkelangen	Brynseng	Kiwi Fjeldset	Kiwi Dalgård
Azimuth°	195	180	205	203	185	200	240
Technology	**mono-Si**						
Capacity [kWp]	20.01	32.1	27.09	35.2	165.585	2.43	8.018
Area [m^2]			267.5	208.2	1046.5		58
Air-gap [mm]	N/A	N/A	48	51	240	N/A	55
1 year	**Specifc yield [kWh/kWp]**						
May 17	88.08	77.88	69.3	-	46.84	61.62	-
Jun 17	88.43	74.17	63.25	-	53.63	56.04	-
Jul 17	95.11	84.64	67.61	-	63.55	56.58	-
Aug 17	87.07	86.42	64.21	-	70.23	68.58	-
Sep 17	58.08	46.32	34.74	-	31.96	22.13	46.58
Oct 17	64.68	67.01	46.2	-	55.18	35.53	16.73
Nov 17	35.54	37.73	30.13	-	37.33	15.33	3.26
Dec 17	15.74	11.28	11.04	14.22	9	3.38	0.74
Jan 18	21.01	10	9.2	13.31	9	4.96	3.85
Feb 18	43.68	44.77	29.61	42.53	40.95	27.43	18.72
Mar 18	80.99	96.73	76.95	92.11	79.93	80.04	48.56
Apr 18	95.68	95.02	75.29	85.31	51.19	80.46	61.84
SUM	774.09	731.97	577.53	-	548.79	512.08	-

It is important to convey that the specific yield is not a performance metric, it is a system value [85]. Although the annual system values differ, the monthly development is very similar, independent on their location and irradiance. The monthly development from each case is shown in Figure 6.11, where the red triangles indicate months with missing data.

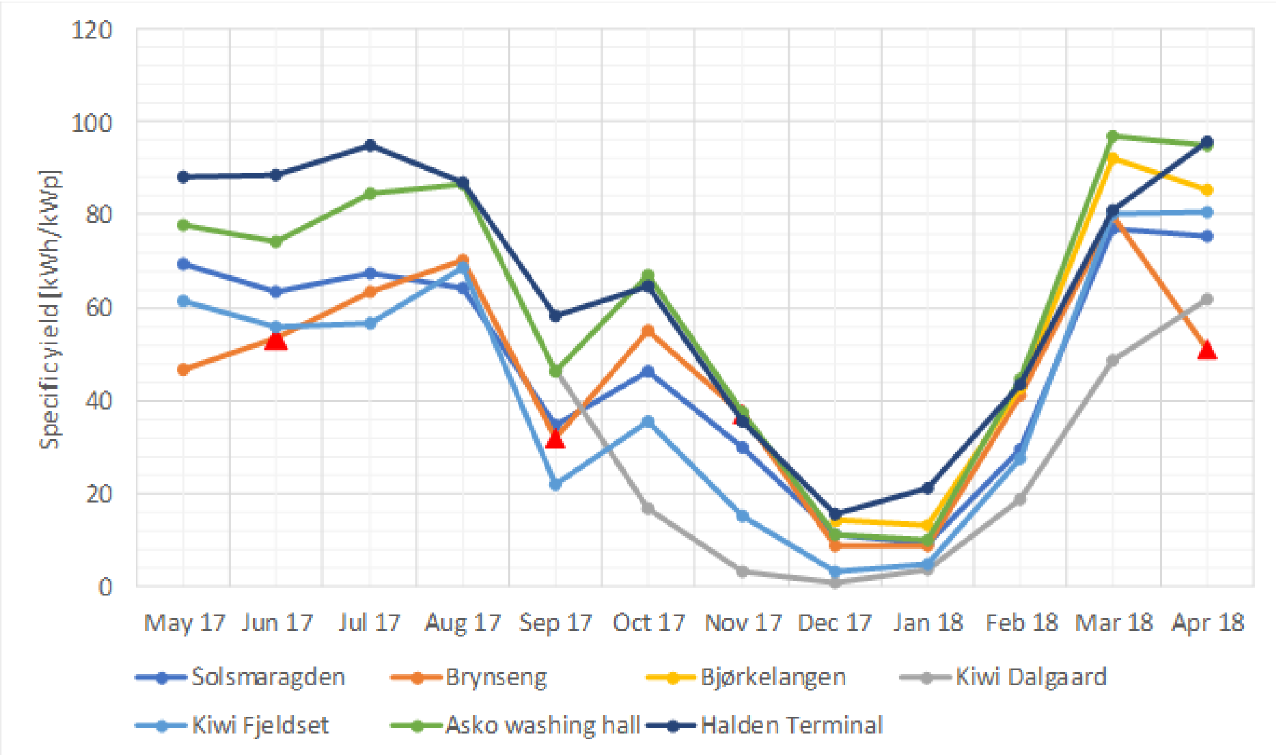

Figure 6.11: Graphically monthly development from May 2017 to April 2018 of each case reviewed in Section 5

The graphically plotted values from Table 19 in Figure 6.11 reveals some variations between the analyzed cases, although the tendency throughout the year is similar for all PV systems. As seen in the individual comparison of simulated and measured specific yield, irradiance is the main contribution for the different system values of specific yield as can be seen in Figure 6.11, as expected from theory (Section 2.2.3). From Figure 6.2, it can be verified that the drop in energy production in September 2017 was due to low irradiance.

6.2.1 Cost comparison

As mentioned in Section 1.3, the absolute cost values numbers on the PV systems are often embedded in the total cost and sometimes a business secret. As input to this master thesis, only three of the seven cases have given insight into the numbers on the cost associated with having a facade of BIPV.

Solsmaragden with an added cost of 29.8 NOK/W_p and Brynseng with 27.5 NOK/W_p for the BIPV system. These buildings are of taylor made modules making them costly, however useful lessons on attachment details and planning have been accomplished. The BAPV system at Bjørkelangen with standard modules had an approximate cost of 13 NOK/W_p, referring to the calculation done in Section 5.3.3.

In a report from B.Thorud [86] in 2013, did an evaluation on different facade materials, with the cost per square meter shown in Figure 6.12.

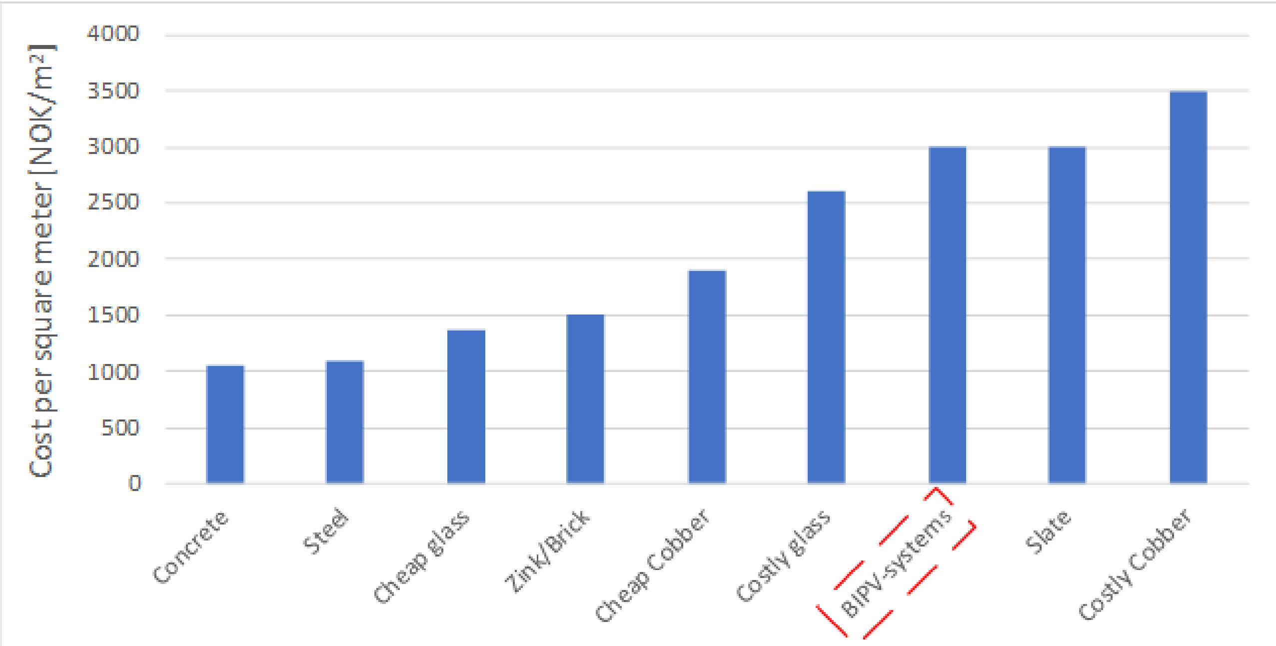

Figure 6.12: Evaluation of different materials used on building facades, retrieved from [86]

The added cost for the BIPV system at Solsmaragden per square meter was 2967 NOK/A_m, which number that has been subtracted as the "normal" facade cost has not been available to the author. The BIPV system at Brynseng had a cost of 7360 NOK/A_m, which are higher then the BIPV system indicated in Figure 6.12. As presented above, the taylor made modules makes the cost associated with the total PV system for Solsmaragden and Brynseng significant higher than a facade with standard modules seen at Bjørkelangen, where the cost is approximately 2200 NOK/A_m.

FUSen is one of the leading companies on PV systems in Norway. Fusen provided in 2018 an updated distribution on cost for a new project. According to FUSen, the cost distribution in Figure 6.13 can be seen as a typical and recently updated cost allocations for a BIPV project [87].

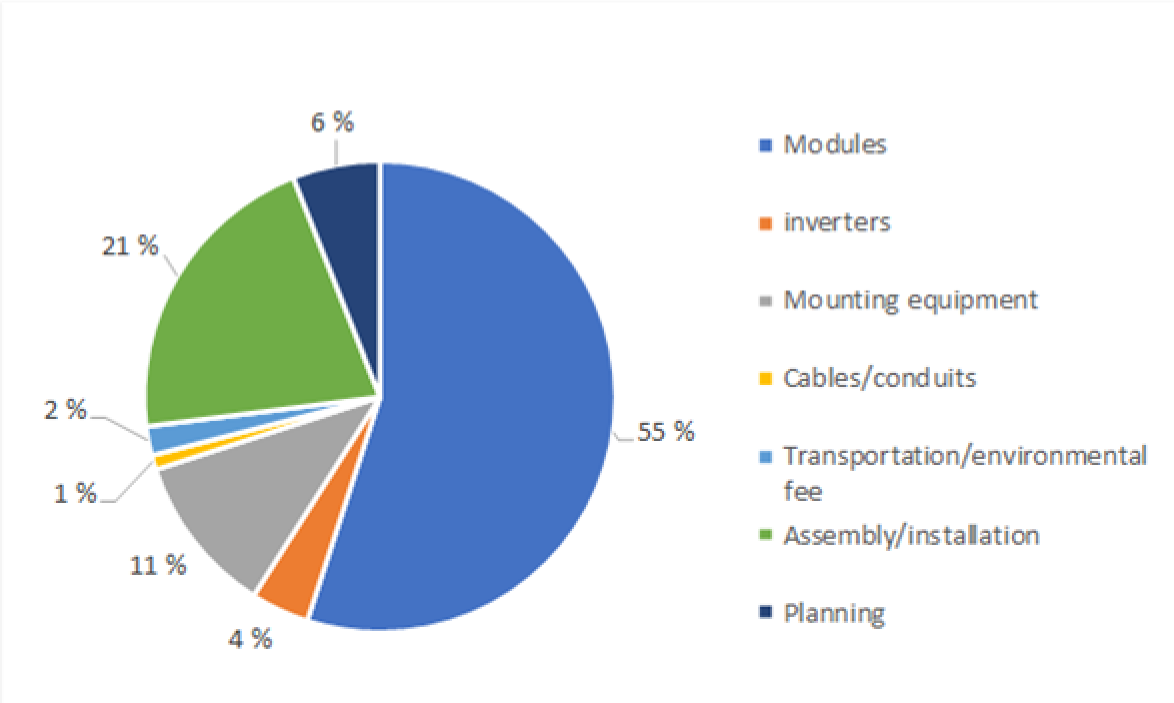

Figure 6.13: Typical cost distribution of the total PV system

The cost distribution in Figure 6.13 from the one in Brynseng in Figure 5.17, where the installation and work was the most prominent cost. Here modules are the highest cost (55 %) which brings promise of cost reduction as BIPV marked grows and costs are expected to go down. The development of mounting details and knowledge about the Norwegian building standards are assumed to reduces the costs associated with installation/assembly, planning and other.

6.3 Lessons learned about the different fastening solutions

The different fastening solutions between the PV modules and the building structure varies, depending on whether using taylor made modules or standard modules with a frame. The fastening solution used on ASKO washing hall and Haldenterminalen has an accessible mounting and is fast to install. This solution seems to be useful for BAPV systems on the facade.

Using PV system of taylor made PV modules with glass-glass structure, as seen on Solsmaragden, Brynseng, and Kiwi Dalgård, the fastening solution has been made specific to the PV system in question. Solsmaragden uses standard glass clamps to attach the PV modules to the brackets (Section 5.1.5).

Brynseng and Kiwi Dalgård both uses a similar fastening solution provided by two different installers, FUSen and Staticus, respectively. Both have a batten/rail glued on to the PV module, with different hook system. The solution at Brynseng presented in Section 5.2.2, have a complicated attachment procedure between the glued batten and the brackets fastened to the building structure (seen in appendix B.1), providing a wide air-gap of 239.5 mm between the PV modules and insulation. The hook system at Kiwi Dalgård and attachment procedure, presented in section 5.4.2, have an easy mounting between the PV module and building structure. The PV module configuration (can be seen in Appendix D.1) is merely clicked on to the vertical rails. The quick installation is beneficial for replacement of the PV modules.

6.4 Summarized discussion of compared cases

The main objective of this master thesis was to contribute to the ongoing research and development of the Norwegian database on BIPV, as part of the national project BIPVNO [5]. As there is limited information available, in addition to short operating time for the BIPV systems, there is no existing basis for comparison of Norwegian BIPVs. The reference basis is of BAPV systems located in Nordic climates. The researchers have mainly been focused on the PR values as this metric is a better foundation for comparing the results. As can be seen in the state of the art Section 3.2, a PR in the region of 0.80 and higher is what is to be expected from a good functioning BAPV system in Nordic conditions.

When elaborating on the results in the Table 19, it can be seen that from May 2017 to August 2017 all of the analyzed systems have a similar tendency of an even development, contrary to the usual summer peak of the typical roof installation. It can be seen that there are some differences in the specific yield. Solsmaragden and Brynseng are not that far in distance from each other, and the irradiation values obtained from PVGIS is quite similar. However, both buildings are not built with the purpose of maximizing the PV system output as for ASKO washing hall and Haldenterminalen, which performs closer to the expected values.

The reason is that the owner in some cases focuses on the aesthetic look, rather than maximizing the energy production of the PV system. This can be seen in Brynseng, where the option of building the south facade as a BIPV came at a late stage in the design phase. The central section of the building has a building extension above the PV modules, also is the depth of the central section broader than the two other. Nevertheless, a BIPV solution can be both aesthetic to look at and have good energy production.

For the individual cases, where there has been performed a comparison between the roof and the facade, the results show that the specific yield of the facade compared with the specific yield of the roof is not that far from each other. The facade systems seem to be operating well at early spring and early autumn. The PV system efficiency is better in the winter season as opposed to the summer, where the module temperature naturally gets higher, because of the higher ambient temperature and intensity of the irradiance (Section 2.2.3).

The facade oriented systems seem to be operating satisfactorily compared with the simulated estimations. It is important to clarify that the values compared are only from one year of data, where longer data series are necessary to give an adequate individual and comparison assessment, respectively.

.

7 Conclusion

The PV systems assessed in this master thesis have a variety of installed capacity, size, and cost. With the rapidly increasing knowledge and research on PV systems, they are well suited to replace traditionally clothed facades. The solution with PV modules on the facade gives an aesthetic look combined with renewable energy production. The common conclusion is that as new knowledge is acquired on the operative PV systems, new projects uses the advantages and becomes more feasible. The PV technology is developing, and new solutions will come on the market.

Facade integrated PV systems in Norway have few available systems and limited data series to analyze. The PV systems examined in this master thesis, cannot be representative of new projects before there are several more years of data series. Nevertheless, the preliminary analysis reveals that the system values seem to be satisfactory. The analyzed cases have similar trends of annual variation on the specific yield. From May 2017 to April 2018, the annual specific yield varies from 500 to 770 kWh/kW_p for the analyzed cases. The variation can to some extent be explained by the geographical location and azimuth angle as can be seen when comparing simulated data from PVGIS.

The locations where there are both roof and facade PV installations shows that the facade energy production is more evenly distributed throughout the year than the roof installation. When comparing the specific yield for the PV systems on the facades with the roof PV systems, the facade systems produced 80-98 % of the roof systems.

Lessons learned so far by assessing the PV systems in this master thesis, are that the technical solution on attaching the PV modules to the facade has improved. As can be seen from Solsmaragden, the first BIPV system analyzed, the time and complexity of the mounting details have been improved significantly to the PV system at Kiwi Dalgård, delivered by the same supplier. Also lessons learned can be used to develop new or improve products, processes, and solutions.

7.1 Recommendations for further work

The recommendations for further work is to keep monitoring the evaluated cases in this master thesis. As more extended data series becomes available, the analysis will become more adequate.

The collection of data from the web software programs is time consuming, and development of a web scraping technique allowing access to all of the data available simultaneously would be beneficial.

The renewable energy community should encourage installers and owners to include irradiance and module temperature sensors. This will give the researchers more metrics to evaluate when analyzing the performance of the PV systems on the facade, with PR and temperature corrected PR.

As several new projects are coming up, they would be interesting to analyze when the time series are available. The combined PV system of CIGS and mono-Si on Kiwi Dalgård is one of those systems.

References

[1] Norges vassdrags og energidirektorat, Nasjonal varedeklarasjon 2016, Accessed 06032018. [Online]. Available: https://www.nve.no/reguleringsmyndigheten-for-energi-rme-marked-og-monopol/varedeklarasjon/nasjonal-varedeklarasjon-2016/

[2] E. Union, "Directive 2009/28/ec of the european parliament and of the council of 23 april 2009 on the promotion of the use of energy from renewable sources and amending and subsequently repealing directives 2001/77/ec and 2003/30/ec," *Official Journal of the European Union*, vol. 5, p. 2009, 2009.

[3] Øystein Holm, "National survey report of pv power applications in norway 2016," *Forskningsrådet and International Energy Agency*, 2017, accessed: 01.02.2018. [Online]. Available: http://www.iea-pvps.org/?id=93

[4] Multiconsult and A. Viak, "Solcellesystemer og sol i systemet," p. 31, 2018, accessed: 15.05.2018. [Online]. Available: http://solenergiklyngen.no/app/uploads/sites/4/180313-rapport_solkraft-markedsutvikling-2017-endelig.pdf

[5] Building Integrated Photovoltaics for Norway project, homepage, Accessed 12.05.2018. [Online]. Available: http://bipvno.no/

[6] IEA-PVPS. (2015) Enabling framework for the acceleration of bipv. Accessed: 06.03.2018. [Online]. Available: http://www.iea-pvps.org/index.php?id=task15

[7] S. R. Wenham, M. A. Green, and M. E. Watt, *Applied Photovoltaics*. Centre for Photovoltaic Devices and Systems, 2005, pages 5-9,46-53, 89-90 ,97-99,127,181-182.

[8] C. Honsberg and S. Bowden, "Standard solar spectra," accessed: 20.01.2018. [Online]. Available: http://www.pveducation.org/pvcdrom/appendices/standard-solar-spectra

[9] pv education. (2018) Solar radiation on a tilted surface. Accessed 15.02.2018. [Online]. Available: https://www.pveducation.org/pvcdrom/properties-of-sunlight/solar-radiation-on-a-tilted-surface

[10] sandia national laboratories. (2018) Plane of array (poa) irradiance. Accessed 11.02.2018. [Online]. Available: https://pvpmc.sandia.gov/modeling-steps/1-weather-design-inputs/plane-of-array-poa-irradiance/

[11] H. Z. A. Garni, A. Awasthi, and M. A. Ramli, "Optimal design and analysis of grid-connected photovoltaic under different tracking systems using homer," *Energy Conversion and Management*, vol. 155, pp. 42 – 57, 2018. [Online]. Available: http://www.sciencedirect.com/science/article/pii/S0196890417310221

[12] G. Masson and I. Kaizuka, "Iea pvps annual trend report of 2017," 2018, chapter 1, Accessed: 10.05.2018. [Online]. Available: http://www.iea-pvps.org/?id=256

[13] I. E. Commission *et al.*, "Standard iec 60904-3: photovoltaic devices," *Part 3: Measurement Principles for Terrestrial Photovoltaic (PV) Solar Devices With Reference Spectral Irradiance Data*, 1987.

[14] F. Fazelpour, M. Vafaeipour, O. Rahbari, and R. Shirmohammadi, "Considerable parameters of using pv cells for solar-powered aircrafts," *Renewable and Sustainable Energy Reviews*, vol. 22, pp. 81 – 91, 2013, accessed: 15.03.2018. [Online]. Available: http://www.sciencedirect.com/science/article/pii/S1364032113000476

[15] G. Stapleton, S. Neill, and G. Miline, "Photovoltaic systems," 2013, accessed: 25.01.2018. [Online]. Available: http://www.yourhome.gov.au/energy/photovoltaic-systems

[16] Manz. Solar. Accessed 12.05.2018. [Online]. Available: https://www.manz.com/markets/solar/

[17] D. Sera, R. Teodorescu, and P. Rodriguez, "Pv panel model based on datasheet values," in *2007 IEEE International Symposium on Industrial Electronics*, June 2007, pp. 2392–2396.

[18] C. Honsberg and S. Bowden, "Solar cell efficiency," accessed: 30.01.2018. [Online]. Available: http://www.pveducation.org/pvcdrom/solar-cell-efficiency

[19] International Electrotechnical Commission, IEC-61853-1:2011, Photovoltaic (PV) module performance testing and energy rating - Part 1: Irradiance and temperature performance measurements and power rating, accessed: 14.05.2018, online: https://webstore.iec.ch/publication/6035.

[20] K. Paghasian and G. TamizhMani, "Photovoltaic module power rating per iec 61853 2013;1: A study under natural sunlight," in *2011 37th IEEE Photovoltaic Specialists Conference*, June 2011, pp. 002 322–002 327.

[21] C. R. et al., "Uncertainties in pv system yield predictions and assessments," iEA-PVPS, Task 13, Subtasks 2.3 & 3.1.

[22] D. C. Jordan and S. R. Kurtz, "Photovoltaic degradation rates—an analytical review," *Progress in photovoltaics: Research and Applications*, vol. 21, no. 1, pp. 12–29, 2013.

[23] PV education.org, Degradation and failure modes, accessed: 14.05.2018, online: https://www.pveducation.org/pvcdrom/modules/degradation-and-failure-modes.

[24] IEA-PVPS, task 13, Performance and Reliability of Photovoltaic Systems, online: http://www.iea-pvps.org/index.php?id=57, accessed: 14.05.2018.

[25] U. E. I. Administration. (2018) Solar explained, photovoltaics and electricity. Accessed: 30.04.2018. [Online]. Available: https://www.eia.gov/energyexplained/?page=solar_photovoltaics

[26] Florida solar energy center,How a PV system works, Accessed: 10.02.2018. [Online]. Available: http://www.fsec.ucf.edu/en/consumer/solar_electricity/basics/how_pv_system_works.htm

[27] B. P. Association. (2018) How solar pv works. Accessed: 12.02.2018. [Online]. Available: http://www.bpva.org.uk/solar-photovoltaic/how-solar-pv-works/

[28] J. S. Stein, “Pv performance modeling methods and practices,” 2017, pages 21-23.

[29] S. S. Technology, “Solar inverters,” 2018, accessed: 13.05.2018. [Online]. Available: https://www.sma.de/en/products/solarinverters.html

[30] N. H. Reich, B. Mueller, A. Armbruster, W. G. J. H. M. Sark, K. Kiefer, and C. Reise, “Performance ratio revisited:,” *Progress in Photovoltaics: Research and Applications*, vol. 20, no. 6, pp. 717–726, 9 2012.

[31] M. Allaby, *Basics of environmental science.* Routledge, 2002.

[32] S. A. Kalogirou, L. Aresti, P. Christodoulides, and G. Florides, “The effect of air flow on a building integrated pv-panel,” *Procedia IUTAM*, vol. 11, pp. 89 – 97, 2014, iUTAM Symposium on Nonlinear Interfacial Wave Phenomena from the Micro- to the Macro-Scale.

[33] International standard, IEC 61724, Accessed: 17.04.2018. [Online]. Available: https://webstore.iec.ch/publication/33622

[34] S. James Mokri and C. Joe Cunningham, “Pv system performance assessment,” *The SAM Virtual Conference*, vol. 2.0, p. 28, Jun. 2014, accessed: 19.03.2018. [Online]. Available: http://sunspec.org/wp-content/uploads/2015/06/SunSpec-PV-System-Performance-Assessment-v2.pdf

[35] J. Meydbray, K. Emery, and S. Kurtz, “Pyranometers and reference cells, what’s the difference?” *NREL/JA*, pp. 1–5, 2012.

[36] J. Meydbray, E. Riley, L. Dunn, K. Emery, and S. Kurtz, “Pyranometers and reference cells: Part 2: What makes the most sense for pv power plants?; preprint,” National Renewable Energy Laboratory (NREL), Golden, CO., Tech. Rep., 2012.

[37] WMO, “Guide to meteorological instruments and methods of observation,” *WMO No.8*, 2008, geneva, Switzerland.

[38] L. Dunn, M. Gostein, and K. Emery, “Comparison of pyranometers vs. pv reference cells for evaluation of pv array performance,” in *2012 38th IEEE Photovoltaic Specialists Conference*, June 2012, pp. 002 899–002 904.

[39] J. U. et al., “Performance, reliability and analysis of photovoltaic systems, task 2,” A part of International Energy Agency Photovoltiac Power Systems Programme, Finished 2010, accessed 08.03.2018. [Online]. Available: http://iea-pvps.org/index.php?id=30

[40] U. Jahn, W. Nasse, T. Nordmann, L. Clavadetscher, and D. Mayer, “19th eupvsec,” in *Achievements of task 2 of IEA PV power systems programme: final results on PV system performance*, Paris, France, 2004, pp. 2813–2816.

[41] J. Leloux, L. Narvarte, and D. Trebosc, “Review of the performance of residential pv systems in france,” *Renewable and Sustainable Energy Reviews*, vol. 16, no. 2, pp. 1369 – 1376, 2012.

[42] J. L. et al., “Review of the performance of residential pv systems in belgium,” *Renewable and Sustainable Energy Reviews*, vol. 16, no. 1, pp. 178 – 184, 2012.

[43] W. G. v. S. Thomas Nordmann, Luzi Clavadetscher and M. Green, “Analysis of long-term performance of pv systems different data resoultion for different purposes,” TNC Conuslting AG, Utrecht Univeristy, M.G.Lightning Electrical Engineering, resreport, Nov. 2014, iEA PVPS Task 13, Subtask 1 Report IEA-PVPS T13-05:2014 ISBN 978-3-906042-21-3.

[44] Øystein Kleven and H. Persson, “Solar power plants in the north,” PiteEnergi AB, techreport, May 2015.

[45] D. M. Mutungi, “Degradation of photovoltaics in central finland: A comparative study of polycrystalline and heterojunction with intrinsic thin layer technologies,” Master’s thesis, University of Jyväskylä, Sep. 2013.

[46] A. G. Imenes, H. G. Beyer, K. Boysen, J. O. Odden, and R. E. Grundt, “Performance of grid-connected pv system in southern norway,” in *2015 IEEE 42nd Photovoltaic Specialist Conference (PVSC)*, June 2015, pp. 1–6.

[47] A. G. Imenes, “Performance of bipv and bapv installations in norway,” in *Photovoltaic Specialists Conference (PVSC), 2016 IEEE 43rd*. IEEE, 2016, pp. 3147–3152.

[48] E. C. Camou, “Performance analysis on pv plant in norway,” mathesis, Dalarna Univeristy, Sep. 2017.

[49] T. B. Åsheim, “Analysis of a photovoltaic power plant at evenstad,” mathesis, Norwegian University of Science and Technology, Jun. 2017.

[50] SMA, “Sunny portal,” 2018, accessed; 26.04.2018. [Online]. Available: https://www.sma.de/en/products/monitoring-control/sunny-portal.html#Professional-Package-10854

[51] IBC. (2018) Ibc solportal pro. Accessed: 05.02.2018. [Online]. Available: https://www.ibc-solar.com/login/

[52] T. E. Commission. (2012) Photovoltaic geographical information system (pvgis). Accessed 05.05.2018. [Online]. Available: http://re.jrc.ec.europa.eu/pvgis/

[53] Interviews performed by Anne Gerd Imenes at Teknova (2017), as part of the project “Building integrated photovoltaics for Norway”, Norwegian Research Council EnergiX project number 244031. Interview subjects: Mr Steinar Nilsen, FUSen, Oslo; and Mr Trond Åsheim, Union Eiendomsutvikling, Drammen.

[54] Interviews performed by Anne Gerd Imenes at Teknova (2017), as part of the project “Building integrated photovoltaics for Norway”, Norwegian Research Council EnergiX project number 244031. Interview subjects: Mrs Magnhild Kallhovd, Undervisningsbygg Oslo KF; and Mrs Bodil Motzke, Utdanningsetaten, Oslo commune.

[55] Interviews performed by Anne Gerd Imenes at Teknova (2018), as part of the project “Building integrated photovoltaics for Norway”, Norwegian Research Council EnergiX project number 244031. Interview subjects: Mr Steinar Nilsen, FUSen, Oslo.

[56] C. Jardine and G. Conibeer, "Pv-compare: Direct comparison of eleven pv technologies at two locations in northern and southern europe," 11 2017.

[57] S. Norge, "Criteria for passive houses and low energy buildings non-residential buildings," *Standard Norge*, 2007, accessed: 13.04.2018. [Online]. Available: http://www.standard.no/en/webshop/ProductCatalog/ProductPresentation/?ProductID=587802

[58] T. Haumann, "A breif look at the performance of pv in norway," Master's thesis, Univeristy of Tromsø, Dec. 2016.

[59] S. B. Lund. Energibygget på union brygge - passivhus med høy standard og solcellefasade. Accessed 15.03.2018. [Online]. Available: https://malling.no/tjenester/markets/finn-lokaler-til-leie/eiendom/?adId=53194726&ismalling=1

[60] ISSOL. (2016) Solsmaragden, union brygge, drammen. Accessed: 09.04.2018. [Online]. Available: http://www.issol.eu/solsmaragden-union-brygge-drammen/

[61] Personal communcaiton, Morten Gregertsen, Union eiendom, 22.05.2018.

[62] P. group, "Glassklemme," 2018, retrived on 09.05.2018. [Online]. Available: http://www.pks.no/glassklemme_modell_40_41/cms/74

[63] ENOVA. (2018) Enova's business strategy. Accessed 27.04.2018. [Online]. Available: https://www.enova.no/om-enova/

[64] Motzke, B. (2018). Et skolebygg å være stolt av. [pdf] p.9. [Accessed 28 May. 2018].

[65] ISSOL, "Photovoltiac system sizing report-brynseng skole," ISSOl, Tech. Rep., 2016, confidental.

[66] Rockwool group, RedAir system, brochure, accessed: 28.05.2018, online :https://www.rockwool.no/konstruksjoner/vegg/fasadeisolering-og-fasaderenovering/redair-flex-ventilerte-fasader/.

[67] Notes from telephone meeting between Anne Gerd Imenes at Teknova and Per Urdahl, Solel, Tuesday 31. August 2017.

[68] Personal communication, Per Urdahl, SolEl ,23.03.2018,.

[69] Personal communication, Ole-Christian Østreng, Aurskog-Høland municipality, 21.03.2018.

[70] Norgesgruppen. Dette er norgesgruppen. Accessed: 19.03.2018. [Online]. Available: http://www.norgesgruppen.no/om-oss/dette-er-norgesgruppen/

[71] T. C. Tuv. (2017) Kiwi åpner norges grønneste butikk. Accessed 07.04.2018. [Online]. Available: https://www.fusen.no/single-post/2017/09/04/KIWI-%C3%A5pner-Norges-gr%C3%B8nneste-butikk

[72] Norgesgruppen. (2017) Dalgård i trondheim. Accessed 27.03.2018. [Online]. Available: https://norgesgruppeneiendom.no/prosjekter/dalgaard-byaasen-i-trondheim/

[73] ——. (2017) Kiwi dalgård. Accessed 20.03.2018. [Online]. Available: https://kiwi.no/Tema/samfunnsansvar/Miljo-og-barekraft/i-dag-apnet-kiwis-nye-miljobutikk-i-trondheim/

[74] Interview performed by Christian Hals Frivold, student at University of Agder (2018), Interview object: Geir Fikke, FUSen AS, 13.03.2018.

[75] Manz. (2018) Thin film modules. Accessed 10.05.2018. [Online]. Available: https://www.manz.com/en/

[76] ENOVA. (2017) Kiwi dalgård miljøbutikk. Accessed 23.04.2018. [Online]. Available: https://www.enova.no/om-enova/om-organisasjonen/teknologiportefoljen/kiwi-dalgard-miljobutikk/

[77] Byggindustrien. (2017) Kiwi dalgård. Accessed 24.04.2018. [Online]. Available: http://www.bygg.no/article/1325407

[78] Personal e-mail communcation, Ine Maribu, Karl Knudsen AS, 28.05.2018.

[79] Byggindustrien, “Kiwi fjeldset,” 2016, retrived 06.05.2018. [Online]. Available: http://www.bygg.no/article/1266692

[80] Kiwi. (2016) Miljøbutikk av hel ved. Accessed 15.04.2018. [Online]. Available: http://www.mynewsdesk.com/no/kiwi-norge/images/kiwi-fjeldset-elverum-529517

[81] K. Group. (2017) Referanseprosjekt asko. Accessed: 12.04.2018. [Online]. Available: https://www.kingspan.com/no/nb-no/produkter/sandwichelement/referanseprosjekter/asko-nn

[82] K. Systems. Speedrail system. Accessed: 12.04.2018. [Online]. Available: https://k2-systems.com/en/products/speedrail-system

[83] John A. Duffie and William A. Beckman, Solar Engineering of Thermal Processes, Second Edition, John Wiley & Sons, USA, 1991.

[84] Norwegian Meteorological Institute, eKlima, homepage, accessed: 28.05.2018, online: http://sharki.oslo.dnmi.no/portal/page?_pageid=73,39035,73_39049&_dad=portal&_-schema=PORTAL.

[85] J. Mokri and J. Cunningham, “Pv system performance assessment,” *SunSpec Alliance, USA*, 2014.

[86] Powerpoint from Dr. Ing. Bjørn Thorud, Multiconsult, Smartgridkonferansen 2013, Solceller i Norge- Når blir det lønnsomt?,online: https://smartgrids.no/wp-content/uploads/sites/4/2013/10/7_3_Thorud.pdf, accessed 25.05.2018.

[87] Personal communication, Steinar Nilsen, FUSen, 27.04.2018.

Appendix A Solsmaragden

Table A1: Efficiency and Performance Ratio on the south facade at Solsmaragden

Month	Eff (inv7) (%)	Eff (Inv8) (%)	PR (Inv7)	PR (Inv8)	Specific Yield (Inv 7)	Specific Yield (Inv 8)	Eff (%) South facade	PR South facade	Specific yield South facade
Jan 17	8.30	8.36	0.84	0.82	9.60	9.33	8.35	0.82	9.41
Feb 17	9.21	9.39	0.93	0.92	36.01	35.39	9.33	0.92	35.56
Mar 17	7.99	8.10	0.81	0.79	63.02	61.56	8.07	0.80	61.97
Apr 17	8.26	8.24	0.84	0.81	73.90	71.01	8.25	0.81	71.83
May 17	8.03	7.98	0.81	0.78	71.46	68.45	7.99	0.79	69.30
Jun 17	8.06	7.99	0.82	0.78	65.34	62.42	8.01	0.79	63.25
Jul 17	7.90	7.84	0.80	0.77	69.81	66.74	7.86	0.78	67.61
Aug 17	7.88	7.83	0.80	0.77	66.21	63.43	7.84	0.77	64.21
Sep 17	7.61	7.69	0.77	0.75	35.41	34.48	7.67	0.76	34.74
Oct 17	7.88	8.04	0.80	0.79	46.77	45.98	7.99	0.79	46.20
Noc 17	8.12	8.20	0.82	0.80	30.71	29.90	8.18	0.81	30.13
Dec 17	7.70	8.04	0.78	0.79	10.99	11.06	7.95	0.78	11.04
Jan 18	6.50	6.74	0.66	0.66	9.20	9.20	6.67	0.66	9.20
Feb 18	7.25	7.37	0.74	0.72	30.04	29.44	7.33	0.72	29.61
Mar 18	7.01	7.05	0.71	0.69	78.67	76.27	7.04	0.70	76.95
Apr 18	7.83	7.78	0.79	0.76	77.66	74.35	7.80	0.77	75.29

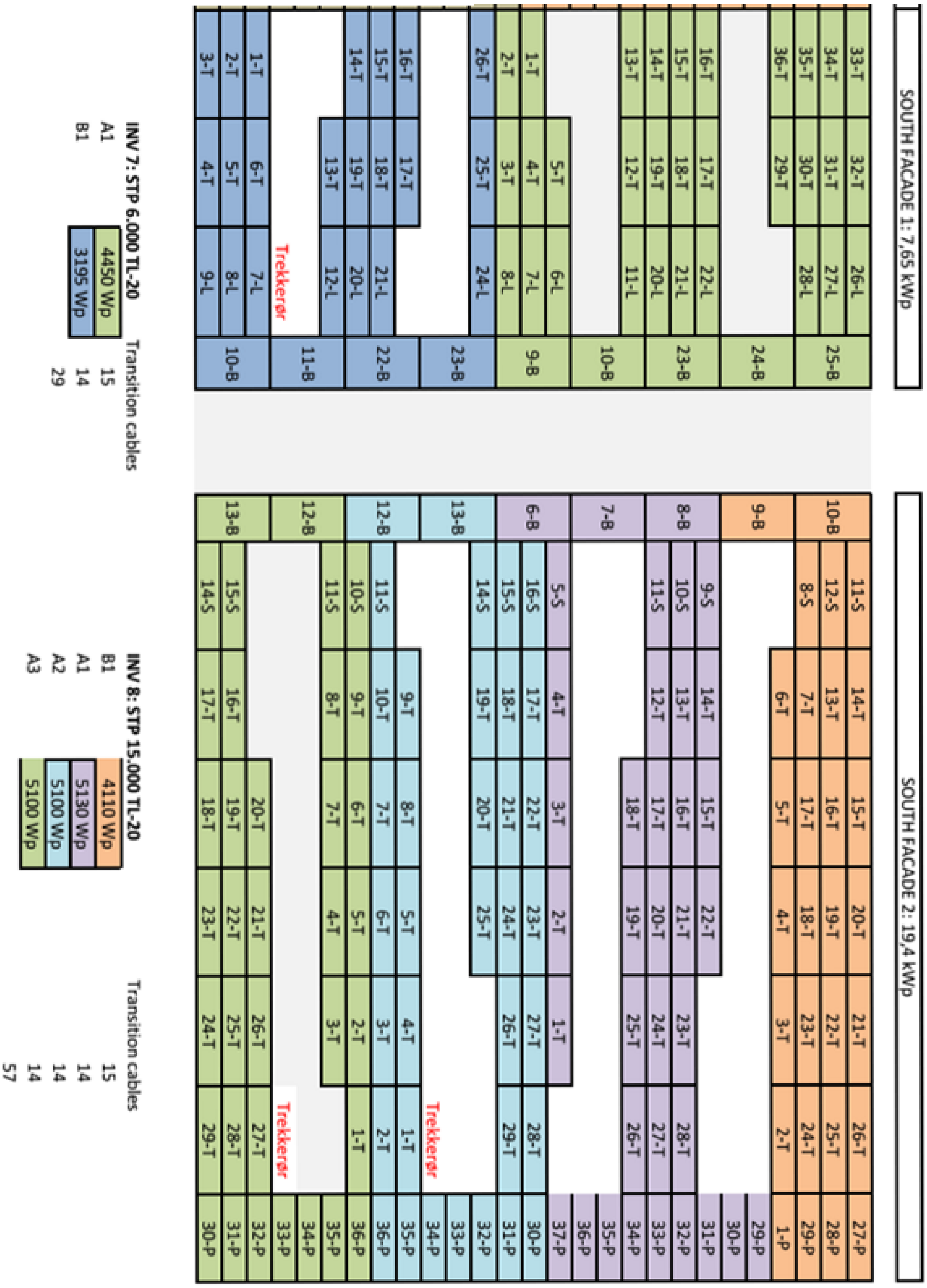

Figure A.1: The string design of inverter 7 and 8 on the south facade of Solsmarageden

Datasheets of the PV modules at the south facade of Solsmaragden

ISSOL - PRODUCT DESIGN

ISSOL Performance & Harmony

ISO 9001 QUALITÉ 1006 OSI GESTION DE QUALITÉ

CENIT 220 - MODEL - 70 - 6112 - Type B

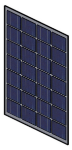

PV module type		Bi-Glass
Dimensions	(mm)	1790x490x8
Module power	(Wp)	70
Cell type		Monocrystalline

Electrical Data				
Nominal power	P_{nom}	70 Wc	Number of cell	20
Cells efficiency	η %	20,0-20,1		
Rated voltage	V_{mpp}	11,00		
Rated current	I_{mpp}	6,44		
Open-circuit voltage	V_{oc}	13,12		
Short-circuit current	I_{sc}	6,93		
Maximum system voltage	IEC	1000		
Temperature coefficient	dP_{mpp}/dT	-0,391 %/°K		
	dV_{oc}/dT	-0,3055 %/°K		
	dI_{sc}/dT	0,0455 %/°K		

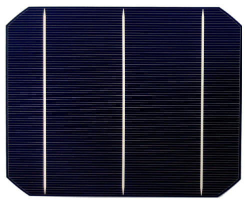

Mono Cell

Mecanical Data		
Cell dimensions	mm	156x156
Module dimensions	mm	1790x490x8
Module weight (unframed)	kg	18
Distance between cells	mm	18
Distance between cells raws	mm	60
Transparency rate	%	0,00
Front glass type		Printed Securit Albarino T
Thickness		4
Rear glass type		Float Securit
Thickness		4
Tedlar		Black

Cabling	
Solar cable	4mm²
Connector type	Connecteur MC4
Cable length	1000mm
Junction Box	
Junction box	PV 1410
Positioning	Behind the cells
Number / module	1
Diode number / box	2
Frame	
Frame type	Unframed
Ribbon	
Color of the ribbon	Black painted

SAINT-GOBAIN   els spelsberg

Insurance / Certification		
CEI 61215 edition2, Safety Class II	VDE Marking	Ethias performance insurance included
IEC	DVE CERTIFICATION IEC 61215 SAFETY CLASS II	ethias

ISSOL - PRODUCT DESIGN

Performance & Harmony

GESTION DE QUALITÉ

CENIT 220 - MODEL - 95 - 6112 - Type L

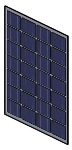

PV module type		Bi-Glass
Dimensions	(mm)	1670x590x8
Module power	(Wp)	95
Cell type		Monocrystalline

Electrical Data

Nominal power	P_{nom}	95 Wc	Number of cell	27
Cells efficiency	η %	20,0-20,1		
Rated voltage	V_{mpp}	14,85		
Rated current	I_{mpp}	6,44		
Open-circuit voltage	V_{oc}	17,71		
Short-circuit current	I_{sc}	6,93		
Maximum system voltage	IEC	1000		
Temperature coefficient	dP_{mpp}/dT	-0,391 %/°K		
	dV_{oc}/dT	-0,3055 %/°K		
	dI_{sc}/dT	0,0455 %/°K		

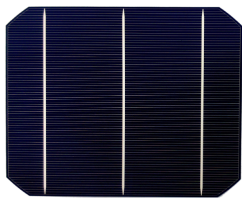

Mono Cell

Mecanical Data

Cell dimensions	mm	156x156
Module dimensions	mm	1670x590x8
Module weight (unframed)	kg	20
Distance between cells	mm	30
Distance between cells raws	mm	26
Transparency rate	%	0,00
Front glass type		Printed Securit Albarino T
	Thickness	4
Rear glass type		Float Securit
	Thickness	4
Tedlar		Black

Cabling

Solar cable	4mm²
Connector type	Connecteur MC4
Cable length	1000mm
Junction Box	
Junction box	PV 1410
Positioning	Behind the cells
Number / module	1
Diode number / box	2
Frame	
Frame type	Unframed
Ribbon	
Color of the ribbon	Black painted

SAINT-GOBAIN els spelsberg

Insurance / Certification

CEI 61215 edition2, Safety Class II	VDE Marking	Ethias performance insurance included

IEC — DVE CERTIFICATION IEC 61215 SAFETY CLASS II — ethias

ISSOL - PRODUCT DESIGN

CENIT 220 - MODEL - 130 - 6312 - Type P

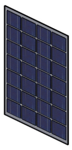

PV module type		Bi-Glass
Dimensions	(mm)	2040x590x8
Module power	(Wp)	130
Cell type		Monocrystalline

Electrical Data				
Nominal power	P_{nom}	130 Wc	Number of cell	36
Cells efficiency	η %	20,0-20,1		
Rated voltage	V_{mpp}	19,80		
Rated current	I_{mpp}	6,44		
Open-circuit voltage	V_{oc}	23,62		
Short-circuit current	I_{sc}	6,93		
Maximum system voltage	IEC	1000		
Temperature coefficient	dP_{mpp}/dT	-0,391 %/°K		
	dV_{oc}/dT	-0,3055 %/°K		
	dI_{sc}/dT	0,0455 %/°K		

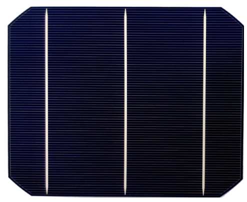

Mono Cell

Mecanical Data		
Cell dimensions	mm	156x156
Module dimensions	mm	2040x590x8
Module weight (unframed)	kg	25
Distance between cells	mm	30
Distance between cells raws	mm	12
Transparency rate	%	0,00
Front glass type		Printed Securit Albarino T
	Thickness	4
Rear glass type		Float Securit
	Thickness	4
Tedlar		Black

Cabling	
Solar cable	4mm²
Connector type	Connecteur MC4
Cable length	1000mm
Junction Box	
Junction box	PV 1410
Positioning	Behind the cells
Number / module	1
Diode number / box	2
Frame	
Frame type	Unframed
Ribbon	
Color of the ribbon	Black painted

Insurance / Certification		
CEI 61215 edition2, Safety Class II	VDE Marking	Ethias performance insurance included

ISSOL - PRODUCT DESIGN

ISSOL Performance & Harmony

ISO 9001 QUALITÉ GESTION DE QUALITÉ

CENIT 220 - MODEL - 150 - 6112 - Type S

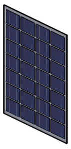

PV module type		Bi-Glass
Dimensions	(mm)	2465x590x8
Module power	(Wp)	150
Cell type		Monocrystalline

Electrical Data				
Nominal power	P_{nom}	150 Wc	Number of cell	42
Cells efficiency	η %	20,0-20,1		
Rated voltage	V_{mpp}	23,10		
Rated current	I_{mpp}	6,44		
Open-circuit voltage	V_{oc}	27,55		
Short-circuit current	I_{sc}	6,93		
Maximum system voltage	IEC	1000		
Temperature coefficient	dP_{mpp}/dT	-0,391 %/°K		
	dV_{oc}/dT	-0,3055 %/°K		
	dI_{sc}/dT	0,0455 %/°K		

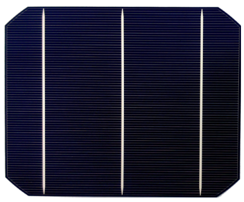

Mono Cell

Mecanical Data		
Cell dimensions	mm	156x156
Module dimensions	mm	2465x590x8
Module weight (unframed)	kg	30
Distance between cells	mm	30
Distance between cells raws	mm	18
Transparency rate	%	0,00
Front glass type		Printed Securit Albarino T
Thickness		4
Rear glass type		Float Securit
Thickness		4
Tedlar		Black

Cabling	
Solar cable	4mm²
Connector type	Connecteur MC4
Cable length	1000mm
Junction Box	
Junction box	PV 1410
Positioning	Behind the cells
Number / module	1
Diode number / box	2
Frame	
Frame type	Unframed
Ribbon	
Color of the ribbon	Black painted

SAINT-GOBAIN els spelsberg

Insurance / Certification		
CEI 61215 edition2, Safety Class II	VDE Marking	Ethias performance insurance included
IEC	DVE CERTIFICATION IEC 61215 SAFETY CLASS II	ethias

ISSOL - PRODUCT DESIGN

CENIT 220 - MODEL - 150 - 6112 - Type T

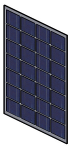

PV module type		Bi-Glass
Dimensions	(mm)	2490x590x8
Module power	(Wp)	150
Cell type		Monocrystalline

Electrical Data

Nominal power	P_{nom}	150 Wc
Cells efficiency	η %	20,0-20,1
Rated voltage	V_{mpp}	23,10
Rated current	I_{mpp}	6,44
Open-circuit voltage	V_{oc}	27,55
Short-circuit current	I_{sc}	6,93
Maximum system voltage	IEC	1000
Temperature coefficient	dP_{mpp}/dT	-0,391 %/°K
	dV_{oc}/dT	-0,3055 %/°K
	dI_{sc}/dT	0,0455 %/°K

Number of cell	42

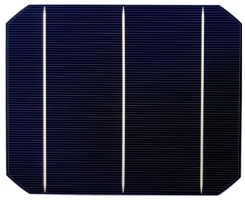

Mono Cell

Mecanical Data

Cell dimensions	mm	156x156
Module dimensions	mm	2490x590x8
Module weight (unframed)	kg	30
Distance between cells	mm	30
Distance between cells raws	mm	20
Transparency rate	%	0,00
Front glass type		Printed Securit Albarino T
	Thickness	4
Rear glass type		Float Securit
	Thickness	4
Tedlar		Black

Cabling

Solar cable	4mm²
Connector type	Connecteur MC4
Cable length	1000mm
Junction Box	
Junction box	PV 1410
Positioning	Behind the cells
Number / module	1
Diode number / box	2
Frame	
Frame type	Unframed
Ribbon	
Color of the ribbon	Black painted

SAINT-GOBAIN els spelsberg

Insurance / Certification

CEI 61215 edition2, Safety Class II	VDE Marking	Ethias performance insurance included

Appendix B Brynseng

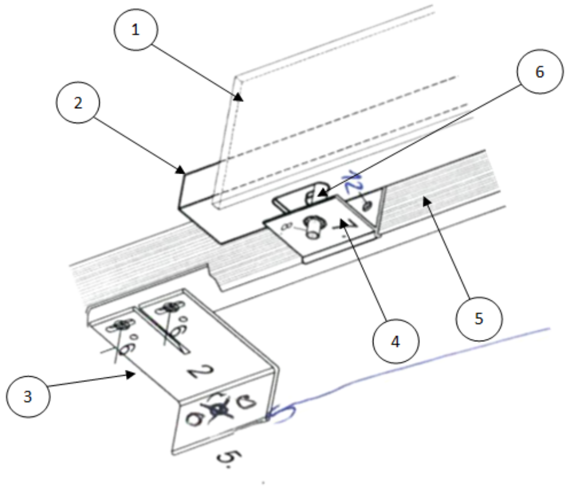

Figure B.1: Detailed mounting specifics on Brynsengfrom confidential pdf, retrived from [54]

The solar panel (1) is fixed to the bracket (2) with gluing, the bottom part of the sliding bracket (3) is fastened with screws. Depending on the location, the sliding brackets are either screwed on wood or concrete. The attachment between the cassette carrier (4) and the T-profile (5), are of self-drilling screws. The connection between the configuration and the hook is of a bolt fastened with nuts on both sides.

Table B1: Explanation of the mounting system at Brynseng

Number	Explanation
1	The solar panel
2	Bracket of Al
3	Sliding bracket (Al) screwed to extruded profile and screwed to either wood/concrete
4	cassette carrier (Al alloy) screwed to extruded profile
5	T-profile (Al)
6	Bolt through the hook and deadlock bracket, fastened with nuts

Tables on missing data, cost and specific yield

Table B2: Detailed information on days of missing data on Brynseng

Days of missing data	Inv 1	Inv 2	Inv 3	Inv4	Inv 5	Inv 6	Inv 7	Inv 8
Jun 17					10			
Sep 17	2	2	2			2	2	2
Nov 17				1				
Apr 18	8	8	8	8	8	8	8	8

Table B3: Calculation of cost with and without ENOVA support

Calculation of cost without the ENOVA support(with the subtraction of traditionally facade materials)	
3.4 Mill NOK/1146m^2 = 2967 NOK/m^2	The amount of NOK paid per square meter
3.4 Mill NOK/114.2kWp = 29.8 NOK/Wp	The amount of NOK paid per watt installed
Subtracting the support from ENOVA of 1.5 Mill NOK	
3.4 Mill NOK − 1.5MillNOK = 1.9 Mill NOK	Cost with ENOVA support
1.9 Mill NOK/1146m^2 = 1658 NOK/m^2	The amount of NOK paid per square meter
3.4 Mill NOK/114.2kWp = 16.64 NOK/Wp	The amount of NOK paid per watt installed

Table B4: The specific yield of each inverter at Brynseng

Brynseng	Total	Left			Central		Right		
		Inv 1	Inv 2	Inv 3	Inv 4	Inv 5	Inv 6	Inv 7	Inv 8
kWh	91233.6	9232.1	9674.4	9276.1	6789.9	8665.9	15108.8	15631	16855.3
kWh/kWp	548.2	530.6	573.5	582.7	390.6	562.7	526.3	561.5	626.4

Table B5: Specific yield of each inverter at Brynseng

Brynseng	Total PV system	Inv1 left side	Inv2 Left side	Inv3 left side	Inv4 central	Inv5 central	Inv6 right side	Inv7-right right side	Inv8 right side
	kWh/kWp	kWh/kWp	kWh/kWp	kWh/kWp	kWh/kWp	kWh/kWp	kWh/kWp	kWh/kWp	kWh/kWp
May 17	46.84	55.07	8.98	21.50	26.91	62.40	53.59	52.87	70.78
Jun 17	53.63	54.53	59.17	64.58	26.12	45.53	54.03	53.61	65.12
Jul 17	63.55	61.40	74.59	74.14	29.44	67.28	59.53	65.19	74.27
Aug 17	70.23	64.82	81.14	81.53	38.92	74.91	66.17	71.74	80.49
Sep 17	31.96	28.05	33.77	34.08	31.04	37.69	28.55	29.29	35.79
Oct 17	55.18	50.66	60.35	61.24	48.56	53.37	52.10	53.90	61.17
Nov 17	37.33	34.92	42.37	35.51	32.78	35.11	38.14	34.36	43.23
Dec 17	8.38	9.04	10.24	6.63	6.05	5.00	10.01	7.11	10.83
Jan 18	9.00	9.06	10.53	8.71	7.53	7.70	9.28	8.05	10.57
Feb 18	40.95	39.30	44.96	45.09	37.11	39.38	38.16	43.63	40.60
Mar 18	79.93	74.93	88.66	90.12	73.70	80.05	70.57	85.28	80.06
Apr 18	51.19	48.83	58.71	59.54	32.39	54.29	46.13	56.41	53.45

String design of the BIPV on Brynseng

Type		Model type	Height [mm]	Width [mm]	Qty [-]	Surfcae [m²]	Surface [m²]	Module Power [wp]	Total power [kWp]
1	Type 1	CENIT220/ Model 290-6112	1790	980	208	1,75	364,87	290	60,32
2	Type 1.2	CENIT220/ Model 240-6112	1790	945	2	1,69	3,38	242	0,48
3	Type 1.3	CENIT220/ Model 195-6112	1790	664	4	1,19	4,75	193	0,77
4	Type 1.4	CENIT220/ Model 195-6112	1790	789	4	1,41	5,65	193	0,77
5	Type 1.5	CENIT220/ Model 195-6112	1790	768	2	1,37	2,75	193	0,39
6	Type 2	CENIT220/ Model 370-6112	2270	980	56	2,22	124,58	369	20,66
7	Type 2.1	CENIT220/ Model 310-6112	2270	969	1	2,20	2,20	309	0,31
8	Type 2.2	CENIT220/ Model 370-6112	2270	1055	6	2,39	14,37	369	2,21
9	Type 3	CENIT220/ Model 240-6112	1625	980	66	1,59	105,11	237	15,64
10	Type 3.1	CENIT220/ Model 200-6112	1625	927	2	1,51	3,01	198	0,40
11	Type 4	CENIT220/ Model 105-6112	730	980	91	0,72	65,10	105	9,56
12	Type 4.2	CENIT220/ Model 090-6112	730	945	1	0,69	0,69	88	0,09
13	Type 4.3	CENIT220/ Model 070-6112	730	768	1	0,56	0,56	70	0,07
14	Type 4.4	CENIT220/ Model 070-6112	730	664	2	0,48	0,97	70	0,14
15	Type 5	CENIT220/ Model 315-6112	2100	980	32	2,06	65,86	316	10,11
16	Type 5.2	CENIT220/ Model 210-6112	2100	723	1	1,52	1,52	211	0,21
17	Type 6	CENIT220/ Model 450-6112	2760	980	24	2,70	64,92	448	10,75
18	Type 6.1	CENIT220/ Model 300-6112	2760	723	1	2,00	2,00	299	0,30
19	Type 6.2	CENIT220/ Model 075-6112	2760	320	6	0,88	5,30	75	0,45
20	Type 6.3	CENIT220/ Model 075-6112	2760	243	1	0,67	0,67	75	0,08
21	Type 6.4	CENIT220/ Model 450-6112	2760	1080	1	2,98	2,98	448	0,45
22	Type 7	CENIT220/ Model 290-6112	1910	980	96	1,87	179,69	290	27,84
23	Type 7.2	CENIT220/ Model 195-6112	1910	723	3	1,38	4,14	193	0,58
24	Type 8	CENIT220/ Model 395-6112	2570	980	2	2,52	5,04	395	0,79
25	Type 9	CENIT220/ Model 055-6112	400	980	38	0,39	14,90	53	2,01
26	Type 9.1	CENIT220/ Model 035-6112	400	664	2	0,27	0,53	35	0,07
27	Type 9.2	CENIT220/ Model 035-6112	400	789	2	0,32	0,63	35	0,07
28	Type 9.3	CENIT220/ Model 045-6112	400	945	1	0,38	0,38	44	0,04
	TOTAL				656		1046,54		165,6

Figure B.2: Different modules used at Brynseng

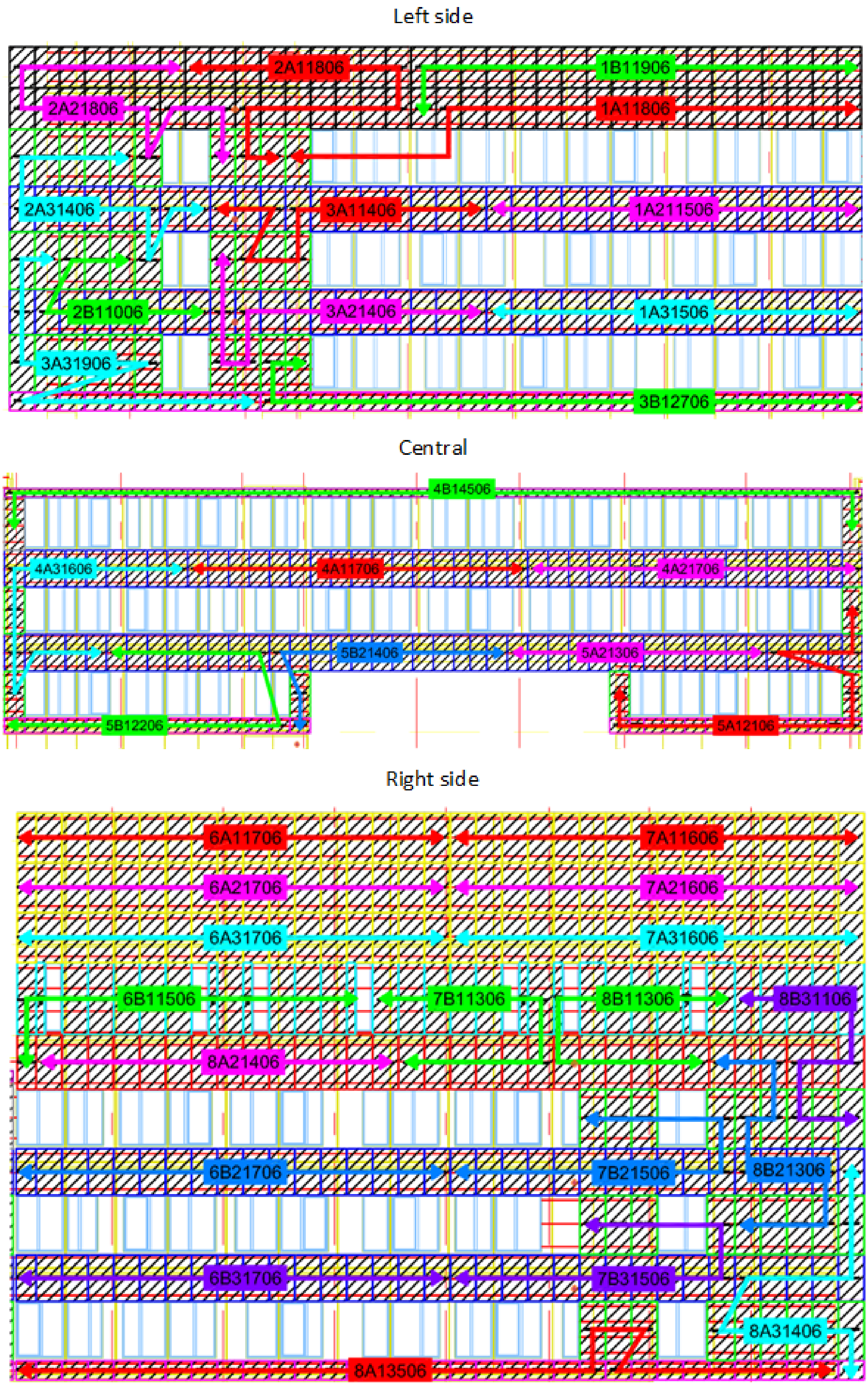

Figure B.3: Electrical scheme of the strings at Brynseng

Verification

Left side

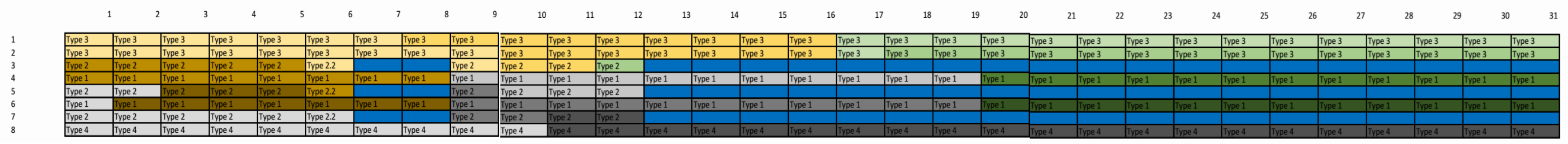

Inverter 1			
Type	Antall	[wp]	kWp
Type 3	18	237	4,266
Type 3.1	1	198	0,198
Type 2	1	369	0,369
Type 3	16	237	3,792
Type 3.1	1	198	0,198
Type 1	15	237	3,555
Type 1	15	237	3,555
Total	67		15,933

Inverter 2			
Type	Antall	[wp]	kWp
Type 3	16	237	3,792
Type 2.2	1	369	0,369
Type 2	1	369	0,369
Type 3	16	237	3,792
Type 2	2	369	0,738
Type 2	5	369	1,845
Type 1	8	290	2,32
Type2.2	1	369	0,369
Type 2	3	369	1,107
Type 1	7	290	2,03
Total	60		16,731

Inverter 3			
Type	Antall	[wp]	kWp
Type 2	7	369	2,583
Type 4	10	105	1,05
Type 1	1	290	0,29
Type 2.2	1	369	0,369
Type 1	11	290	3,19
Type 2	3	369	1,107
Type 2	3	369	1,107
Type 1	11	290	3,19
Type 2	2	369	0,738
Type 4	24	105	2,52
Total	73		16,144

Central side

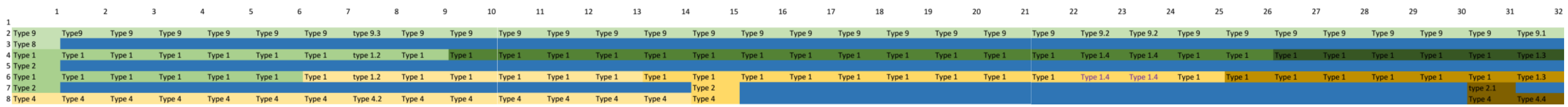

Inverter 4			
Type	Antall	[wp]	kWp
Type 8	2	395	0,79
Type 9	38	38	1,444
Type 9.1	2		
Type 9.2	2		
Tyype 9.3	1	44	0,044
Type 1	14	290	4,06
Type 2	2	369	0,738
Type 1.2	1	242	0,242
Type 1	15	290	4,35
Type 1.4	2	193	0,386
Type 1	15	290	4,35
Type 1.3	2	193	0,386
Total	96		16,79

Inverter 5			
Type	Antall	[wp]	kWp
Type 1	6	290	1,74
Type 1.2	1	242	0,242
Type 4	13	105	1,365
Type 4.2	1	88	0,088
Type 1	10	290	2,9
Type 1.4	2	193	0,386
Type 2	1	369	0,369
Type 4	1	105	0,105
Type 1	12	290	3,48
Type 1.3	1	193	0,193
Type 1	4	290	1,16
Type 1.3	1	193	0,193
Type 2	2	369	0,738
Type 2.1	1	309	0,309
Type 4	11	105	1,155
Type 4.4	2	70	0,14
Total	69		14,563

Right side

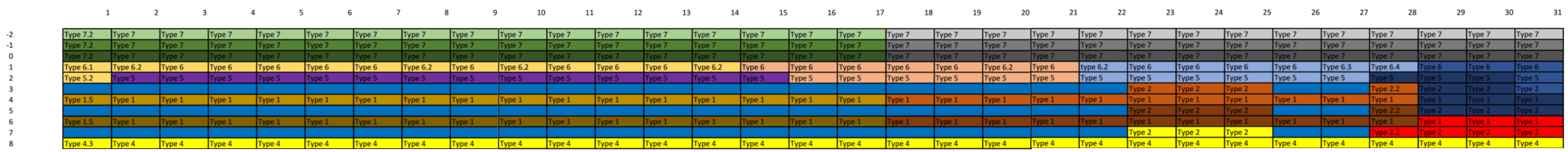

Inverter 6			
Type	Antall	wp	kWp
Type 7	16	290	4,64
Type 7.2	1	193	0,193
Type 7	16	290	4,64
Type 7.2	1	193	0,193
Type 7	16	290	4,64
Type 7.2	1	193	0,193
Type 6	9	448	4,032
Type 6.1	1	299	0,299
Type 6.2	4	75	0,3
Type 5.2	1	211	0,211
Type 1	16	290	4,64
Type 1.5	1	193	0,193
Type 1	16	290	4,64
Type 1.5	1	193	0,193
Total	100		29,007

Inverter 7			
Type	Antall	wp	kWp
Type 7	16	290	4,64
Type 7	16	290	4,64
Type 7	16	290	4,64
Type 5	6	316	1,896
Type 6	6	448	2,688
Type 6.2	1	75	0,075
Type 1	11	290	3,19
Type 2	3	369	1,107
Type 2.2	1	369	0,369
Type 1	11	290	3,19
Type 2	3	369	1,107
Type 2.2	1	369	0,369
Total	91		27,911

Inverter 8			
Type	Antall	wp	kWp
Type 5	6	316	1,896
Type 6	4	448	1,792
Type 6.2	1	75	0,075
Type 6.3	1	75	0,075
Type 6.4	1	448	0,448
Type 6	5	448	2,24
Type 2	3	369	1,107
Type 5	3	316	0,948
Type 1	4	290	1,16
Type 2	6	369	2,214
Type 5	3	316	0,948
Type 1	6	290	1,74
Type 2	6	369	2,214
Type 2.2	1	369	0,369
Type 4	1	105	0,105
Type 2	3	369	1,107
Type 4	31	105	3,255
Type 4.3	1	70	0,07
Type 5	14	316	4,424
Total	100		26,187

Appendix C Bjørkelangen

Cost calculation and specific yield from December 2017 to April 2018, on each string inverter

Table C1: Cost approximation of the BAPV on Bjørkelangen

Steps	Cost approximation of the BAPV on Bjørkelangen
(i)	Cost of Rockwool insulation x installation cost
	$450kr/m^2 \cdot 75kr/m^2 = 525kr/m^2$ (excluded VAT)
(ii)	Cost of installed PV: 13000 kr/kWp
(iii)	Cost for the BAPV part
	$\frac{\text{Cost of installed PV}}{\text{Module per installed kWp}\cdot\text{Area of Module}}$
	$\frac{1300\ NOK/kWp}{\frac{1000}{270\ Wp}\cdot(1640mm\cdot 992mm\cdot 10^{-6})}$
	$\approx 2200NOK/m^2$ (excluded VAT)

Table C2: Yield and specific yield of Bjørkelangen School

Bjørkelangen	Yield [kWh]	Specific Yield [kWh/kWp]	Inv1 [kWh]	Inv2 [kWh]
Dec 17	500.57	14.22	252.15	248.42
Jan 18	468.67	13.31	230.52	238.15
Feb 18	1496.94	42.53	729.48	767.45
Mar 18	3242.10	92.11	1546.67	1695.44
Apr 18	3002.80	85.31	1390.89	1611.91

The technical building integration

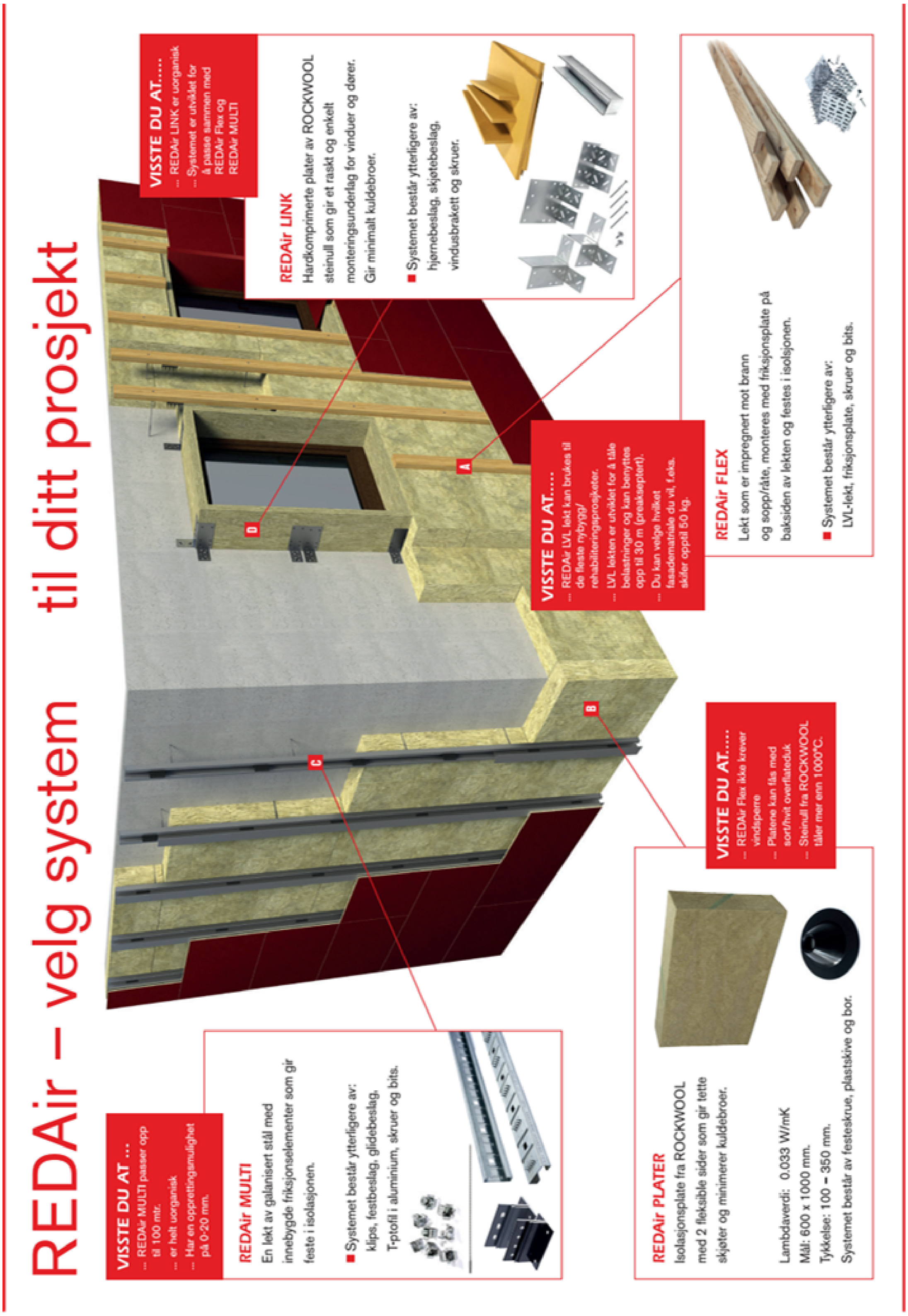

Figure C.1: RedAir system, retrived from [66]

Datasheet of the PV standard PV module

Nordic Solar

We Make Solar Evolve

EliTe BLACK

Monocrystalline Module

ET-M660275BB 275W
ET-M660270BB 270W
ET-M660265BB 265W

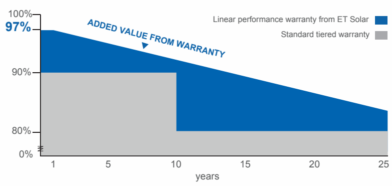

25 25-year performance warranty

10 10-year warranty on materials and workmanship

Rich Product Portfolio & Innovative Product Strategy, satisfy customer needs to the best, and keep the customers' overall costs to the lowest.

High Conversion Efficiency
Industry-leading processing techniques realize great module efficiency, steady power output guaranteed.

Anti-reflective Coating and Reduce O&M Costs
Easier to clean by rainwater to remove dirt on the glass surface, making higher power output and lower maintenance costs.

Visually Appealing Appearance
Good for architectural aesthetics.

0 to +5W

0 to +5W Positive Tolerance
Gain more power yields than expected.

Excellent Loading Capability
2400Pa wind loads, 5400Pa snow loads.
Durable and long-lasting.

Top-quality & Trustworthy Product
Rigorous Quality Management System built.
Multiple internationally recognized PV industry standard certifications attained.

IEC 61215 Ed.2
IEC 61730
UL 1703

CONFORMS TO UL STD. 1703
CERTIFIED TO ULC/ORD STD.C 1703-01

PV CYCLE

BABT8510

Towards Excellence

www.etsolar.com

M/ET-PD-EN-WW2016V4-T

ELECTRICAL SPECIFICATIONS (STC)

Model Type	ET-M660275BB	ET-M660270BB	ET-M660265BB
Peak Power (Pmax)	275W	270W	265W
Module Efficiency	16.90%	16.60%	16.29%
Maximum Power Voltage (Vmp)	30.97V	30.83V	30.64V
Maximum Power Current (Imp)	8.88A	8.76A	8.65A
Open Circuit Voltage (Voc)	39.08V	38.68V	38.29V
Short Circuit Current (Isc)	9.14A	9.12A	9.10A
Power Tolerance		0 to +5W	
Operating Temperature		- 40 ~ + 85℃	
Maximum System Voltage		DC 1000V	
Nominal Operating Cell Temperature		45±2℃	
Fire Safety		Class C(IEC) / Type 1(UL)	
Maximum Series Fuse Rating		20A(IEC) / 15A(UL)	

ELECTRICAL SPECIFICATIONS (NOCT)

Model Type	ET-M660275BB	ET-M660270BB	ET-M660265BB
Peak Power (Pmax)	203.4W	198.5W	194.1W
Maximum Power Voltage (Vmp)	29.3V	28.8V	28.4V
Maximum Power Current (Imp)	6.95A	6.89A	6.84A
Open Circuit Voltage (Voc)	35.80V	35.5V	35.1V
Short Circuit Current (Isc)	7.38A	7.36A	7.35A

MECHANICAL SPECIFICATIONS

Cell Type	156.75mm x 156.75mm
Number of Cells	60 cells in series
Weight	18.5 kg (40.79 lbs)
Dimension	1640×992×35 mm (64.57×39.06×1.38 inch)
Max Load	5400 Pascals (112 lb/ft^2)
Junction Box	IP67 rated
Connector	MC4 Compatible
Output cable	4mm^2(IEC) / 12AWG:PV Wire(UL)

TEMPERATURE COEFFICIENT

Temp. Coeff. of Isc (TK Isc)	0.06% /℃
Temp. Coeff. of Voc (TK Voc)	-0.30% /℃
Temp. Coeff. of Pmax (TK Pmax)	-0.43% /℃

PACKING MANNER

Container	40' HQ
Pieces per Pallet	30
Pieces per Container	840

PHYSICAL CHARACTERISTICS

Unit:mm (inch)

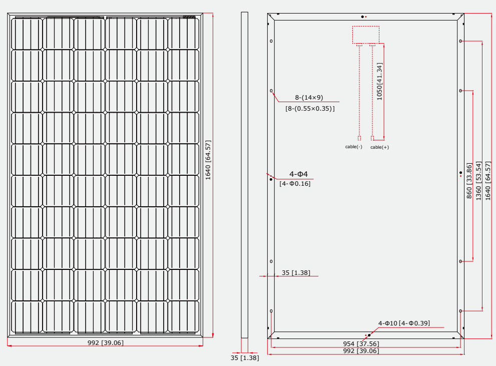

ELECTRICAL CHARACTERISTICS

Temperature Dependence of Isc, Voc and Pmax

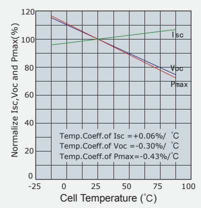

Irradiance Dependence of Isc, Voc and Pmax
(AM1.5,Cell Temperature 25℃)

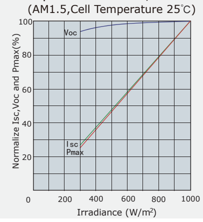

Note: the specifications are obtained under the Standard Test Conditons (STCs): 1000 W/m^2 solar irradiance, 1.5 Air Mass, and cell temperature of 25℃. The NOCT is obtained under the Test Conditions: 800 W/m^2, 20℃ ambient temperature, 1m/s wind speed, AM 1.5 spectrum.
Please contact ***support@etsolar.com*** for technical support. The actual transactions will be subject to the contracts. This parameters is for reference only and it is not a part of the contracts.
The specifications are subject to change without prior notice.

Appendix D Kiwi Dalgård

Yield and specific yield of the BIPV system on Kiwi Dalgård

Table D1: Yield and specific yield at Kiwi Dalgård main facade of Mono-Si

Kiwi Dalgård	Inverter 2 main facade Mono-Si [kWh]	Inverter 2 main facade Mono-Si [kWh/kWp]
Sep 17	373.50	46.58
Oct 17	134.17	16.73
Nov 17	26.17	3.26
Dec 17	5.97	0.74
Jan 18	30.84	3.85
Feb 18	150.07	18.72
Mar 18	389.32	48.56
Apr 18	495.87	61.84

The technical parts modelled by the author in Solid works, from viewing pictures

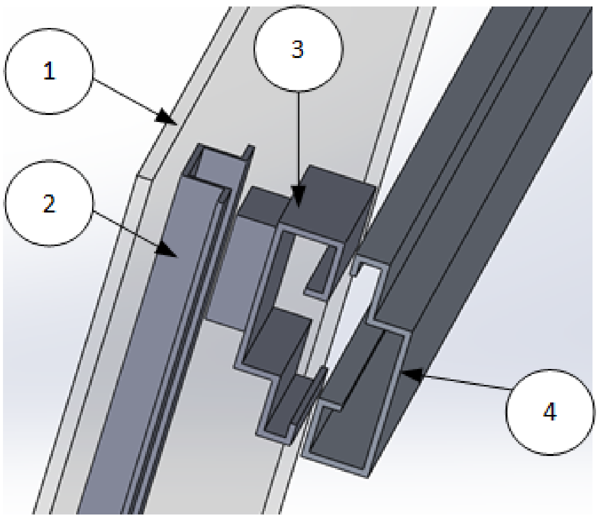

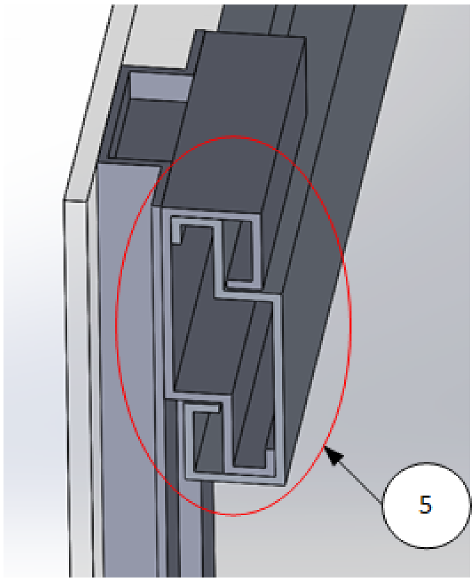

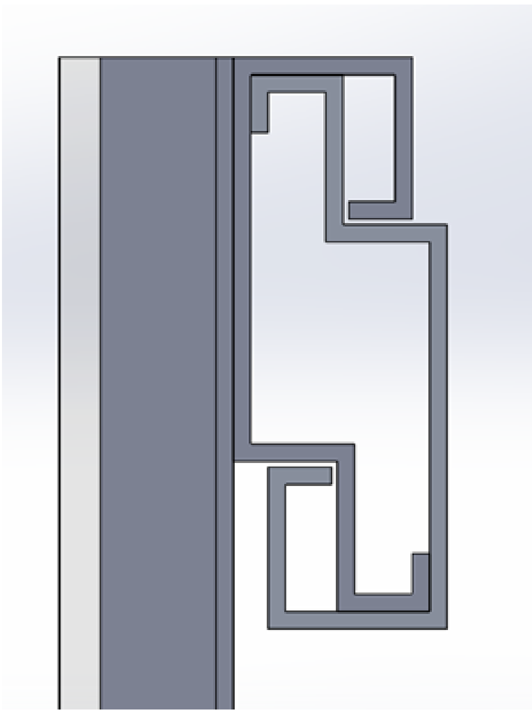

(1) The Solar Panel
(2) The vertical rail glued on the solar panel
(3) The bracket screwed on the vertical rail
(4) The horizontal rail screwed on to the building structure
(5) The bracket is hooked on the horizontal rails

Figure D.1: Illustration of the mounting details at Kiwi Dalgård innos.no

Innos Black Facade
Greener than Green

STC*

Pn	Wp	295	300
Vmpp	V	31,3	31,2
Impp	A	9,42	9,63
Voc	V	39,3	39,4
Isc	A	9,87	9,97
IR****	A	20	20
η	%	18,0	18,3

NOCT**

Pn	W	215	219
Vmpp	V	28,2	28,4
Voc	V	36,2	36,3
Isc	A	7,99	8,07

Temperature Coefficients

Pn	-0,40%/K
Voc	-0,29%/K
Isc	0,050%/K

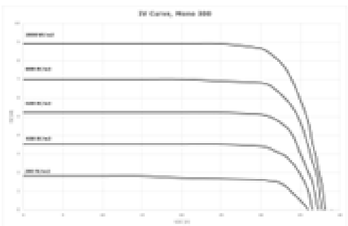

NOCT**	46 °C
Module efficiency reduction at 200W/m2***	-0,6(+/-0,3%) abs.
Max. system voltage	1000V
IP Protection level	IP67
Module design	Glass-Glass with laminated colored foil
Frame	Frameless
Glass	2 layer solarglass with treatment. 3,2mm
No. & type of Solar Cells	Mono crystaline solar cells 156*156mm, 180 μm
Cables	Junction box with MC4 pluggable connectors. Cable 2*0,9m/4mm²
Bypass-Diodes	upp to 3 pcs depending on number of cells
Dimensions (l*w*h)	Up to 1630*982*7mm @ 60 cells
Weight	30,2kg at maximum size
Operating temp. Range	-40 to +85 °C
Mechanical ratings	Suction pressure of 2400Pa approved (wind speed 130km/h with safety factor 3), load 2400 Pa approved
Certification	IEC61215:2005 IEC61730-1/-2:2004 IEC61701:1995 (salt mist) EN50583-1_2016 Category C EN12600 EN12150 EN572-2
Positive sorting	0Wp/+5Wp
Product warranty	12 years
Performance warranty	12 years 90%/25 years 80% output power

The Innos Façade module is produced in a wide variation of format, sizes and colors. Due to that fact the specification above only present the general values for the product. A more precise product definition will follow the delivered product.

Figure D.2: The standard sized PV module from Innos, the taylor made PV modules was not available to the author

Appendix E Kiwi Fjeldset

Yield and Specific yield of the string inverter connected to the facade BAPV system on Kiwi Fjeldset

Table E1: Yield and specific yield of BAPV at Kiwi Fjeldset

Inv 5, south oriented BAPV		
Month	kWh	kWh/kWp
Mar 16	109.13	44.91
Apr 16	131.54	54.13
May 16	153.35	63.11
Jun 16	72.9	30.00
Jul 16	153.19	63.04
Aug 16	143.18	58.92
Sep 16	142.25	58.54
Oct 16	76.44	31.46
Nov 16	31.96	13.15
Dec 16	9.93	4.09
Jan 17	16.36	6.73
Feb 17	72.54	29.85
Mar 17	171.69	70.65
Apr 17	171.94	70.76
May 17	149.73	61.62
Jun 17	136.17	56.04
Jul 17	138.14	56.85
Aug 17	166.66	68.58
Sep 17	53.77	22.13
Oct 17	86.35	35.53
Nov 17	37.26	15.33
Dec 17	8.21	3.38
Jan 18	12.05	4.96
Feb 18	66.66	27.43
Mar 18	194.49	80.04
Apr 18	195.52	80.46

Table E2: Days of missing data of BAPV on Kiwi Fjeldset

Days of missing data	May	Jun	Sep	Oct	Nov	Dec
2016	-	14	1	4	1	1
2017	1	-	5	-	2	2

Datasheet for the PV standard PV modules on Kiwi Fjeldset

Kiwi Fjeldset

ISSOL

270Wp / 984mm x 1637mm / Glass-Glass

Front View with Frame in mm

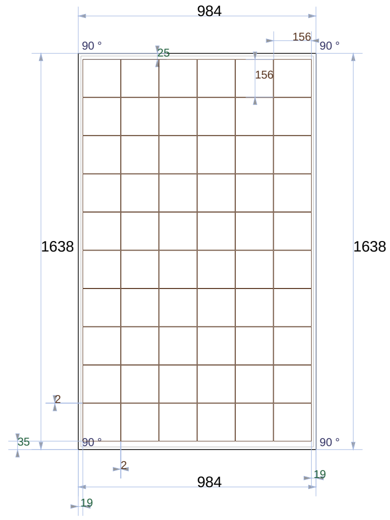

High quality PV glazing

Designed for building integration in respect of the strictest construction norms

ISSOL offers highly-technological content solutions for building integration (BIPV). This PV glazing is valid for all countries following local building regulations. It has been designed to play an essential architectural function and to replace conventional non active building materials. More than just producing electricity, this PV glazing can be used as an essential part of the building envelope making it watertight, isolated, protected from the sun or aesthetical.

ISSOL is a glass manufacturer and a project developer. The company operates in the construction industry by providing active glazing solutions. In collaboration with the world's most famous contemporary designers, ISSOL develops beautiful active buildings that generate their own electricity using the free energy of the sun.

The ISSOL production plant is located in Belgium and is under periodic audit of the German VDE Testing and Certification Institute. The design office and production are certified ISO 9001.

Electrical Data

Peak Power: 270 Wp
VOC: 39.36 V
Vmpp: 33 V
Impp: 8.19 A
Isc (A): 8.81 A
Maximum voltage: 1000 V
Tolerances: +/- 1.5%
Power per sq m: 167.52 W/sq m
T° coef. VOC: -0.3055 %/K
T° coef. Isc: 0.0455 %/K
T° coef. Pmpp: -0.391 %/K

Cell Type

No of Cells: 60
Efficiency: 20.05%
Peak power: 4.79 Wp
Size: 156mm x 156mm
Shape: Pseudo Square
Technology: Monocrystalline
Color: Black
No of Bus Bar: 3

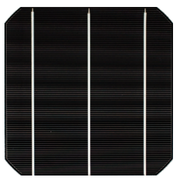

Mechanical Data

Surface: 1.61 sq m
Width: 984 mm
Length: 1,637 mm
Thickness with Frame: 50 mm
Weight: 37.36 kg
Weight per sq m: 23.18 kg/sq m
Frame Type: Vari Sole Dbl

Glass Properties

Front Panel Thickness: 4 mm
Front Panel Pattern: None
Tempered Glass
Back Panel Thickness: 4.5 mm
Front Panel Type: Albarino T Glass
Back Panel Type: Glass Planilux

Other Data

Transparency: 0 %
DC Cables: 1000 mm
Ribbon: Paint Black
Frames: Black Anodized Finish
Junction Box: Spelsberg PV1410
Output connectors: Outer Edge

Page 1/2

ISSOL sa/nv | Z.I. des Plènesses - Rue du Progrès 18 B 4821 Dison (Liège)) - Belgium
TVA/VAT : BE 0879.446.738 | Tel : +32 87338164 | Fax : +32 42900504 | www.issol.eu | infopv@issol.eu © 2015, ISSOL sa/nv

Kiwi Fjeldset

270Wp / 984mm x 1637mm / Glass-Glass

Back View without Frame in mm

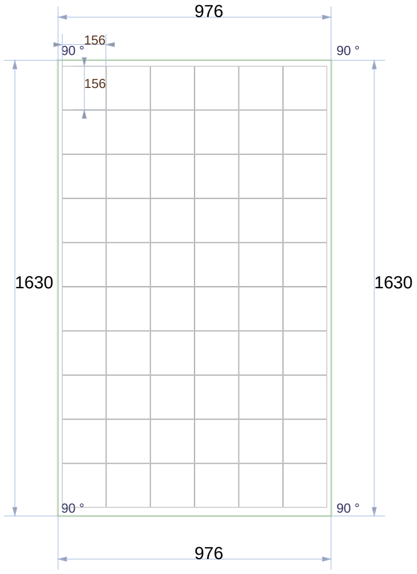

Section

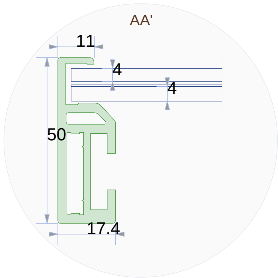

Profile

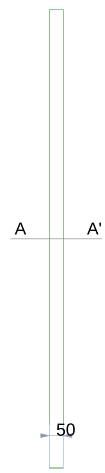

Certifications

EN 12150 Toughened safety glass:EN 12150 Glass in building. Thermally toughened soda lime silicate safety glass: this product is manufactured according to the norm. Tempered safety glass SECURIT®

EN 572-5 Patterned glass:þÿEN 572-5 Basic soda lime silicate glass product. Patterned glass for glass in buil according to the norm.

EN 12600 Pendulum test:EN 12600 Glass in building. Pendulum Test: a pendulum impact test was performed with this glass and get a classification following the norm.

IEC 61701 Salt and mist corrosion:IEC 61701 Salt and mist corrosion of photovoltaic modules: this product passes the test sucessfully.

Factory Inspection Certificate:VDE Factory Inspection Certificate : validity < 1 year the surpervision of the manufacturing site of ISSOL is performed annually by VDE according to the European Factory Inspection Procedure ECS/CIG 021-024 Factory # 30017695 Licence holder # 5007371 Process steps in factory Developpment/Cells Stringing/Assembly/Lamination/Electrical tests/Classification

ISO 9001:ISO 9001: ISSOL's manufacturing plant and engineering office are certified ISO9001:2009 and under permanent surveillance by SGS Certificate BE11/22357/4389

European manufacturing certificate: European manufacturing certificate: product manufactured in the European Economic Area - issued by ELIOSYS certificate #20131127CPE-001

Manufactured IEC 61215: Product manufactured according to IEC 61215 ed. II: crystalline silicon terrestrial photovoltaic (PV) modules. Design qualification and type approval Delivered by VDE Prüf- und Zertifizierungsinstitut - Offenbach - Allemagne

Manufactured IEC 61730: Product manufactured according to IEC 61730 Safety Class II: photovoltaic (PV) module safety qualification Delivered by VDE Prüf und Zertifizierungsinstitut - Offenbach - Allemagne

DIN VDE 0100 Low voltage:DIN VDE 0100-712 Erection of low-voltage systems solar photovoltaic (PV) power supply systems : this product is permitting the respect of the norm

IEC 60664/60243 Insulation testing max Voltage:EC 60664/60243 : Insulation coordination for equipment within low-voltage systems : this product is manufactured in respect of the norm.

VDE Marking:VDE marking : the product is marked with VDE ID # 40022635

Declaration of conformity CE: Declaration of conformity CE : the product conforms to the norms IEC 61215 Ed. 2 - SC II - IEC 61730 - IEC 61701 and to the criterion of the Directive 73/23/CEE.

Junction Box IEC 61215, IEC 61646: The juction box is certified according to the norms IEC 61215 and IEC 61646. TÜV ID 6511005400 - PVS 21200494

STC: Our electrical tests are performed under Stantard Test Condtions (STC) unless stated otherwised _ temperature of 25 °C and an irradiance of 1000 W/m2 with an air mass 1.5 (AM1.5) spectrum

Page 2/2

ISSOL sa/nv | Z.I. des Plènesses - Rue du Progrès 18 B 4821 Dison (Liège)) - Belgium
TVA/VAT : BE 0879.446.738 | Tel : +32 87338164 | Fax : +32 42900504 | www.issol.eu | infopv@issol.eu

Appendix F ASKO washing hall

Tables of yield/specific yield and DC/AC power (Inverter efficiency)

Table F1: Energy production and specific yield of ASKO washing hall

ASKO washing hall	Inv3 [kWh]	Inv3 [kWh/kWp]
Mar 17	1152.00	35.89
Apr 17	2705.00	84.27
May 17	2500.00	77.88
Jun 17	2381.00	74.17
Jul 17	2717.00	84.64
Aug 17	2774.00	86.42
Sep 17	1487.00	46.32
Oct 17	2151.00	67.01
Nov 17	1211.00	37.73
Dec 17	362.00	11.28
Jan 18	321.00	10.00
Feb 18	1437.00	44.77
Mar 18	3105.00	96.73
Apr 18	3050.00	95.02

Table F2: South facade inverter efficiency at ASKO washing hall

ASKO washing hall	Efficiency (%)	Mean Temperature (C)
Apr 17	97.92	26.367
May 17	97.94	29.7048
Jun 17	97.92	31.3374
Jul 17	97.91	32.0941
Aug 17	97.92	31.3633
Sep 17	97.89	28.2448
Oct 17	97.95	26.1414
Nov 17	97.97	24.8717
Dec 17	97.97	24.9136
Jan 18	97.97	24.6744
Feb 18	97.94	24.6524
Mar 18	97.97	27.9134
Apr 18	97.97	32.131

Datasheet of the standard PV module

EN

LG NeON™ 2 Black

LG300N1K-G4

60 cell

LG's new module, NeON™ 2 Black, adopts Cello technology. Cello technology replaces 3 busbars with 12 thin wires to enhance power output and reliability.
NeON™ 2 Black demonstrates LG's efforts to increase customer's values beyond efficiency. It features enhanced warranty, durability, performance under real environment, and aesthetic design suitable for roofs.

Intertek

Key Features

Enhanced Performance Warranty

LG NeON™ 2 Black has an enhanced performance warranty. The annual degradation has fallen from -0.7%/yr to -0.6%/yr. Even after 25 years, the cell guarantees 2.4%p more output than the previous NeON™ modules.

High Power Output

Compared with previous models, the LG NeON™ 2 Black has been designed to significantly enhance its output efficiency making it efficient even in limited space.

Aesthetic Roof

LG NeON™ 2 Black has been designed with aesthetics in mind; thinner wires that appear all black at a distance. The product can increase the value of a property with its modern design.

Outstanding Durability

With its newly reinforced frame design, LG has extended the warranty of the NeON™ 2 Black for an additional 2 years. Additionally, LG NeON™ 2 Black can endure a front load up to 6000 Pa, and a rear load up to 5400 Pa.

Better Performance on a Sunny Day

LG NeON™ 2 Black now performs better on a sunny days thanks to its improved temperature coefficient.

Double-Sided Cell Structure

The rear of the cell used in LG NeON™ 2 Black will contribute to generation, just like the front; the light beam reflected from the rear of the module is reabsorbed to generate a great amount of additional power.

About LG Electronics

LG Electronics is a global big player, committed to expanding its operations with the solar market. The company first embarked on a solar energy source research program in 1985, supported by LG Group's vast experience in the semi-conductor, LCD, chemistry, and materials industries. In 2010, LG Solar successfully released its first MonoX® series to the market, which is now available in 32 countries. In 2013, the NeON™ (previous. MonoX® NeON) won the "Intersolar Award", which demonstrates LG Solar's lead, innovation and commitment to the industry.

LG Life's Good

EN

LG300N1K-G4

LG NeON™ 2 Black

Mechanical Properties

Cells	6 x 10
Cell Vendor	LG
Cell Type	Monocrystalline / N-type
Cell Dimensions	156.75 x 156.75 mm / 6 x 6 inch
# of Busbar	12 (Multi Wire Busbar) NEW
Dimensions (L x W x H)	1640 x 1000 x 40 mm
	64.57 x 39.37 x 1.57 inch
Front Load	6000 Pa / 125 psf NEW
Rear Load	5400 Pa / 113 psf NEW
Weight	17.0 ± 0.5 kg / 37.48 ± 1.1 lbs
Connector Type	MC4, MC4 Compatible, IP67
Junction Box	IP67 with 3 Bypass Diodes
Length of Cables	2 x 1000 mm / 2 x 39.37 inch
Glass	High Transmission Tempered Glass
Frame	Anodized Aluminum

Certifications and Warranty

Certifications (In Progress)	IEC 61215, IEC 61730-1/-2, UL 1703,
	ISO 9001, IEC 62716 (Ammonia Test),
	IEC 61701(Salt Mist Corrosion Test),
Module Fire Performance	Type 2 (UL 1703)
Product Warranty	12 Years NEW
Output Warranty of Pmax (Measurement Tolerance ± 3%)	Linear Warranty* NEW

* 1) 1st year: 98%, 2) After 2nd year: 0.6%p annual degradation, 3) 83.6% for 25 years

Temperature Coefficients

NOCT	46 ± 3 °C
Pmpp	-0.38 %/°C NEW
Voc	-0.28 %/°C
Isc	0.02 %/°C

Characteristic Curves

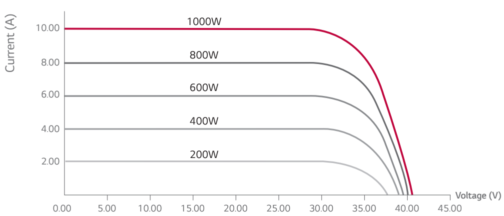

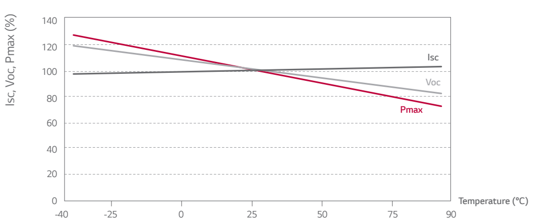

Electrical Properties (STC*)

	300 W
MPP Voltage (Vmpp)	32.5
MPP Current (Impp)	9.26
Open Circuit Voltage (Voc)	39.7
Short Circuit Current (Isc)	9.70
Module Efficiency (%)	18.3
Operating Temperature (°C)	-40 ~ +90
Maximum System Voltage (V)	1000
Maximum Series Fuse Rating (A)	20
Power Tolerance (%)	0 ~ +3

* STC (Standard Test Condition): Irradiance 1000 W/m², Module Temperature 25 °C, AM 1.5
* The nameplate power output is measured and determined by LG Electronics at its sole and absolute discretion.
* The typical change in module efficiency at 200 W/m² in relation to 1000 W/m² is -2.0%.

Electrical Properties (NOCT*)

	300 W
Maximum Power (Pmpp)	218
MPP Voltage (Vmpp)	29.5
MPP Current (Impp)	7.38
Open Circuit Voltage (Voc)	36.5
Short Circuit Current (Isc)	7.83

* NOCT (Nominal Operating Cell Temperature): Irradiance 800 W/m², ambient temperature 20 °C, wind speed 1 m/s

Dimensions (mm / in)

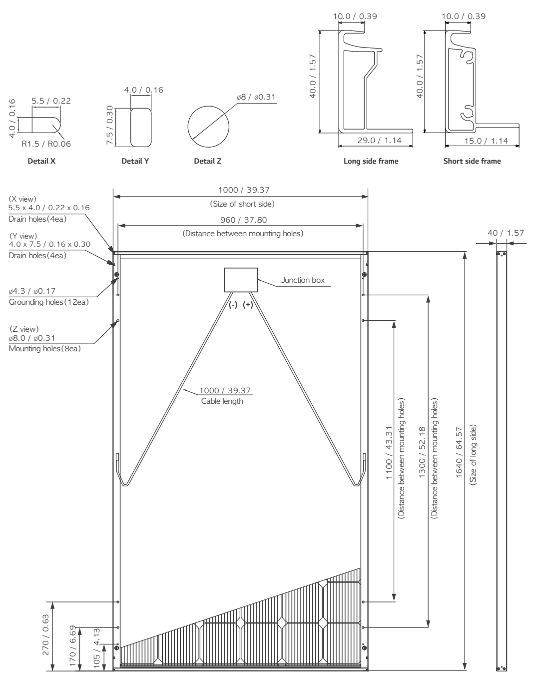

* The distance between the center of the mounting/grounding holes.

LG Life's Good

LG Electronics Inc.
Solar Business Division
Seoul Square 416, Hangang-daero, Jung-gu, Seoul 100-714, Korea

www.lg-solar.com

Product specifications are subject to change without notice.
DS-N2-60-K-G-F-EN-50427

01/04/2015

Appendix G Haldenterminalen

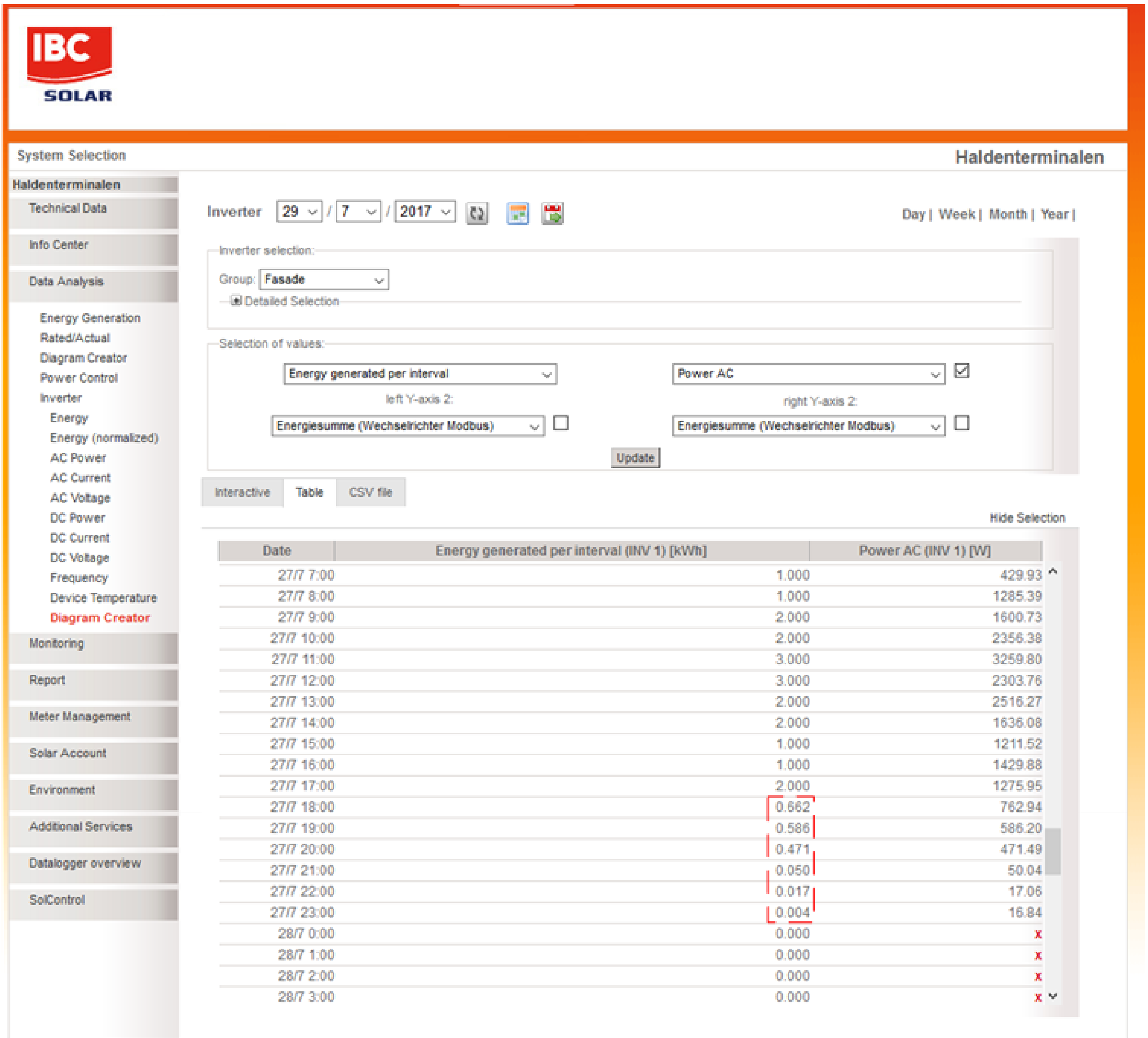

Figure G.1: IBC solar monitoring changing the values on energy generated per interval

Tables with measured data from SolPortal

Table G1: Efficiency and mean temperature at Haldenterminalen

Halden Terminal		
South Facade	Eff %	Temp C
Jan 16	96.02	29.83
Feb 16	96.91	30.59
Mar 16	97.06	30.74
Apr 16	96.34	31.50
May 16	97.22	32.54
Jun 16	97.19	34.69
Jul 16	97.27	35.22
Aug 16	97.20	34.76
Sep 16	97.37	33.94
Oct 16	96.58	32.22
Nov 16	95.00	30.76
Dec 16	94.86	30.30
Jan 17	95.53	30.84
Feb 17	96.21	31.82
Mar 17	97.15	34.26
Apr 17	97.30	35.97
May 17	97.17	37.55
Jun 17	97.14	38.75
Jul 17	97.37	42.41
Aug 17	97.26	42.34
Sep 17	97.01	38.20
Oct 17	97.15	40.93
Nov 17	96.43	39.10
Dec 17	94.33	36.23
Jan 18	94.72	34.32
Feb 18	96.77	35.44
Mar 18	97.26	36.83
Apr 18	97.78	38.90

Table G2: Yield and Specific yield of the south oriented BAPV on Haldenterminalen

Halden Terminal	Facade Inv 1 [kWh]	Facade Inv 1 [kWh/kWp]
Oct 15	1334.2	66.65
Nov 15	665.3	33.23
Dec 15	288.0	14.38
Jan 16	644.2	32.18
Feb 16	1117.9	55.84
Mar 16	1396.7	69.77
Apr 16	1541.7	77.01
May 16	1854.2	92.62
Jun 16	1822.3	91.02
Jul 16	2024.3	101.11
Aug 16	1691.3	84.48
Sep 16	1670.8	83.45
Oct 16	1015.4	50.72
Nov 16	466.8	23.32
Dec 16	389.8	19.47
Jan 17	512.7	25.61
Feb 17	819.6	40.94
Mar 17	1578.5	78.85
Apr 17	1838.5	91.84
May 17	1763.3	88.08
Jun 17	1770.3	88.43
Jul 17	1904.1	95.11
Aug 17	1743.1	87.07
Sep 17	1162.8	58.08
Oct 17	1294.9	64.68
Nov 17	711.5	35.54
Dec 17	315.2	15.74
Jan 18	420.5	21.01
Feb 18	874.5	43.68
Mar 18	1621.4	80.99
Apr 18	1915.4	95.68

Datasheet of the standard PV module and the sandwich panel

Smart Systems for Solar Power

IBC SOLAR

IBC EcoLine – For particulary stable output

IBC MonoSol 255 CS Black, 260 CS Black, 265 CS Black

Solar modules made by monocrystalline silicon

Regardless of whether it is used on detached houses, the roofs of industrial properties or on open spaces, tried and tested IBC MonoSol CS Black photovoltaic modules are suitable for any application requiring a high quality, efficiency and profitability. Continuous quality assurance and process audits during production guarantee a particularly long service life of the modules with a maximum of output, efficiency and reliability. Thanks to the anti-reflective coating on the front glass panels, these modules capture even more light to be more efficient and produce optimum yields.
IBC MonoSol CS Black modules live up to maximum aesthetic demands. These completely black modules with black cell, black frame and black foil visually integrate on any roof and are even suitable for listed buildings.

Highlights:

- 10-year product warranty*
- 25 years linear power warranty*
- Positive power tolerance –0/+5 Wp
- Highly effective with low-iron photovoltaic glass and anti-reflective coating (thickness 3.2 mm)
- Sturdy hollow-chamber frame
- Tested according IEC 61215 for snow loads up to 5400 Pa (ca. 550 kg/m^2)
- IEC 61730, application class A for system voltages up to 1000 V, protection class II
- Produced in facilities certified as per ISO 9001, ISO 14001 and OHSAS 18001
- Regular product/process/quality assurance audits in production
- Quality tested by IBC SOLAR in own laboratory with climate chambers and flasher with integrated electroluminescence measurement

CE

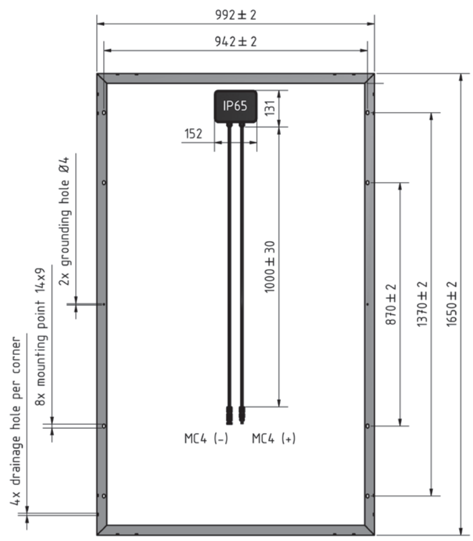

Progression of the power warranty

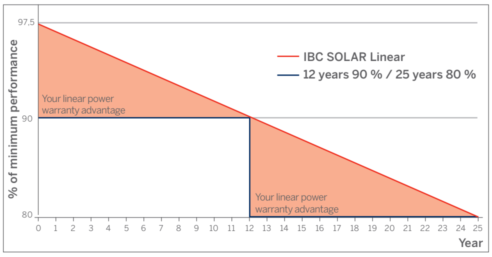

TECHNICAL DATA

IBC MonoSol	255 CS Black	260 CS Black	265 CS Black
STC Power Pmax (Wp)	255	260	265
STC Nominal Voltage Umpp (V)	30.73	31.07	31.4
STC Nominal Current Impp (A)	8.30	8.37	8.44
STC Open Circuit Voltage Uoc (V)	38.32	38.44	38.54
STC Short Circuit Current Isc (A)	8.87	8.93	8.99
800 W/m² NOCT AM 1.5 Power Pmax (Wp)	183.07	186.81	190.55
800 W/m² NOCT AM 1.5 Nominal Voltage Umpp (V)	27.95	28.14	28.33
800 W/m² NOCT AM 1.5 Open Circuit Voltage Uoc (V)	35.66	36.16	36.68
800 W/m² NOCT AM 1.5 Short Circuit Current Isc (A)	6.85	6.89	6.93
Rel. efficiency reduction @ 200 W/m² (%)	3.42	2.81	2.18
Tempcoeff Isc (%/°C)	+0.034	+0.041	+0.041
Tempcoeff Uoc (mV/°C)	–137	–138	–138
Tempcoeff Pmpp (%/°C)	–0.47	–0.493	–0.493
Module Efficiency (%)	15.6	15.9	16.2
NOCT (°C)	46	46	46
Max. System Voltage (V)	1000	1000	1000
Max. Reverse Current Ir (A)	20	20	20
Current value String fuse (A)	15	15	15
Fuse protection from parallel strings	4	4	4
Length (mm)	1650	1650	1650
Width (mm)	992	992	992
Height (mm)	45	45	45
Weight (kg)	19.5	19.5	19.5
Article number	2003800012	2003800014	2003800015

2015-01-16

Presented by:

* The linear power warranty is only valid for installations within Europe and Japan. For further information, please refer to the corresponding product and power warranty in accordance with the version of the full warranty conditions received from your specialized IBC SOLAR partner at the time of installation. This warranty is valid only when the product is installed in accordance with the applicable installation instructions. Electrical values under standard test conditions: 1000 W/m²; 25 °C, AM 1.5. 800 W/m², NOCT. Specifications according EN 60904-3 (STC). All datas according DIN EN 50380. Subject to modifications that represent progress.

IBC SOLAR AG | Am Hochgericht 10 | 96231 Bad Staffelstein, Germany | Phone +49 (0)9573-92 24 0 | info@ibc-solar.com | www.ibc-solar.com

Datasheet
KS1200 NL

Application

The new KS1200 NL is a through fixed wall system for horizontal and vertical installation and is suitable for wall claddings on all types of buildings. For the KS1200 NL follow the manufacturer's instructions given in the Controlled Environments section for special requirements relating to the cladding of cold stores.

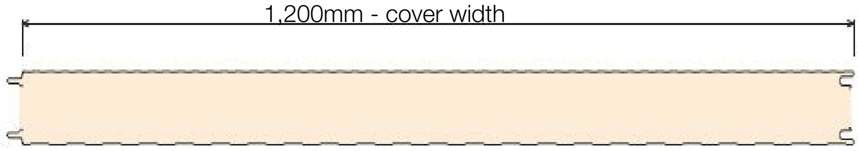

Facing Profiles (V/H, H/H, E/H)

Slightly profiled (H)

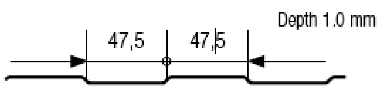

M-Profile

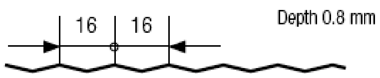

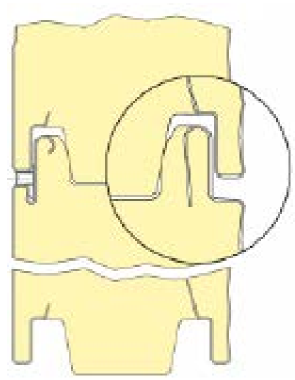

Options:
- Compression tape at the internal side
-Elast sealing at the external side

Panel Thickness (mm)	40	60	80	100	120	150	170	200	220
U-value according to EN ISO 10211-2 (W/m²K)	0,49	0,34	0,26	0,21	0,17	0,14	0,12	0,11	0,10
Weight kg/m²	11,04	11,67	12,30	12,93	13,59	14,51	15,15	16,09	16,73
Element length (mm)	2000mm - 20000mm								
Element width (mm)	1200mm								
Sheet (mm): external	0,5mm 0,6mm/0,7mm on request								
Sheet (mm): internal	0,5mm								

Materials

Steel

Galvanic protection options

1. Hot-dip zinc coated steel with a total of 275 g/m2 of zinc, according to EN 10147:2000. This can be finished with a number of coatings – Polyester, Spectrum™, PVDF and Foodsafe finishes.
2. Galvalloy (hot-dip coated with eutectic alloy of approx. 95% Zn, 5% Al and other elements) in accordance with EN 10214.

Thickness of external and internal sheet is 0.50 mm.

External Coating Options

- Standard Polyester
  PES Polyester is a universal, economic coating system suitable for exterior and interior applications. The nominal coating thickness is 25 µm.

- PVDF
  PVDF offers unequalled colour and gloss retention and good corrosion resistance. The nominal coating thickness is 25 µm. It can be used in climates with extremely high UV radiation combined with extreme temperatures and relative humidity. The standard colour range includes metallic silver.

Datasheet
KS1200 NL

- Spectrum™
  Kingspan Spectrum™ is a 50µm Polyurethanecoated semi gloss finish with a slight granular effect.It offers an outstanding durability- and weather resistance performance, excellent corrosion and UV-resistance as well as high color & gloss retention characterstics.Its superior flexibility enables high resistance against mechanical damages. Kingspan Spectrum is available in a wide range of solid and metallic colours. Furthermore it is free of clorine, phtalates and plasticizers and 100% recyclable

Internal Coating Options

- Polyester
  Polyester coating with a nominal thickness of 15 µm. The standard colour is grey white, (similar RAL 9002) .
- Foodsafe
  The surface of this 150 µm thick polymer coating is non-toxic and resistant to mould, durable and easy to clean. It is chemically inert and safe for continuous contact with unpacked food. The standard colour is white. Consult Kingspan about the availability of other colours. Other coating systems are available by discussion with Kingspan. Plain and coloured aluminium is available on a project specific basis. Contact Kingspan Technical Services.

Insulation Core

Firesafe IPN closed-cell foam is the standard insulating core used. It is made to a non-deleterious specification with Zero Ozone Depletion Potential ODP and is CFC / HCFC free.

Joint Geometry

We have redesigned the joint geometry for horizontal installation, as an asymmetrical panel joint offers a range of benefits. On the outside, the inclination of the groove flank prevents water from penetrating. Even in the case of driving rain, the water can run off in a controlled manner without getting into the joint. This prevents the joints from freezing. The opposite side of the joint has a groove for accommodating some well-proven finishing profiles. Thus, a visually homogenous wall surface is created inside building and and achieves hygienic conditions if required.

Biological

Kingspan panels are immune to attack from mould, fungi, mildew and vermin. No urea formaldehyde is used in the construction, and the panels are nondeleterious.

Fire

KS1200 NL insulated sandwich panels have been tested and approved and comply with National Building Regulations and standards. Panels with FIREsafe IPN core are classified as B-s1,d0 according EN 13501-1

Acoustics

Independend from the panel thickness and without any additional actions a single figure weigthed sound reduction R‘w of 25dB is accomplished.

Building Regulations

Kingspan KS1200 NL insulated sandwich panels apply to the european standard EN 14509: Self-supporting double skin metal faced insulating panels and conform to additional National Building Regulations and standards.

Quality

Kingspan insulated sandwich panels are manufactured from the highest quality materials, using state of the art production equipment to rigorous quality control standards, complying with ISO9001:2000 standards, ensuring long term reliability and service life.

Guarantees & Warranties

Kingspan will provide external coating, product guaranties on an indiviual project basis.

Packing

Standard packing – road transportation
KS1200 NL panels are stacked weather side to internal side. The top, bottom, sides and ends are protected with foam and timber packing and the entire palette is wrapped in plastic. The number of panels in each pack depends on panel thickness and length. The table below is shown as a guide. Quantities are reduced for exceptionally long panels. Typical palette height is 1.100 mm. Maximum palette weight is 4.200 kg.

Panel Thickness (mm)	40	60	80	100	120	150	170	200	220
Number of panels in package	27	17	13	11	9	7	6	5	5

Delivery

All deliveries (unless indicated otherwise) are by road transport to project site. Off loading is the responsibility of the client.

Site Installation

Site assembly instructions are available from Kingspan. Kingspan will arrange training of the site fitters and supervisors if requested.

Appendix H Screen shot of web-based monitoring software

Figure H.1: Screen shot of the diagram creator of IBC Solar Pro

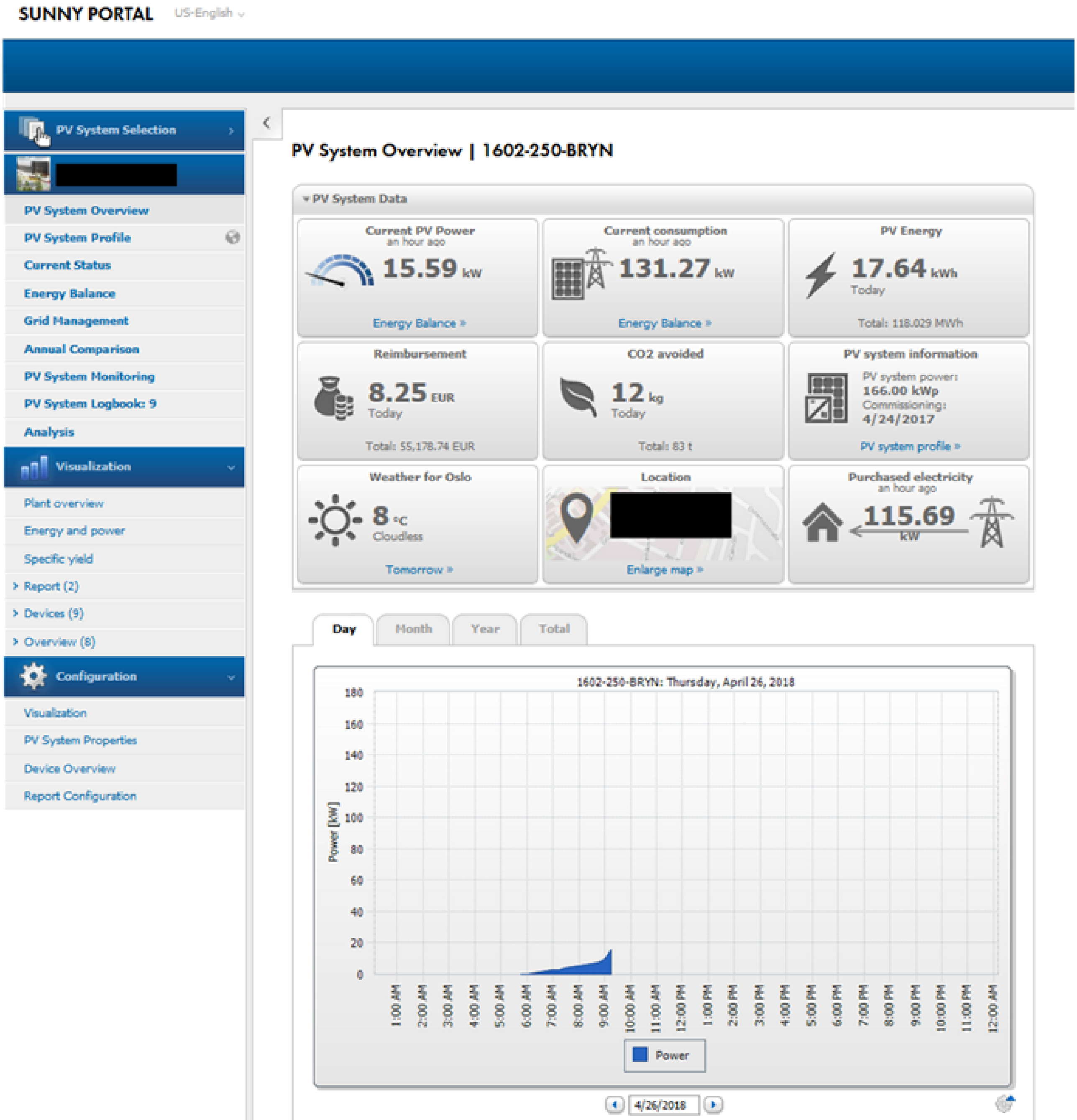

Figure H.2: Example of front page on Sunny Portal and different analysis parameters